Origin, characterization and roles of matrix vesicles in physiological and pathological mineralization.

Cyril Thouverey

N° d'ordre: 95-2008 Année 2008

THESE

Présentée devant

Nencki Institute of Experimental Biology,

Polish Academy of Sciences

Université Claude Bernard Lyon 1,

Pour l'obtention

Du DIPLOME DE DOCTORAT

(Arrêté du 7 août 2006 et arrêté du 6 janvier 2005)

Présentée et soutenue publiquement le 20 juin 2008

Par

Cyril Thouverey

Origin, characterization and roles of matrix vesicles in physiological and pathological mineralization

Directeurs de thèse:

Pr René Buchet et Pr Sławomir Pikuła

JURY: Mme Françoise Bleicher

Mme Joanna Bandorowicz-Pikuła

Mme Martime Cohen-Solal

Mr René Buchet

Mr Sławomir Pikuła

Mr Aleksander Sikorski

UNIVERSITE CLAUDE BERNARD - LYON I

Président de l'Université	**M. le Professeur L. COLLET**
Vice-Président du Conseil Scientifique	M. le Professeur J.F. MORNEX
Vice-Président du Conseil d'Administration	M. le Professeur J. LIETO
Vice-Président du Conseil des Etudes et de la Vie Universitaire	M. le Professeur D. SIMON
Secrétaire Général	M. G. GAY

SECTEUR SANTE

Composantes

UFR de Médecine Lyon R.T.H. Laënnec	Directeur : M. le Professeur P. COCHAT
UFR de Médecine Lyon Grange-Blanche	Directeur : M. le Professeur X. MARTIN
UFR de Médecine Lyon-Nord	Directeur : M. le Professeur J. ETIENNE
UFR de Médecine Lyon-Sud	Directeur : M. le Professeur F.N. GILLY
UFR d'Odontologie	Directeur : M. O. ROBIN
Institut des Sciences Pharmaceutiques et Biologiques	Directeur : M. le Professeur F. LOCHER
Institut Techniques de Réadaptation	Directeur : M. le Professeur MATILLON
Département de Formation et Centre de Recherche en Biologie Humaine	Directeur : M. le Professeur P. FARGE

SECTEUR SCIENCES

Composantes

UFR de Physique	Directeur : Mme. le Professeur S. FLECK
UFR de Biologie	Directeur : M. le Professeur H. PINON
UFR de Mécanique	Directeur : M. le Professeur H. BEN HADID
UFR de Génie Electrique et des Procédés	Directeur : M. le Professeur G. CLERC
UFR Sciences de la Terre	Directeur : M. le Professeur P. HANTZPERGUE
UFR de Mathématiques	Directeur : M. le Professeur M. CHAMARIE
UFR d'Informatique	Directeur : M. le Professeur S. AKKOUCHE
UFR de Chimie Biochimie	Directeur : Mme. le Professeur H. PARROT
UFR STAPS	Directeur : M. C. COLLIGNON
Observatoire de Lyon	Directeur : M. le Professeur R. BACON
Institut des Sciences et des Techniques de l'Ingénieur de Lyon	Directeur : M. le Professeur J. LIETO
IUT A	Directeur : M. le Professeur M. C. COULET
IUT B	Directeur : M. le Professeur R. LAMARTINE
Institut de Science Financière et d'Assurances	Directeur : M. le Professeur J.C. AUGROS

NENCKI INSTITUTE OF EXPERIMENTAL BIOLOGY

Polish Academy of Sciences

Board of Directors

Director	Jerzy Duszyński
Deputy Director for Scientific Research	Urszula Sławińska
Deputy Director for Scientific Research	Hanna Fabczak
Deputy Director for Scientific Research	Adam Szewczyk
Administrative Director	Anna Jachner-Miśkiewicz

Scientific Departments and Laboratories

Department of Cell Biology	Katarzyna Kwiatkowska
Laboratory of Cell Membrane Physiology	Elżbieta Wyroba
Laboratory of Transcription Regulations	Bożena Kamińska-Kaczmarek
Laboratory of Physiology of Cell Movements	Stanisław Fabczak
Laboratory of Plasma Membrane Receptors	Andrzej Sobota
Laboratory of Regeneration and Morphogenesis of Protozoa	Maria Jerka-Dziadosz
Department of Biochemistry	Sławomir Pikuła
Laboratory of Biochemistry of Lipids	Sławomir Pikuła
Laboratory of Bioenergetics and Biomembranes	Jerzy Duszyński
Laboratory of Cell Signaling and Metabolic Disorders	Agnieszka Dobrzyń
Laboratory of Cellular Metabolism	Krzysztof Zabłocki
Laboratory of Comparative Enzymology	Wojciech Rode
Laboratory of Intracellular Ion Channels	Adam Szewczyk
Laboratory of Molecular Basis of Cell Motilty	Maria Jolanta Rędowicz
Laboratory of Motor Proteins	Andrzej A. Kasprzak
Laboratory of Molecular Bases of Aging	Ewa Sikora
Department of Molecular and Cellular Neurobiology	Jolanta Skangiel-Kramska
Laboratory of Bioinformatics and Systems Biology	Krzysztof Pawłowski
Laboratory of Calcium Binding Proteins	Anna Filipek
Laboratory of Epileptogenesis	Katarzyna Łukasiuk
Laboratory for Mechanisms of Transport Through Biomembranes	Katarzyna A. Nałęcz
Laboratory of Molecular Basis of Brain Plasticity	Jolanta Skangiel-Kramska
Laboratory of Molecular Neurobiology	Leszek Kaczmarek
Laboratory of Neurobiology of Development and Evolution	Krzysztof Turlejski
Laboratory of Neuroplasticity	Magorzata Kossut
Department of Neurophysiology	Andrzej Wróbel
Laboratory of Defensive Conditioned Reflexes	Tomasz Werka
Laboratory of Ethology	Ewa Joanna Godzińska
Laboratory of Limbic System	Stefan Kasicki
Laboratory of Molecular and Systemic Neuromorphology	Grzegorz Wilczyński
Interinstitute Laboratory of Neuromuscular Plasticity	Urszula Sławińska
Laboratory of Neuropsychology	Elżbieta Szeląg
Laboratory of Psychophysiology	Anna Grabowska
Laboratory of Reinnervation Processes	Julita Czarkowska-Bauch
Laboratory of Visual System	Andrzej Wróbel
Laboratory of Preclinical Studies in Neurodegenerative Diseases	Grażyna Niewiadomska
Supporting Units	
The Animal House	Anna Passini
Laboratory of Confocal Microscopy	Wanda Kłopocka
Laboratory of Electron Microscopy	Elżbieta Wyroba
Information Technology Unit	Mirosław Sikora

Acknowledgements

This thesis was prepared under the co-supervision of Professors René BUCHET and Slawomir PIKULA. I would like to thank them for their guidance, encouragement, and enthusiasm.

I wish to thank following people for their suggestions, discussions, teaching and technical help:

Laboratory of Biochemistry of Lipids (Warsaw):
Joanna BANDOROWICZ-PIKULA
Agnieszka STRZELECKA-KILISZEK
Aleksandra DABROWSKA
Aneta KIRILENKO
Karolina Maria GORECKA
Magdalena Malgorzata HAMCZYK
Marcin BALCERZAK
Michalina KOSIOREK
Paulina PODSZYWALOW-BARTNICKA
Anna SEKRECKA
Małgorzata Eliza SZTOLSZTENER
Tanuja TALUKDAR

Laboratory of Confocal Microscopy (Warsaw):
Artur WOLNY
Jarosław KORCZYNSKI
Wanda KLOPOCKA

Institute of Biochemistry and Biophysics (Warsaw):
Agata MALINOWSKA
Michal DADLEZ

Laboratory ODMB (Lyon):
Anne BRIOLAY
Françoise BESSON
Geraldine BECHKOFF
Jacqueline RADISSON
Jamel BOUZENZANA
Laurence BESUEILLE
Le ZHANG
Lina LI
Mélanie DELOMENEDE
Michèle BOSCH
Nicolas SINDT
Noëlle CALAS
Pierre BROQUET
Saida MEBAREK-ASSAM
Véronique ROCHE

University Lyon 1:
Françoise BLEICHER
John CAREW

Many thanks to the Members of the Jury: Françoise BLEICHER, Joanna BANDOROWICZ-PIKULA, Martine COHEN-SOLAL, René BUCHET, Slawomir PIKULA and Aleksander SIKORSKI.

To my parents, Marie-Do and François,
My sister, Adeline,
My brother, Gillian,
My family, my friends,

To my girlfriend, Karelle, and her son, Clément

CONTENTS

Abbreviations

AnxA	-vertebrate annexin
AA	-ascorbic acid
ADP	-adenosine diphosphate
AMP	-adenosine monophosphate
5'-AMPase	-5'-adenosine monophosphatase or 5'-nucleotidase
Arf	-ADP-ribosylation factor
AR-S	-Alizarin Red-S
ATP	-adenosine triphosphate
ATPase	-adenosine triphosphatase
BCIP	-bromo-chloro-indolyl phosphate
β-GP	-β-glycerophosphate
bis-*p*-NPP	-bis-*p*-nitrophenyl phosphate
CCD	-cytochalasin D
CHOL	-cholesterol
CPPD	-calcium pyrophosphate dihydrate
DAG	-diacylglycerols
ER	-endoplasmic reticulum
ESI	-electrospray ionization
FACS	-fluorescence activated cell sorter
FBS	-fetal bovine serum
FFA	-free fatty acids
FITC	-fluorescein isothiocyanate
FPR	-false positive rate

FTIR -Fourier transformed infrared spectroscopy

GPI -glycosylphosphatidylinositol

GTP -guanosine triphosphate

HA -hydroxyapatite

HBSS -Hank's balanced salt solution

K_M -Michaelis-Menten constant

K_i -Inhibition constant

MAG -monoacylglycerols

MMP -matrix metalloprotease

MS -mass spectrometry

MS/MS -tandem mass spectrometry

MVs -matrix vesicles

NBT -nitroblue tetrazolium

NPP1 -nucleoside triphosphate pyrophosphatase phosphodiesterase 1

PA -phosphatidic acid

PAGE -polyacrylamide gel electrophoresis

PBS -phosphate-buffered saline

PC -phosphatidylcholine

PDE -phosphodiesterase

PE -phosphatidylethanolamine

PHL -phalloidin

PI -phosphatidylinositol

PI-PLC -phosphatidylinositol specific phospholipase C

PME -phosphomonoesterase

pMV	-pellet of MVs treated by PI-PLC
p-NPP	-*p*-nitrophenyl phosphate
P_i	-inorganic phosphate
PP_i	-inorganic pyrophosphate
PS	-phosphatidylserine
SDS	-sodium dodecyl sulfate
SCL	-synthetic cartilage lymph
SDS	-sodium dodecyl sulfate
SLC_A_	-solute carrier family _ member _
SM	-sphingomyelin
sMV	-supernatant of MVs treated by PI-PLC
TAG	-triacylglycerols
TBS	-Tris-buffered saline
TTBS	-Tween Tris-buffered saline
TNAP	-tissue non-specific alkaline phosphatase
TRITC	-tetramethylrhodamine isothiocyanate
UTP	-uridine triphosphate
VDAC	-voltage-dependent anion channel

CHAPTER I

INTRODUCTION

1. Bone

Bone and cartilage are complex, dynamic and highly specialized forms of connective tissues that together make up the skeleton [1]. However, they are structurally and functionally different. Bone matrix is composed of an organic phase, containing mostly type-I collagen, providing tensile strength, and an inorganic phase, hydroxyapatite (HA), which gives it mechanical resistance [2]. Osteoclasts, osteoblasts and osteocytes are the three major cell types present in bone. Plasticity of the skeleton and its ability to adapt relies on continuous modeling and remodeling that require osteoclastic resorption of bone matrix and deposition of a new mineralized matrix by osteoblasts [3]. Osteocytes maintain the osseous matrix, participate in extracellular exchanges and are involved in the mechanotransduction [3].

2. Cartilage

On the other hand, articular cartilage matrix is mainly composed of type-II collagen and proteoglycans and is highly hydrated giving it elasticity and ability to deform. Therefore, cartilage matrix does not mineralize, except at the growth plates of long bones [3]. Chondrocytes are the only cell type present in cartilage. They maintain a stable non-hypertrophic phenotype at the sites of articular cartilage, do not proliferate and produce extracellular matrix components [4,5]. In contrast, non-hypertrophic chondrocytes undergo a series of differenciation in embryonic cartilage and growth plates: cell proliferation, maturation, hypertrophy, terminal differentiation and cell apoptosis [6,7]. Hypertrophic chondrocytes initiate and regulate the extracellular matrix mineralization in embryonic cartilage and growth plates which are the sites of endochondral ossification [8-11].

3. Mineralization

Physiological mineralization is a highly regulated process that takes place during the formation, development, remodeling and repair of skeletal tissues (Table 1) [12]. In prenatal and early postnatal life, skeletal tissues develop either by intramembranous ossification, where bone is formed within craniofacial fibrous tissue, or by endochondral bone formation, which leads to the replacement of the embryonic cartilaginous skeleton by the definitive bone skeleton [12]. Early postnatal endochondral ossification also occurs in the case of long bone growth from so-called growth plate cartilage. Then, throughout life, the mineralization process continues to play a crucial role in bone modeling, remodeling and repair [12]. Mineralization is tightly controlled both temporally and spatially by mineralization-competent cells [8].

Table 1. Sites of biomineralization.

	Period	Tissue	Ossification	Promineralizing cells
Craniofacial bone formation	Prenatal and early postnatal life	Craniofacial fibrous tissues	Intramembranous ossification	Osteoblasts
Skeletal bone formation	Fœtal life	Fœtal cartilaginous skeleton	Endochondral ossification	Hypertrophic chondrocytes
Long bone growth	Early postnatal life	Growth plate cartilages	Endochondral ossification	Hypertrophic chondrocytes
Bone remodeling and repairing	Throughout the life	Bones	Haversian ossification	Osteoblasts

4. Mineralization-competent cells

Chondrocytes and osteoblasts have a mesenchymal origin. Multipotent mesenchymal stem cells generate pluripotent progenitor cells that can differentiate into various cell types: adipocytes, fibroblasts, chondrocytes and pre-osteoblasts. In response to environmental factors, chondrocytes and pre-osteoblasts differentiate into hypertrophic chondrocytes and osteoblasts respectively [13]. These two cell types are mineralization-competent cells that regulate matrix calcification by modifying extracellular matrix composition and releasing matrix vesicles (MVs) [9,10]. The initiation of HA deposition is one of the most important events in mineralization and thus, subjected to intensive scrutiny. Several different mechanisms of HA deposition have been suggested. One mechanism involves non-collagenous extracellular matrix proteins that serve as nucleation sites [14], whereas another proposes that extracellular MVs accumulate Ca^{2+} and inorganic phosphate (P_i) leading to HA formation [15]. Metastable equilibrium of Ca^{2+} and P_i in extracellular matrix can also lead to mineral formation and can contribute to the growth of HA, released by MVs or initiated by the extracellular matrix protein or by both [16].

5. Matrix vesicles

MVs have been discovered for the first time by Anderson [17] and Bonucci [18] in cartilage and by Anderson and Reynolds [19]. These extracellular organelles (between one hundred to four hundred nanometers in diameter) are involved in the initial step of extracellular matrix calcification by promoting the deposition of HA, e.g. $Ca_{10}(PO_4)_6(OH)_2$ in their lumen [9,10,15,20]. Ion channels and transporters present in MV membrane act for Ca^{2+} [13,21,22] and P_i uptakes into these organelles [23-

27]. By accumulating Ca^{2+} and P_i, MVs create an optimal environment to induce the formation of HA (Fig. 1) [9-11]. Then, the breakdown of MV membrane releases HA crystals in the extracellular matrix where mineralization is propagated [9]. These crystals serve as a template for the formation of crystalline arrays, leading to a tissue calcification [10]. The extracellular matrix contains sufficiently high concentrations of Ca^{2+} and P_i concentrations to propagate the mineralization [10]. Negatively charged proteins of the matrix interact with minerals and thus, control their growth, orientation and size.

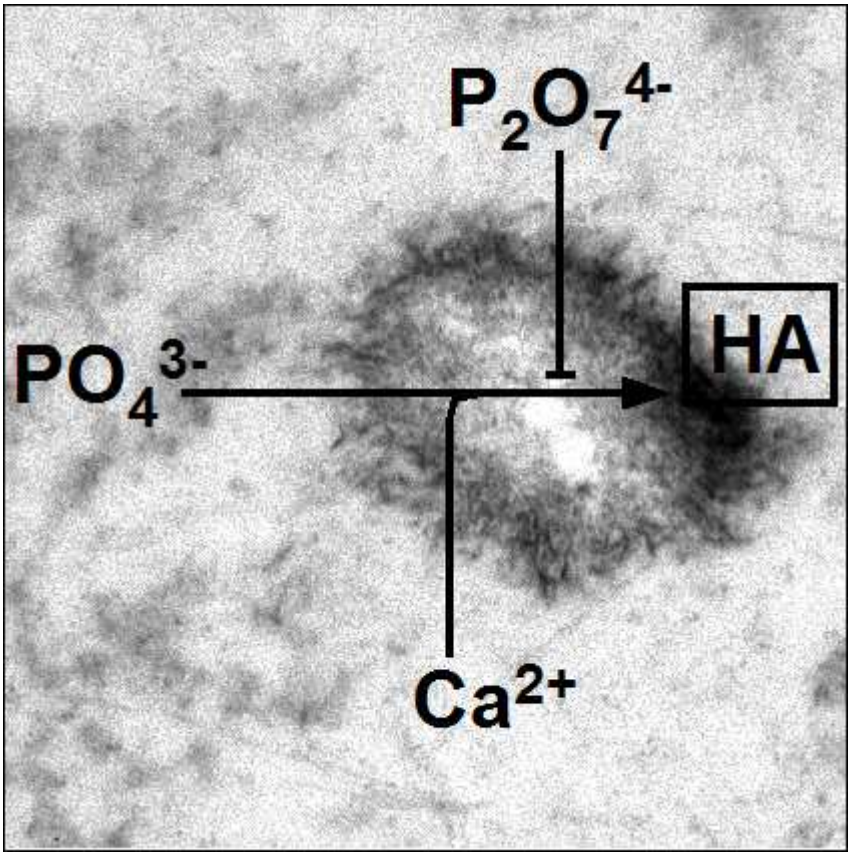

Figure 1. Electron micrograph of a calcifying matrix vesicle isolated from Saos-2 cell cultures. (Magnification, x 100,000).

6. Matrix vesicle biogenesis

It has been demonstrated that MVs derive from the plasma membrane of hypertrophic chondrocytes [28,29]. Four hypotheses have been proposed concerning the mechanisms of MV formation [28]. As areas of mineralization coincide with chondrocyte apoptosis in growth plate cartilages, it was suggested that MVs derive from the rearrangement of apoptotic cell membrane [30]. This was not confirmed by Kirsch et al. [31] who showed that MVs and apoptotic bodies are structurally and functionally different. Only mature osteoblasts mineralize their matrix, while only terminally differentiated growth-plate chondrocytes release MVs [32]. Electron microscopic

observations indicated that MVs could be formed by secretion of preformed cytoplasmic structures in the extracellular matrix [33,34]. The findings of Rabinovitch and Anderson [28] favored other hypotheses of subunit secretion followed by their extracellular assembly and, above all, the budding from cells. Then, Cecil and Anderson [35] confirmed this last hypothesis that MVs appear to bud from the tips of plasma membrane microvilli of hypertrophic chondrocytes (Fig. 2) [9]. Furthermore, MVs may arise from the membrane adjacent to newly formed extracellular matrix [36]. Cell surface microvilli of hypertrophic chondrocytes were found to be the precursors of MVs and the actin network appeared to be essential for their formation [37,38].

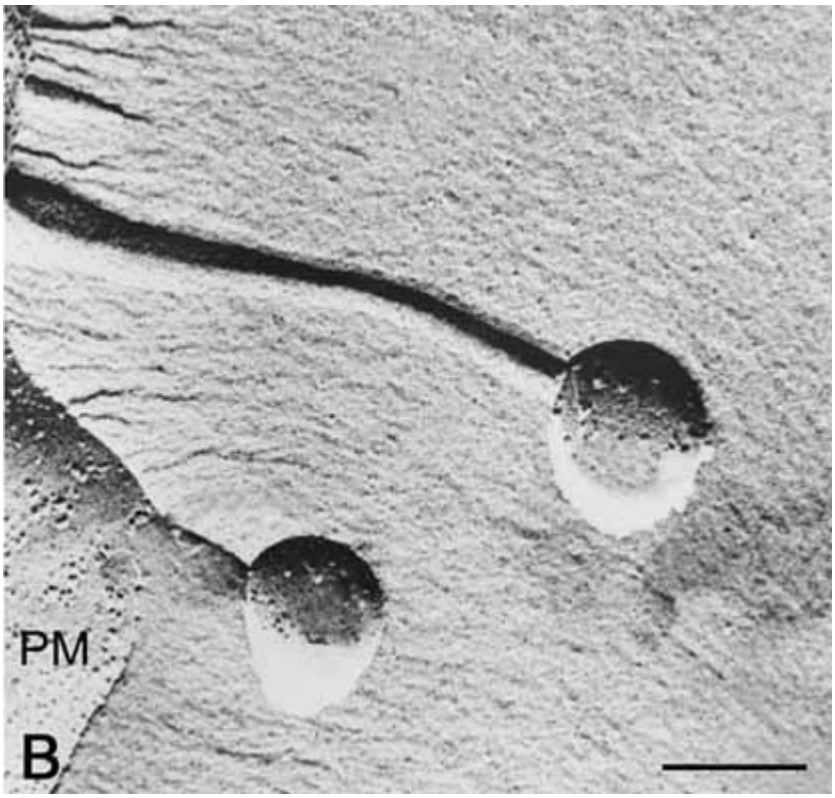

Figure 2. This freeze-fracture replica illustrates vesicles appearing to bud from the tips of hypertrophic chondrocyte plasma membrane microvilli [35]. PM, plasma membrane. (Magnification, x 47,000; bar: 200 nm).

7. Structure and functions of matrix vesicles

The proportion of free cholesterol and the cholesterol/phospholipid ratio is nearly twice as high in the MVs as in the chondrocyte plasma membrane [39]. MV membrane exhibits lower content in phosphatidylcholine (PC) and phosphatidylethanolamine (PE) and higher content in sphingomyelin (SM) and phosphatidylserine (PS) in comparison to plasma membrane [39]. High levels in cholesterol, SM and PS are characteristic of MV membrane [40]. It has been proposed that MV lipids may be involved in the control of normal mineralization in vivo [41].

Recently, the whole proteomes of MVs isolated from chicken embryo growth plate cartilage [42] and from pre-osteoblast MC3T3-E1 cell cultures [43] have been described. PHOSPHO1 [44], 5'-nucleotidase [45], ion-motive ATPases [45,46], tissue non-specific alkaline phosphatase (TNAP) [47,48] provide P_i from the hydrolysis of their respective substrate, while ectonucleotide pyrophosphatase phosphodiesterase 1 (NPP1) is responsible for the production of inorganic pyrophosphate (PP_i) [49], a potent inhibitor of HA growth [50]. NPP1 and TNAP have antagonistic effects on mineral formation due to their opposing activities [51-54]: either production of PP_i by NPP1 or its hydrolysis by TNAP. P_i transport into MVs may be performed by alkaline pH-specific P_i-transporter [23,24] or by sodium-dependent P_i transporter (a member of the type III Glvr-1gene family) [25-27].

Several annexins (AnxA1, AnxA2, AnxA4-A7 and AnxA11) have been identified in MVs. These proteins are involved in Ca^{2+} homeostasis by mediating Ca^{2+} influx into MVs [13,21,22]. Annexins exhibit Ca^{2+}-regulated phospholipid-binding properties [55] and thus, can interact with both outer and inner leaflets of MV membrane due to high Ca^{2+} concentration inside and outside MVs. Anionic phospholipids, including PS, are enriched in the inner leaflet of MV membranes [56] and serve with annexins as nucleation sites for mineral formation due to their Ca^{2+}-binding properties [57-59]. Annexins associated to the outer leaflet of MV membrane can interact with extracellular matrix proteins and anchor MVs. In chicken growth plate, types II and X collagens enhance Ca^{2+} influx into MVs by promoting activity of ion channels formed by annexins [21,22].

Extracellular matrix proteins such as collagens [21,22,60,61] and proteoglycans [62,63], interact with the external surface of MVs. These interactions between extracellular matrix components and MVs are necessary to control the mineral growth and its directional expansion [9,10]. Furthermore, several enzymes such as matrix metalloproteases (MMP-2, MMP-9, MMP-13) [64], proteoglycanases [65,66], carboxypeptidase M [42] and aminopeptidases [43] are present at the outer surface of MVs. They catalyze degradation of the extracellular matrix, hydrolyze mineralization inhibitory proteins and increase the access of MVs to extracellular ions. Numerous protein kinases and G proteins traditionally involved in signal transduction were detected in MVs [42,43,67]. Actin [68,69] as well as actinins, filamins, gelsolin and myristoylated alanine-rich C kinase substrate (MARCKS) [42,43] were major cytoskeletal proteins identified in MVs. Finally, phospholipase A2 [70], phospholipase D [71], lactate dehydrogenase [72], carbonic anhydrase II [73] have been detected in MVs.

8. Extracellular ATP

Extracellular nucleotides, such as ATP, seem to be crucial regulatory molecules in the mineralization [74]. Recent advances in the area of mineralization revealed a dual character of ATP,

i.e. (1) as a signaling molecule, ligand for purine and pyrimidine P2 receptors, involved in the differentiation and activation of bone forming and resorbing cells, osteoblasts, osteoclasts and chondrocytes, and (2) as a substrate and precursor of regulatory factors, e.g. P_i and PP_i, determining the type of mineral formed inside MVs at the initial steps of mineralization [75].

Among the main regulatory factors affecting mineralization are transforming growth factor-β, bone morphogenetic protein-2, all-trans retinoic acid, 1α,25-dihydroxyvitamin D3, 3,5,30-triiodi-L-thyronine and extracellular nucleotides (ATP, ADP and UTP) [74]. In skeletal tissues, osteoblasts [76,77] continuously release ATP in the extracellular environment. Several actors have been proposed for ATP release: vesicular release, conductive channels, connexin hemichannels or stretch-activated channels, or ABC transporters [78]. They also release ATP upon mechanical stimulation or in response to hypoxia, osmotic swelling and cell lysis. In resting HOBIT cells (a human osteoblast cell line), for example, the extracellular ATP concentration is 5 nmol/l, but can reach 20 nmol/l under hypotonic stimulation [79]. Chondrocytes can also release nucleotides, maintaining extracellular ATP at a concentration of 1–3 nmol/l [80-82].

Once released, extracellular nucleotides are metabolized by a variety of cell-surface-located enzymes (ecto-nucleotidases) that sequentially hydrolyze nucleoside 5'-triphosphates to their respective nucleoside 5'-di and 5'-monophosphates, nucleosides and P_i or PP_i, therefore regulating the extracellular nucleotide concentration under physiological conditions [82]. They were found to be potent Ca^{2+} mobilizing agents, substrates and/or modulators of tissue transglutaminases and ectoprotein kinases that modify matrix proteins, regulating crystal deposition or growth [82]. They also act on both ionotropic (P2X) and metabotropic (P2Y) plasma membrane receptors that are implicated in a variety of biological processes including cell growth, proliferation, differentiation, energy metabolism and tissue mineralization [74,83-86].

9. Regulation of osteoblast functions by extracellular ATP

In mineralization, signaling through P2 receptors is of particular importance for the regulation of osteoblastic proliferation (P2X5) and differentiation (with a shift from P2X to P2Y expression during differentiation in culture) [87], osteoclast differentiation (P2X7) [88], and survival (P2Y6) [89]. Activation of P2Y1 receptors on osteoblasts enhances expression of receptor activator of nuclear factor kB ligand leading indirectly to an increase in osteoclast formation and resorption. Signals produced were found to activate gap junctions and hemichannels, and resulted in the release of signaling molecules into the bone fluid: ATP, nitric oxide and prostaglandins [90].

Eight subtypes of P2Y ($P2Y_{1,2,4,6,11–14}$) and seven subtypes of P2X ($P2X_{1–7}$) receptors have been identified in mammals [91]. P2Y receptors have seven-transmembrane spanning regions, are coupled

to G-proteins [92], and are responsible for inositol triphosphate generation and Ca^{2+} release from intracellular stores. P2X receptors are ATP-gated cation channels related to *Caenorhabditis elegans* degenerins and mammalian amiloride-sensitive Na^{+} channels, expressed in nerve, muscle, bone, glands and the immune system. Their subunits consist of two transmembrane domains [86,91,93].

Strong evidence is provided that extracellular ATP, acting through multiple P2 receptors, may participate in the regulation of bone metabolism, by activating signaling cascades in osteoblasts such as extracellular signal-regulated kinase 1/2 and p38 mitogen-activated protein kinase pathways. This activation results in increased $[Ca^{2+}]_{in}$ from intracellular stores. Among the signaling pathways, Src kinases were shown to be key enzymes [87]. Extracellular ATP acts as a potent agent mediating cell-cell contacts [94], inducing apoptosis [95,96] and stimulating proliferation [97] of bone marrow mesenchymal stem cells, from where osteoblasts originate, whereas their homing is likely regulated by extracellular UTP [98]. Furthermore, it has been reported that P2Y receptor-mediated and gap junction mediated mechanisms of intracellular calcium signaling play different roles during differentiation of bone-forming cells [99]. Concerning the role of osteoblast P2X receptors (Fig. 3), the function of P2X2 receptors is not yet established, although their expression in these cells has been reported. P2X5 receptors were found to stimulate proliferation and/or differentiation of preosteoblasts [74]. P2X7 receptors were reported to mediate blebbing in osteoblasts in response to ATP, mechanical or inflammatory stimuli. These receptors are coupled to the activation of phospholipases D and A2 leading to the production of lysophosphatidic acid. It is suggested that this pathway may contribute to osteogenesis during skeletal development and mechanotransduction [91]. The osteoblast responses to nucleotides increase during differentiation [84]. In addition to P2 receptors, it has been shown that human osteoprogenitor cells produce extracellular adenosine and express all four types of P1 receptors that are activated by adenosine. Adenosine is therefore suggested to be an important regulator of differentiation of osteoblast precursor cells and significantly contribute to the regulation of bone formation and resorption [100].

10. Regulation of osteoclast functions by extracellular ATP

The second type of bone cells where nucleotides can interact are osteoclasts which resorb bone extracellularly. They are multinucleated cells formed by the proliferation of hematopoietic, mononuclear progenitors of the monocyte and macrophage lineage, and their subsequent fusion into multinucleated osteoclasts. The process is regulated by macrophage colony-stimulating factor and receptor activator of nuclear factor κB ligand [74,101-103]. Bone resorption begins with the migration of osteoclasts to the site of resorption, their attachment to the bone, their polarization, and the formation of a sealed extracellular vacuole into which H^{+} and hydrolyzing enzymes (cathepsin K) are secreted by osteoclasts to dissolve bone mineral and degrade the collagenous organic matrix [90,103].

Osteoclasts also secrete L-glutamate and the bone degradation products upon stimulation with ATP in a Ca^{2+}-dependent manner [102]. This seems of particular importance since glutamate signaling is suggested to play a significant role in bone homeostasis. In addition, it has been shown that targeted disruption of the c-Src tyrosine kinase-encoding gene impairs osteoclast bone resorbing activity and leads to osteopetrosis. This suggests that c-Src kinase activity, not only on the plasma membrane but also on the mitochondria, is essential for the regulation of osteoclastic bone resorption [101] and may be a target of rational drug design [104]. The regulation of activity of osteoclasts, which develop from cell precursors, fusion, activation and functions is triggered by P2 receptors, e.g. P2X2, P2X4, P2X5, P2X7 and P2Y1 [74]. It must be stressed, however, that bone resorption may indirectly be regulated by ADP via the P2Y1 receptors residing on osteoblasts. Moreover, UTP and ATP, via P2Y2 receptors, inhibit the bone formation catalyzed by osteoblasts.

11. Regulation of chondrocyte functions by extracellular ATP

Another tissue extremely active in the mineralization process is cartilage. It is built up by chondrocytes which exist in the organism at various levels of development and differentiation from progenitor to hypertrophic cells. Chondrocytes, just like osteoblasts/osteocytes, are affected by mechanical forces that are remodeling the cartilage extracellular matrix. These forces induce time-dependent expression of certain genes in chondrocytes regulated by $[Ca^{2+}]_{in}$ and cAMP [105]. Mechanically induced calcium waves were observed in chondrocytes, related to stimulation of P2Y receptors and concomitant release of Ca^{2+} from internal stores, triggering further release of ATP from adjacent cells [106]. Activation of P2X receptors may also enable Na^{+} influx triggering membrane depolarization and activation of voltage-operated Ca^{2+} channels as reported in chondrocytes in monolayer subjected to substrate deformation [107].

Chondrocytes also express P2X2, P2X5, P2Y1 and P2Y2 receptors (Fig. 3). The role of P2 receptors in the production of prostaglandins has been suggested. It has been shown that ATP and ADP, and less strongly UTP, stimulate the production of prostaglandin E by cultured human chondrocytes, which was enhanced by the proinflammatory cytokines interleukin-1β, interleukin-1α and tumor necrosis factor-α. Additionally, extracellular ATP and UTP, but not ADP, have been shown to stimulate cartilage resorption; again, this was enhanced by simultaneous application of interleukin-1β and tumor necrosis factor-α. The overall function of chondrocytes (especially articular chondrocytes) is also regulated by intracellular pH and external O_2 tension [108], and mechanical stimuli [105]. It has been shown *in vitro* that the inhibition of various channels alters chondrocyte mechanotransduction [109]. Some of these channels, as recently identified in articular chondrocyte ATP-sensitive potassium channels, are of particular importance since they are involved in coupling metabolic and electrical activities in chondrocytes and in the metabolic regulation [110].

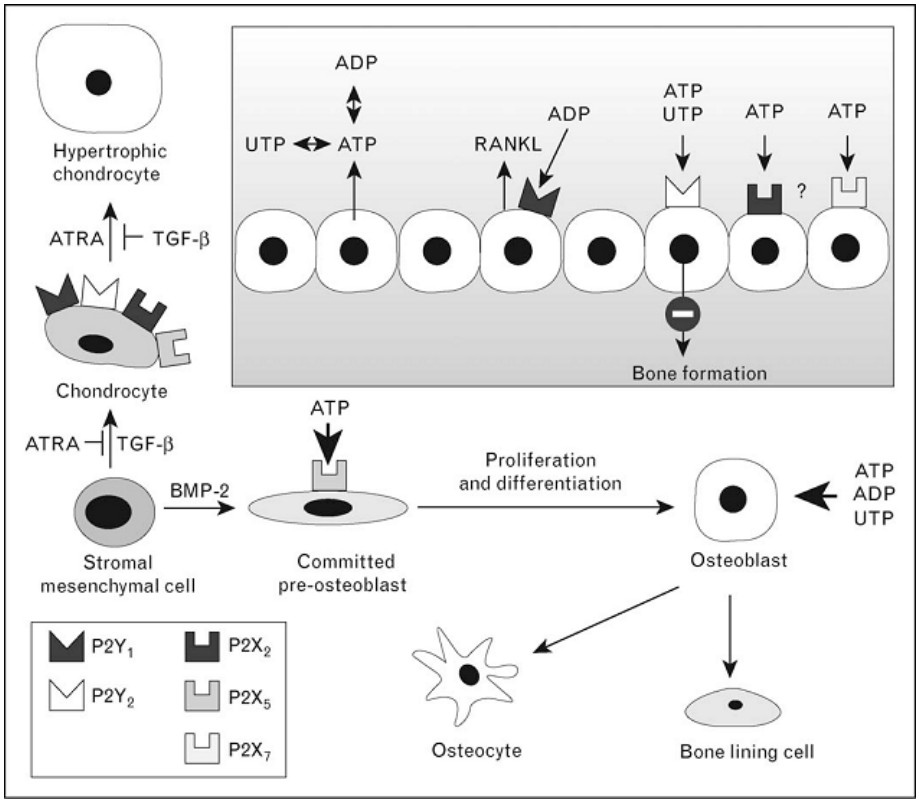

Figure 3. Extracellular ATP acting via P2 receptors as a potent mediator of differentiation and metabolism of mineralizationcompetent cells: osteoblasts and chondrocytes.

Pluripotent stem cells are progenitors of fibroblasts, adipocytes, osteoblasts and chondrocytes. Their fate is regulated by various physiological factors: transforming growth factor (TGF)-β, bone morphogenetic protein (BMP)-2, all-trans retinoic acid (ATRA), 1α,25-dihydroxyvitamin D3, 3,5,30-triiodi-Lthyronine and ATP. ATP is constitutively released by the osteoblast monolayer on the surface of growing bone tissue subjected to shear stress. Then, ATP could be transformed to ADP or to UTP by ecto-nucleotidases. All these nucleotides may then affect, through their specific P2 receptors, the differentiation, metabolism and function of all cell types engaged in the mineralization process, e.g. chondrocytes (characterized by two phenotypes, i.e. non hypertrophic characteristic for articular cartilage and hypertrophic in growth plate) and osteoblasts (as well as deriving from osteoblasts bone lining cells and osteocytes residing within bone matrix). The third important cell lineage, i.e. osteoclasts, playing a role in bone resorption, whose development from cell precursors, fusion, activation and functions is also regulated by P2 receptors, e.g. P2X2, P2X4, P2X5, P2X7 and P2Y1, is not shown. It must be stressed that bone resorption may be indirectly regulated by ADP via the P2Y1 receptors residing on osteoblasts. On the other hand, UTP and ATP, via P2Y2 receptors, inhibit bone formation catalyzed by osteoblasts. The role of P2X2 receptors on the functioning of osteoblasts is not yet established; however, their expression was reported. P2X5 receptors were found to augment proliferation and/or differentiation of preosteoblasts. P2X7 receptors mediate blebbing in osteoblasts in response to ATP, mechanical or inflammatory stimuli. These receptors are coupled to activation of phospholipases D and A2, which leads to the production of lysophosphatidic acid. It is suggested that this pathway may contribute to osteogenesis during skeletal development and mechanotransduction. P2X2, P2X5, P2Y1 and P2Y2 receptors were identified in chondrocytes, and their role in the production of prostaglandins has been suggested. Other explanations are in the text. RANKL, receptor activator of nuclear factor κB ligand. Adapted from [74].

12. ATP as a prerequisite of mineral formation by matrix vesicles

Due to the physiological role of extracellular ATP in bone formation and remodeling, and its persisting presence in the calcification environment, ATP is expected to be one of the main sources of both P_i and PP_i during the initial steps of mineralization occurring in MVs; both compounds having opposite roles in bone formation and remodeling.

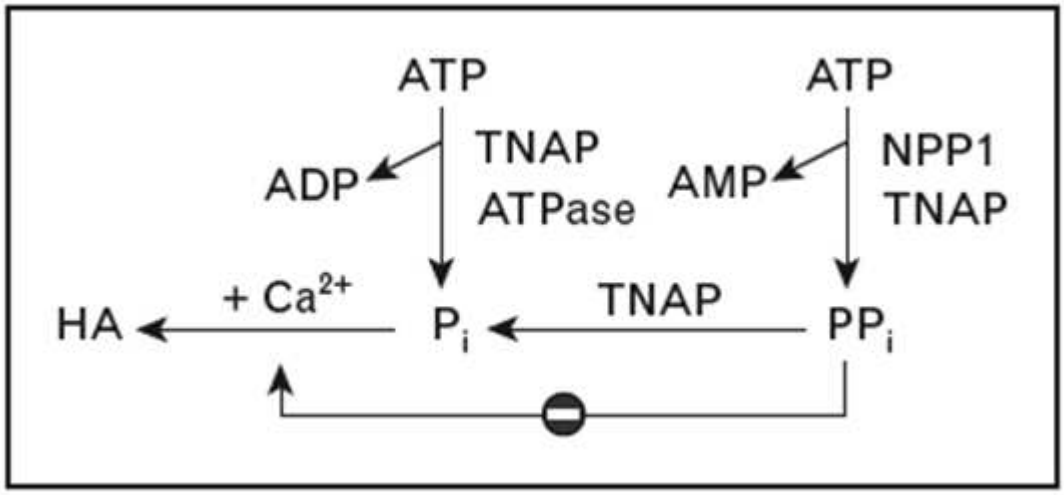

Figure 4. Antagonistic effects of pyrophosphate (PP_i) and inorganic phosphate (P_i) on the mineralization process occurring in matrix vesicles released by competent mineralization cells.

A substrate of mineralization, P_i, arises from distinct sources, including the hydrolytic activity of tissue nonspecific alkaline phosphatase (TNAP) and various ATPases present in matrix vesicles. Accumulation of P_i and Ca^{2+} inside matrix vesicles is a prerequisite for the formation of hydroxyapatite (HA). PP_i, the inhibitor of hydroxyapatite formation, is produced at least partly by nucleotide triphosphate pyrophosphatase phosphodiesterase 1 (NPP1). PP_i is then hydrolyzed by TNAP which speeds up the formation of hydroxyapatite. Under certain conditions, however, TNAP may also produce PP_i from ATP [111]. The interrelationship between ATP generating systems and ATP-consuming processes leading to the changes in intracellular ATP concentration (some of them leading to ATP depletion) underlines the importance of adenosine nucleotide homeostasis for the functioning of cells active in the mineralization process. The changes in ATP concentration are likely to be propagated by various effector proteins leading to specific functional responses. Adapted from [111].

MVs are markedly enriched in TNAP, the enzyme providing P_i from various phosphorylated substrates for hydroxyapatite crystallization and to hydrolyze PP_i, a potent inhibitor of mineralization (Fig. 4) [111]. In addition to TNAP, another enzyme of opposite function, NPP1, is present in MVs. NPP1 exhibits a broad substrate specificity and is able to catalyze the reactions involving phosphate diesters. In addition, several kinases have been identified in MVs, including protein kinase C isoforms that also require ATP for their activity [42,43]. It is worth noting that among phospholipases present in

MVs, such as phospholipase A2 [70], the activity of phospholipase D may be regulated by phosphorylation [71].

Changing the source of P_i can modulate the rate of mineralization and the quality of mineral formed [75]. Hydrolysis of monophosphoester substrates, like glucose-6-phosphate, AMP or phosphocholine (substrates for TNAP, 5'-nucleotidase and PHOSPHO1), yields P_i leading to the formation of mature crystalline mineral, while the hydrolysis of ATP by NPP1 and possibly by TNAP inhibits the formation of hydroxyapatite due to the production of PP_i. Since phosphodiesterase activity of NPP1 and also of TNAP towards ATP has a high impact on MV-mediated mineralization, nucleotides can affect mineral formation as well [111].

MVs are organelles whose membrane reflects the same orientation as plasma membranes with the glycosylphosphatidylinisotol-anchored TNAP pointing towards the extracellular matrix while the catalytic domains of ATPases are directed into the lumen of MVs [112]. Thus, ATP can be hydrolyzed outside MVs by TNAP and NPP1, but by ATPases inside MVs. The mechanism of the transport of the nucleotide and/or products of its hydrolysis from the extracellular matrix to the interior of MVs has, however, not yet been described. It can be speculated that transport of ATP and related compounds (PP_i) to the MV lumen could occur through a voltage-dependent anion channel (VDAC) [113], on the basis of observation that a VDAC is responsible for ATP translocation into the lumen of sarcoplasmic reticulum [114]; a VDAC has been shown to be present in MVs [42,43]. In line with this hypothesis is the identification of a VDAC in the extramitochondrial compartment, including endoplasmic reticulum and plasma membrane [114]. Analysis of human osteoblast membrane proteins revealed the presence of two VDAC isoforms, VDAC 1 and 2 [115]. Due to the presence of numerous extracellular nucleotide hydrolases, however, VDAC may rather transport products of ATP hydrolysis. Current information on the effect of ATP on MV-mediated mineralization concerns mainly the generation of PP_i [75,111].

13. Pathological calcification in osteoarthritis

The regulation of physiological mineralization is mediated at cellular and tissue levels, and requires coordination between stimulatory and inhibitory factors [116]. Indeed, changes in the mineralization can have serious ramifications. Pathological mineralization may be due to an unbalance between pro- and anti-mineralization regulatory components and molecules. For example, articular cartilage calcification leads to joint inflammation and the progression of osteoarthritis.

Osteoarthritis is a common age-related joint disease characterized by a degradation of the proteoglycan and collagen matrix [117]. Articular chondrocytes maintain a stable phenotype throughout life. However, they lose their phenotype in osteoarthritic cartilage and undergo terminal

differentiation similar to that in growth plate cartilages [116]. Osteoarthitic articular chondrocytes express proteins usually restricted to the sites of bone formation: annexins, TNAP, type-I and type-X collagen (markers of osteoblasts and hypertrophic chondrocytes respectively), osteonectin, osteocalcin, bone morphogenetic proteins (which induce new bone formation) and RUNX2 (a transcription factor regulating hypertrophic chondrocyte differentiation) [118-120]. Moreover, these cells release MVs [122-124], which are responsible for the initial formation of basic calcium phosphate (BCP) [122-124] or calcium pyrophosphate dihydrate (CPPD) minerals [125-128] in degenerative joints. Several factors can stimulate terminal differentiation of articular chondrocytes such as a loss of transforming growth factor β [129] or the presence of interleukine 8 [130]. It has been demonstrated that an excessive deposition of BCP crystals in joints alters gene expression of MMPs and catabolic cytokines [131], and stimulate articular chondrocyte apoptosis [132], resulting in accelerated cartilage degradation. Overexpression of AnxA5 leads to the terminal differentiation of chondrocytes and finally their apoptosis [118,132], suggesting that this protein play an important role in terminal differentiation of osteoarthritic chondrocytes. NPP1 and ANK (a transmembrane PP_i exporter present in chondrocyte plasma membrane) are overexpressed in osteoarthritic joints leading to accumulation of PP_i and CPPD formation. Although the role of these crystals in osteoarthritis is not fully understood, there is evidence suggesting that these crystals take a share in joint damage.

CHAPTER II

AIMS

1. Regulatory effect of PP_i on mineralization.

Physiological mineralization is a process restricted to skeletal tissues and regulated by a subtle coordination between stimulatory and inhibitory factors. However, ectopic pathological calcification can occur in any soft tissues and may be due to an unbalance between pro- and anti-mineralization molecules. For example, in calcifying osteoarthritic joints, articular chondrocytes lose their stable phenotype and undergo a series of differentiation to generate terminally differentiated hypertrophic chondrocytes usually present in sites of endochondral bone formation. These cells become able to release MVs structurally and functionally similar to those present in embryonic and growth plate cartilages. It has been suggested that a balance between levels of P_i and PP_i is required for physiological mineralization. Therefore, to test the hypothesis that $[P_i]/[PP_i]$ ratio could be a determinant factor regulating pathological calcification or its inhibition, we created a pathological model of mineralization involving MVs isolated from 17-day-old chicken embryo growth plates. MVs were incubated in a synthetic cartilage lymph (SCL) mimicking extracellular cartilage fluid in the presence of Ca^{2+} and different phosphate substrates. The effects of phosphate substrates (P_i, AMP, ATP, PP_i) as well as the effects of $[P_i]/[PP_i]$ ratios on the MV-mediated mineralization were determined. In this respect, enzymatic activity assays, turbidimetry measurements and infrared spectroscopy were conducted to determine MV phosphomonoesterase, phosphodiesterase, pyrophosphatase activities, kinetic parameters of mineralization and the nature of minerals formed. The mains findings of the regulating effect of PPi on mineralization are presented in chapter 1 of the Result Part.

2. Origin, biogenesis and functions of matrix vesicles.

Since their discovery in 1967, MVs were subjected to intensive investigations. Although MVs exhibit similar structural and functional properties, they differ from a tissue to another or from species to another. Differences between their proteome can underline a new mechanism (functions, regulations, formation). Despite growing knowledge about the structures and the functions of MVs, little is known regarding their biogenesis, especially from osteoblasts. It has been demonstrated that growth plate MVs are released from chondrocyte microvilli and that actin microfilaments may be involved in MV formation. Human osteosarcoma Saos-2 cells express the entire osteoblastic differentiation sequence from proliferation to mineralization and spontaneously release mineralization-competent MVs. Thus, we selected osteoblast-like Saos-2 cells to analyze the mechanisms involved in the release of MVs into the extracellular matrix. To verify the hypothesis that microvilli are the precursors of MVs, microvilli from apical Saos-2 cell plasma membrane were purified and two different approaches were used to determine the origin, biogenesis and functions of MVs. Firstly, the morphological and biochemical properties (protein profiles, lipid compositions, ability to mineralize)

of microvilli were compared with those of MVs. The role of actin network in MV formation was investigated by employing two drugs which affect microfilament polymerization and depolymerization and monitoring MV release. The overall findings were presented in Chapter 2 of the Result Part. Secondly, a proteomic analysis was performed on both MVs and microvilli. Their proteomes were compared and interpreted to identify an *in vivo* mechanism of MV biogenesis. An overview of the different class of proteins, their functions during mineral formation, as well as the presence of protein markers for lipid rafts, microvilli and MVs are presented and discussed in Chapter 3 of the Result Part.

CHAPTER III

METHODS AND RESULTS

Inorganic Pyrophosphate as a Regulator of Hydroxyapatite or Calcium Pyrophosphate Dihydrate Mineral Deposition by Matrix Vesicles

[1,2]Cyril Thouverey, [2]Géraldine Bechkoff, [1]Sławomir Pikuła and [2]René Buchet

[1]Department of Biochemistry, Nencki Institute of Experimental Biology, Polish Academy of Sciences, PL-02093 Warsaw, Poland.

[2]Université de Lyon, Lyon, F-69003, France ; Université Lyon 1, Villeurbanne, F-69622, France ; INSA-Lyon, Villeurbanne, F-69622, France; CPE Lyon, Villeurbanne, F-69616, France; ICBMS CNRS UMR 5246, Villeurbanne, F-69622, France.

Running title: Regulatory effect of PP_i on mineralization

*Keywords***:** Alkaline phosphatase, calcium pyrophosphate dihydrate, cartilage, hydroxyapatite, mineralization, osteoarthritis, pyrophosphate.

*Abbreviations***:** AnxA2-6, vertebrate annexin 2-6; AMP, adenosine monophosphate; 5'AMPase, 5' adenosine monophosphatase; ATP, adenosine triphosphate; ATPase, adenosine triphosphatase; BCIP, bromo-chloro-indolyl phosphate; bis-*p*-NPP, bis-*p*-nitrophenyl phosphate; CPPD, calcium pyrophosphate dihydrate; GPI, glycosylphosphatidylinositol; HA, hydroxyapatite; MVs, matrix vesicles; NBT, nitroblue tetrazolium; NPP1, nucleoside triphosphate pyrophosphatase phosphodiesterase 1; PAGE, polyacrylamide gel electrophoresis; PDE, phosphodiesterase; PI-PLC, phosphatidylinositol specific phospholipase C; PME, phosphomonoesterase; pMV, pellet of MVs treated by PI-PLC; *p*-NPP, *p*-nitrophenyl phosphate; P_i, inorganic phosphate, PP_i, inorganic pyrophosphate; SDS, sodium dodecyl sulfate; SCL, synthetic cartilage lymph; sMV, supernatant of MVs treated by PI-PLC; TNAP, tissue non-specific alkaline phosphatase.

ABSTRACT

Objective: Pathological mineralization is induced by an unbalance between pro- and anti-mineralization factors. In calcifying osteoarthritic joints, articular chondrocytes undergo terminal differentiation similar to that in growth plate cartilage and release MVs responsible for hydroxyapatite (HA) or calcium pyrophosphate dihydrate (CPPD) deposition. Inorganic pyrophosphate (PP_i) is a likely source of inorganic phosphate (P_i) to sustain HA formation when hydrolyzed but is also a potent inhibitor preventing apatite mineral deposition and growth. Moreover, an excess of PP_i can lead to CPPD formation, a marker of pathological calcification in osteoarthritic joints. It has been suggested that the P_i/PP_i ratio during biomineralization is a turning point between physiological and pathological mineralization. The aim of this work was to determine the conditions favoring either HA or CPPD formation initiated by MVs.

Methods: MVs were isolated from 17-day-old chicken embryo growth plate cartilages and subjected to mineralization in the presence of various P_i/PP_i ratios. The mineralization kinetics and the chemical composition of minerals were determined by light scattering and infrared spectroscopy, respectively.

Results: The formation of HA is optimal when the P_i/PP_i molar ratio is above 140, but is completely inhibited when the ratio decreases below 70. The retardation of any mineral formation is maximal at P_i/PP_i ratio around 30. CPPD is exclusively produced by MVs when the ratio is below 6, but it is inhibited for the ratio exceeding 25.

Conclusions: Our findings are consistent with the P_i/PP_i ratio being a determinant factor leading to pathological mineralization or its inhibition.

INTRODUCTION

Physiological mineralization takes place during the formation and the development of mineralized tissues, e.g. bones and teeth [1-3]. In the prenatal and early postnatal life, biomineralization is the last essential event in the endochondral and intramembranous bone formation leading to the replacement of cartilaginous skeleton and craniofacial fibrous tissue by the definitive bone skeleton. Throughout life, the mineralization process continues to play a crucial role in bone remodeling and repair. The regulation of physiological mineralization is mediated at molecular, cellular and tissue levels [4] and involves coordination between stimulatory and inhibitory factors [3-6]. However, uncontrolled or pathological mineralization, due to an unbalance between pro- and anti-mineralization factors [3-6], can occur during ageing, degenerative joint diseases, or genetic and various metabolic disorders. This causes an excessive mineral deposition in articular cartilages [7,8] that leads to joint inflammation and the progression of osteoarthritis. Several calcified diseases are characterized by the deposit of calcium pyrophosphate dihydrate (CPPD) or of hydroxyapatite (HA) in degenerative joints [3-10].

During endochondral ossification, chondrocytes undergo a series of differentiation: cell proliferation, hypertrophy, terminal differentiation and cell apoptosis [11-14]. Hypertrophic chondrocytes initiate mineralization by releasing matrix vesicles (MVs) [14-16]. MVs are involved in the initial step of mineralization by promoting the formation of HA in their lumen [17]. Preformed HA crystals are released from MVs into the extracellular matrix, so that HA crystals continue to grow [6]. In contrast, chondrocytes in healthy articular cartilage maintain a stable phenotype [13] and their released MVs are unable to calcify [6]. These chondrocytes do not proliferate but produce extracellular matrix components such as chondroitin-4-sulfate, chondroitin-6-sulfate, keratansulfate, as well as types II, III, VI, IX and XI collagen [18].

Osteoarthritis is characterized by a degradation of the proteoglycan and collagen matrix [19] as well as articular chondrocytes undergoing terminal differentiation similar to that in growth plate cartilage [3]. Osteoarthritic articular chondrocytes release MVs [20-23], which are responsible for the initial formation of HA [20-23] or CPPD minerals [8,9,24,25] in degenerative joints. MVs from osteoarthritic cartilage have a protein machinery similar to that of MVs from growth plate cartilage, necessary for Ca^{2+} uptake into MV lumen: annexin A2 (AnxA2), AnxA5 and AnxA6 [26], as well as for P_i homeostasis: tissue non-specific alkaline phosphatase (TNAP) [27,28], 5'AMPase [28], ion-motive ATPases [28], and nucleotide pyrophosphatase/phosphodiesterase-1 (NPP1) [8,9,29]. In addition to these proteins, osteoarthitic articular chondrocytes express type X collagen (a marker of hypertrophic chondrocytes), osteonectin, bone morphogenetic proteins (which induce new bone formation) and RUNX2 (a transcription factor regulating hypertrophic chondrocyte differentiation) [26,30-32].

At enzymatic and molecular levels, NPP1 and TNAP have antagonistic effects [33-36] on mineral formation due to their opposing activities: production of PP_i by NPP1 or its hydrolysis by TNAP. TNAP provides P_i from various phosphate substrates during mineralization [37,38], whereas NPP1, and possibly TNAP [39], supplies PP_i from ATP or UTP hydrolysis. At low concentrations, PP_i prevents the seeding of calcium phosphate minerals [40-44], while an excessive accumulation of PP_i in cartilage matrix leads to deposits of pathologic CPPD crystals, e.g. $Ca_2P_2O_7$ x 2 H_2O [45-47]. ANK, a transmembrane protein that transports intracellular PP_i to the extracellular matrix [48-50], and NPP1, are overexpressed in chondrocytes of osteoarthritic articular cartilage, contributing to increase PP_i, where CPPD crystal formation occurs [29-51-53].

P_i/PP_i ratio could be a turning point to discern between physiological and pathological mineralization and therefore is subjected to tight regulation [37]. Since osteoarthritic MVs and growth plate MVs exhibit similar structural and functional properties, we selected MVs isolated from chick embryo growth plate cartilage to investigate their role in the regulating effect of the P_i/PP_i ratio on HA and CPPD mineral depositions.

MATERIALS AND METHODS

Purification of Matrix Vesicles

MVs were isolated from growth plate and epiphyseal cartilage slices of 17-day-old chicken embryos by collagenase digestion [54], with slight modifications [55]. 17-day-old chicken embryo leg bones were cut into 1-3-mm thick slices and washed 5 times in a synthetic cartilage lymph (SCL) containing 100 mM NaCl, 12.7 mM KCl, 0.57 mM $MgCl_2$, 1.83 mM $NaHCO_3$, 0.57 mM Na_2SO_4, 1.42 mM NaH_2PO_4, 5.55 mM D-glucose, 63.5 mM sucrose and 16.5 mM TES (pH 7.4). Growth plate and epiphyseal cartilage slices were digested at 37 °C for 3.5 – 4 hours in the SCL buffer with 1 mM Ca^{2+} and collagenase (500 units/g of tissue, type IA, Sigma). It was vortexed and filtered through a nylon membrane. The suspension was centrifuged at 600 x *g* for 10 min to pellet intact hypertrophic chondrocytes. The supernatant was centrifuged at 13,000 x *g* for 20 min. The pellet was discarded and the supernatant was submitted to a third centrifugation at 70,000 x *g* for 1 hour. The final pellet containing MVs was suspended in 300 µL of SCL buffer and stored at 4 °C. The protein concentration in the MV fraction was determined using the Bradford assay kit (Bio-Rad). Proteins of MVs were separated in 7.5 or 10 % (w/v) SDS-polyacrylamide gels [56]. The gels were stained with Coomassie Brilliant Blue R-250.

Transmission electron microscopy

A 20 µL aliquot of MV fraction was transferred to carbon-coated grids. The grids were negatively stained with 2 % uranyl acetate and dried. The grids were viewed with an electron microscope Philips CM140 at 80 kV accelerating voltage.

Treatment of MVs by Phosphatidylinositol Specific Phospholipase C

MVs (1 µg of MV proteins/µL) were incubated in SCL with 10 mM Mg^{2+}, 5 µM Zn^{2+} and 1 unit of phosphatidylinositol specific phospholipase C (PI-PLC) per mL for 7 hours at 37 °C under gentle agitation. The supernatant (sMV) containing MV GPI-anchored proteins and the pellet (pMV) were separated by centrifugation at 90,000 x *g* for 30 min. The pMV was resuspended in the same volume of SCL as before the centrifugation.

Immunodetection of Chicken Caveolin-1

Proteins of MVs were separated in 12 % (w/v) SDS-polyacrylamide gels [56] and then electro-transferred (Mini-ProteanII™ Kit, Bio-Rad) onto nitrocellulose membranes (Hybond™-ECL™, Amersham Biosciences) [57]. The nitrocellulose membranes were blocked with 5 % (w/v) milk in a buffer (20 mM Tris-HCl, pH 7.5, 150 mM NaCl) for 1 hour at room temperature, then incubated with 3 % (w/v) milk and 0.1 % (v/v) mouse monoclonal IgG against chicken caveolin-1 (BD Biosciences) in TTBS buffer (20 mM Tris-HCl, pH 7.5, 150 mM NaCl, 0.05 % (v/v) Tween 20) at 4 °C overnight. The nitrocellulose membranes were washed several times with TTBS and incubated with 3 % (w/v) milk and 0.05 % (v/v) goat anti-mouse IgG conjugated with alkaline phosphatase (Immuno-Blot Assay Kit, Bio-Rad) in TTBS buffer. The membranes were washed, and bands were visualized by addition of color-developing solution according to the manufacturer's instructions.

Specific Revelation of Alkaline Phosphatase

MV proteins were incubated under mild denaturing conditions (without heating before the gel migration) in the Tris buffer containing 2 % SDS but no β-mercaptoethanol to preserve the TNAP activity. After the migration, SDS-polyacrylamide gels were incubated in a solution containing 0.1 M Tris-HCl (pH 9.6), 0.1 M NaCl, 5 mM $MgCl_2$, 0.24 mM bromo-chloro-indolyl phosphate (BCIP), a TNAP substrate and 0.25 mM nitroblue tetrazolium (NBT) until the blue band associated with alkaline phosphatase was visible [39].

Enzymatic Assays

The phosphomonoesterase (PME) activity was measured at pH 7.4 or 10.4, using 10 mM *p*-nitrophenyl phosphate (*p*-NPP) as a substrate [58], in 25 mM piperazine and 25 mM glycylglycine buffer, by monitoring the release of *p*-nitrophenolate at 420 nm (ε = 9.2 cm^{-1} mM^{-1} at pH 7.4; ε = 18.5 cm^{-1} mM^{-1} at pH 10.4, M^{-1}). One unit of PME activity corresponds to the amount of enzyme hydrolyzing 1 µmol of *p*-NPP per min at 37 °C. The phosphodiesterase (PDE) activity of MVs was measured at pH 7.4 or at 9, with 2 mM bis-*p*-nitrophenyl phosphate (bis-*p*-NPP) as substrate in 25 mM piperazine and 25 mM glycylglycine buffer, and monitoring the release of *p*-nitrophenolate at 420 nm (ε = 9.2 cm^{-1} mM^{-1} at pH 7.4; ε= 17.8 cm^{-1} mM^{-1} at pH 9) [39]. One unit of PDE activity corresponds to the amount of enzymes hydrolyzing 1 µmol of bis-*p*-NPP per min at 37 °C. To determine the pyrophosphatase activity, MVs were incubated in 25 mM piperazine and 25 mM glycylglycine buffer (at the indicated pH) containing 0.25 mM to 2 mM PP_i, for 20 min at 37 °C. The reaction was stopped by adding 10 mM levamisole and stored at 4 °C. Aliquots of the reaction mixture were collected to

determine PP_i concentrations with the Sigma reagent kit. One unit of pyrophosphatase activity corresponds to the amount of enzymes hydrolyzing 1 µmol of PP_i per min at 37 °C.

Determination of Mineralization Kinetics

Aliquots of the MV stock solution were diluted to a final concentration of 20 µg of MV proteins/mL in the SCL buffer containing 2 mM Ca^{2+} and different concentrations of ions (P_i, PP_i) or phosphate substrates (AMP, ATP), as indicated in the figure legends. They were incubated at 37 °C and their absorbances at 340 nm were measured at 15-min intervals with Uvikon spectrophotometer model 932 (Kontron Instruments). When MVs were incubated in SCL containing 2 mM Ca^{2+} but not P_i, PP_i and other phosphate substrates, there were no changes in turbidity. Thus, the increase in turbidity was due to mineral formation [59,60].

Identification of Minerals by Infrared Spectroscopy

The minerals were determined by infrared spectroscopy (Nicolet 510M FTIR spectrometer). They were centrifuged at 3,000 x *g* for 10 min and washed several times with water. They were dried and incorporated by pressing into 100 mg of KBr. Standard CPPD was prepared by incubating stoichiometric proportions of Ca^{2+} and PP_i at 37 °C for 2 weeks. Standard HA was purchased from Sigma.

RESULTS

Biochemical Characterization of Matrix Vesicles

The MVs extracted from chicken embryo growth plate cartilages were round structures with a diameter ranging from 100 to 250 nm, (Fig. 1), in agreement with Anderson *et al.* [61] and Balcerzak *et al.* [55]. The electrophoretic profile of MVs exhibited, among others, three major bands with apparent molecular weights of 44, 38 and 31 kDa (Fig. 2A) [59]. Caveolin-1, a marker of caveolae, present in the plasma membrane of hypertrophic chondrocytes (26 kDa, Fig. 2B, lane 2), was absent in MVs (Fig. 2B, lane 1), indicating that isolated MVs are not contaminated by the fragments of plasma membrane. TNAP, a marker enzyme of MVs [62], involved in the P_i homeostasis in mineralizing tissues [63-65], was enriched in the MV fractions. The phosphomonoesterase (PME) activity associated with TNAP of MVs at pH 10.4 was 25.0 ± 3.4 units per mg of proteins, approximately 5-times higher in comparison to hypertrophic chondrocytes (Table 1), indicating a high degree of purity of MV preparations.

TABLE I. Phosphomonesterase activity at pH 10.4 of chondrocytes, cellular debris and MVs.

	Digest	Hypertrophic chondrocytes	Second pellet	Matrix vesicles	Last supernatant
Specific PME activity (U/mg)*	2.1 ± 0.2	5.2 ± 0.8	5.7 ± 0.6	25.0 ± 3.4	0.3 ± 0.1
Percentage of total activity (%)	100	18.2 ± 2.7	34.4 ± 3.5	39.7 ± 3.6	11.1 ± 1.1
Enrichment	1	2.5	2.7	11.9	0.1

Growth plate cartilages were digested by collagenase. Hypertrophic chondrocytes were obtained by a centrifugation at 600 x *g* for 10 min, the second pellet by a centrifugation at 13,000 x *g* for 20 min and MVs by a last centrifugation at 70,000 x *g* for 60 min.

*Phosphomonoesterase activity is expressed as µmol of *p*-nitrophenyl phosphate hydrolysed per minute, per mg of MV proteins at pH 10.4.

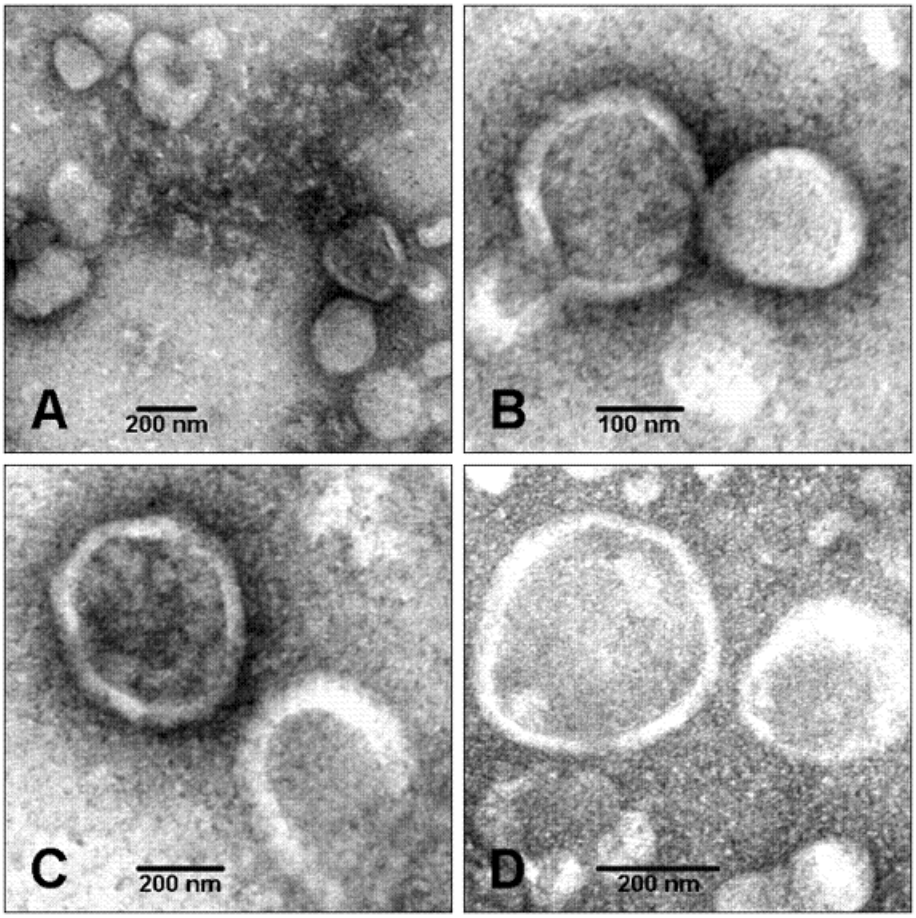

Figure 1. Electron microscope view of MVs. MVs exhibit spherical shapes with a 100-250 nm diameter. (Magnifications: A, x 53,000 – B, x 100,000 – C, x 75,000 – D, x 100,000).

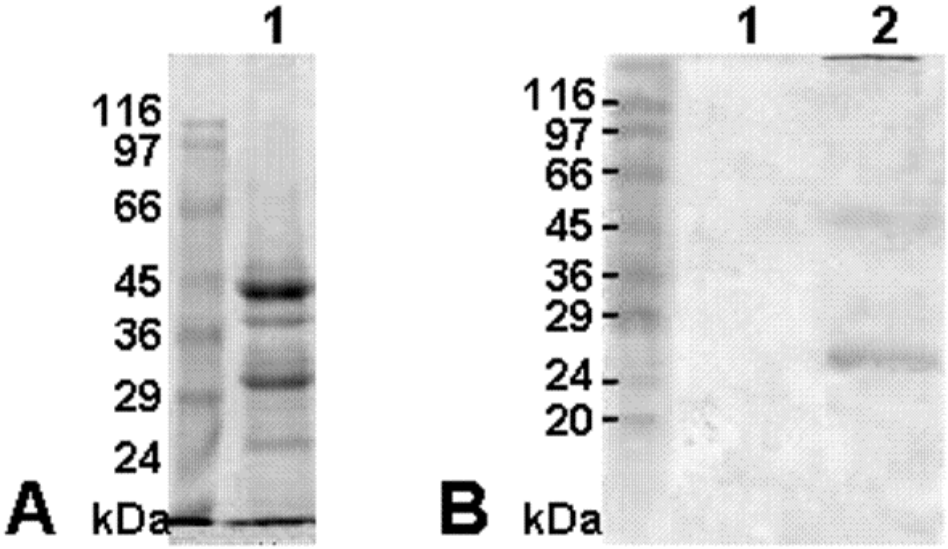

Figure 2. (A) Protein pattern of MVs in a 10 % SDS-polyacrylamide gel. Lane 1, MVs. (B) Western-Blot of MVs and hypertrophic chondrocytes for the detection of caveolin-1. Lane 1, MVs; Lane 2, co-isolated chondrocytes.

Extravesicular P_i and PP_i homeostasis by Matrix Vesicles

To delineate the importance of TNAP in PME and pyrophosphatase activities of MVs, the enzyme was digested out from MVs by a cleavage of its glycosylphosphatidylinositol (GPI) anchor with PI specific phospholipase C (PI-PLC). GPI-anchored TNAP in untreated MVs exhibited an apparent molecular weight of 118 kDa (Fig. 3, lane 1). After centrifugation, TNAP without GPI anchor was detected in the supernatant (sMV, Fig. 3, lane 2), but not in the pellet containing MVs devoid of GPI anchored proteins (pMV, Fig.3, lane 3).

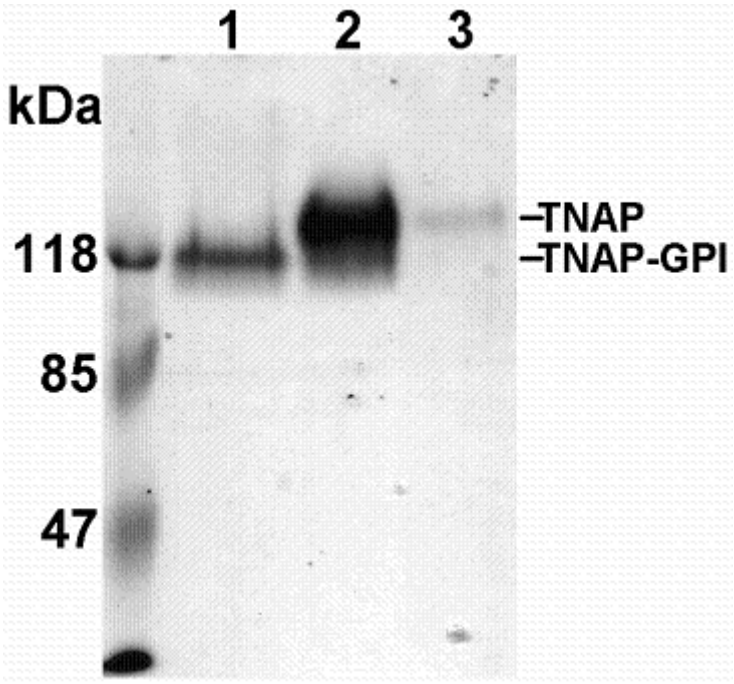

Figure 3. BCIP-NBT visualization of tissue non-specific alkaline phosphatase in a 7.5 % SDS-polyacrylamide gel. Lane 1, MVs; Lane 2, sMV (supernatant of MVs treated by PI-PLC); Lane 3, pMV (pellet of MVs treated by PI-PLC).

The specific PME activity of MVs amounted to 0.62 ± 0.10 units per mg of MV proteins at physiological pH, i.e. 40 times lower than at pH 10.4 (Table 2). The percentage of total PME activity of the sMV was 92 ± 3.7 % at pH 10.4 and 91 ± 3 % at pH 7.4 (Table 2), indicating that more than 91 % of PME activity is associated with TNAP in MVs. The PDE activity of MVs reflecting both TNAP [39] and NPP1 activities [35] was 2.66 ± 0.30 units per mg of MV proteins at optimal conditions (pH 9). It was 0.52 ± 0.08 units per mg of MV proteins at pH 7.4. When the substrate concentration was reduced from 2 to 0.5 mM, the optimal pH for the activity shifted from 8.8 to 8.2 (Fig. 4). In the presence of 2 mM PP_i, the pyrophosphatase activity of MVs was 3.70 ± 0.31 units per mg of MV proteins at pH 8.8, and 1.00 ± 0.08 units per mg of MV proteins at physiological pH (Table 2). The apparent K_m of PP_i hydrolysis at physiological pH was identical for MVs, sMV and pMV, and amounted to 355 ± 6 µM. The pyrophosphatase activity of all these samples was also inhibited in the same competitive manner by P_i; K_i amounted to 3.63 ± 0.14 mM. Over 96 ± 5.2 % of the

pyrophosphatase activity was attributed to the sMV at pH 7.4 (Table 2), indicating that the ability of MVs to hydrolyse PP_i was due to TNAP.

TABLE II. Hydrolysis of *p*NPP and PP_i by matrix vesicles (MVs), the supernatant fraction (sMV) and the pellet fraction (pMV) of MVs treated by PI-PLC.

	MVs	sMV	pMV
	U/mg*	% of total MV activity	
$PME_{10.4}$	25.0 ± 3.40	92.0 ± 3.7	9.8 ± 0.9
$PME_{7.4}$	0.62 ± 0.10	91.0 ± 3.0	12.0 ± 1.0
$PP_{i8.8}$	3.70 ± 0.31	95.2 ± 2.8	6.0 ± 1.0
$PP_{i7.4}$	1.00 ± 0.09	96.0 ± 1.7	5.2 ± 0.8

Phosphomonoesterase activity was measured by hydrolysis of *p*NPP at pH 10.4 ($PME_{10.4}$) and at pH 7.4 ($PME_{7.4}$). Pyrophosphatase activity was determined by hydrolysis of PP_i at pH 8.8 ($PP_{i8.8}$) and at pH 7.4 ($PP_{i7.4}$). The activities of MVs are expressed as µmol of substrate hydrolysed per minute, per mg of MV proteins, under described conditions. The activities of sMV and pMV are expressed as percentages of total MV activities.
*Activities are expressed as µmol of substrate hydrolysed per minute, per mg of MV proteins at pH 10.4.

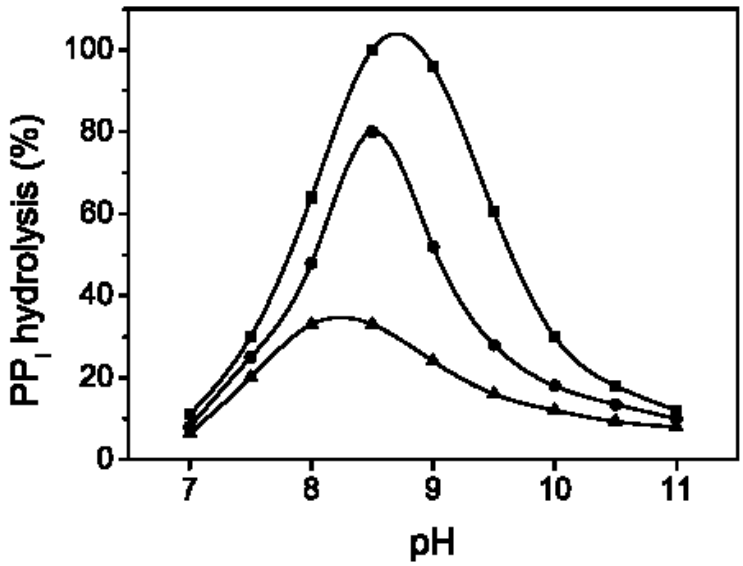

Figure 4. The effect of pH on the PP_i hydrolysis by MVs. The pyrophosphatase activity of MVs was measured at different pH from 7 to 11, in the presence of different concentrations of PP_i: (■) 2 mM, (●) 1 mM, and (▲) 0.5 mM.

P_i and Nucleotide-Initiated Mineralization by Matrix Vesicles

The isolated MVs incubated in the SCL buffer with 2 mM Ca^{2+} were able to induce mineral formation, after a short lag period of 3.5 – 4 hours, corresponding to the time of accumulation of Ca^{2+}

and P_i within MVs [60]. Then, the mineral formation increased rapidly and reached saturation (Fig. 5). MVs in SCL medium without Ca^{2+} was not able to mineralize, indicating that the presence of 0.57 mM Mg^{2+} in SCL medium containing MVs cannot induce mineral formation. No mineral was formed in the SCL buffer with 2 mM Ca^{2+} devoid of MVs, indicating that MVs are essential to initiate mineralization. The MV-induced mineral was identified by infrared spectroscopy. The infrared spectrum of mineral formed by MVs in SCL buffer exhibited five peaks at 1090 cm^{-1}, 1030-1034 cm^{-1}, 960-961 cm^{-1}, 600-602 cm^{-1} and 561-562 cm^{-1} (Fig. 6, spectrum: SCL), corresponding to the peaks of HA (Fig. 7, spectrum: HA) [66,67], indicating the ability of MVs to produce HA. Addition of 1 mM or 2 mM P_i (corresponding respectively to a total P_i concentration of 2.42 mM or 3.42 mM in SCL) into the mineralization medium reduced the lag period of mineral formation induced by MVs from 3.5 – 4 hours to 1.5 – 2 hours or to 0.5 hour, respectively (Fig. 5). In both cases, the minerals formed by MVs were identified as crystalline HA (Fig. 6, spectrum: P_i). Addition of 1 mM AMP reduced the induction phase from 3.5 – 4 hours to 2.5 – 3 hours (Fig. 5), i.e. to a lower extent as compared with the addition of 1 mM P_i, due to the time required for hydrolysis of AMP by TNAP. The mineral formed was also HA (Fig. 6, spectrum: AMP). However, addition of 0.33 mM ATP increased the time delay of mineral formation from 3.5 – 4 hours to 18 – 20 hours (Fig. 5). This retardation was due to the inhibitory effect of ATP on HA deposition [68] or the formation of PP_i, a potent inhibitor of calcium-phosphate deposition [41-43]. The mineral phase produced by MVs in the presence of 0.33 mM ATP revealed HA and a small amount of other minerals, as suggested by the presence of a broad contour in the 1200 cm^{-1} to 1000 cm^{-1} region (Fig. 6, spectrum: ATP), and as reported elsewhere [37].

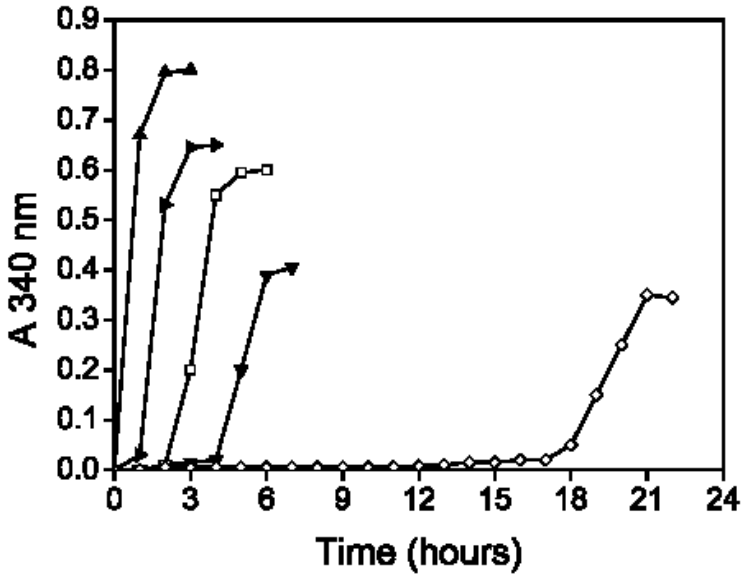

Figure 5. Kinetics of mineral formation by matrix vesicles. MVs were incubated at 37 °C in SCL buffer containing 2 mM Ca^{2+} and 1.42 mM P_i with additional inorganic phosphate (P_i) or phosphate substrates, as follows: (▼) without additional substrates, (►) Total P_i = 2.42 mM (▲) Total Pi = 3.42 mM, (□) 1 mM AMP, and (◊) 0.33 ATP. Mineral formation was assessed by light scattering at 340 nm.

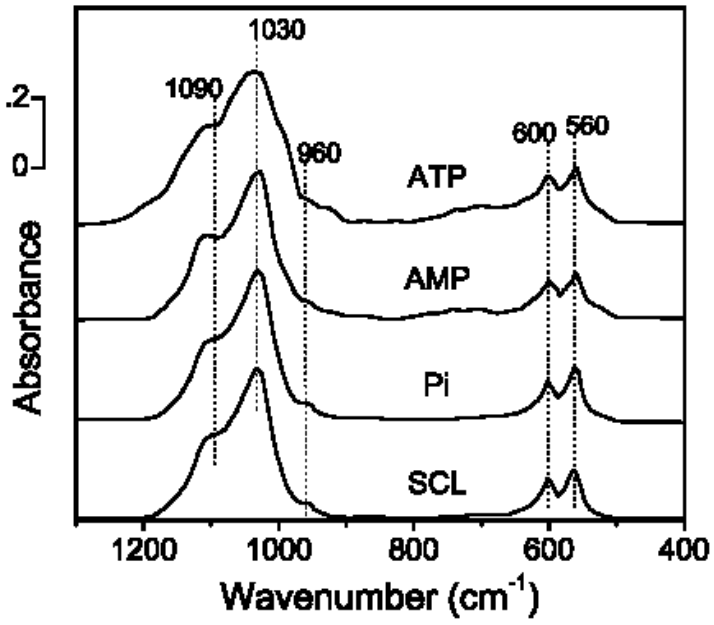

Figure 6. Infrared spectra of minerals formed by MVs in the presence of different concentrations of P_i or different phosphate substrates. MVs were incubated at 37 °C in SCL buffer containing 2 mM Ca^{2+} and 1.42 mM P_i with additional P_i or phosphate substrates: without additional substrates as a control (spectrum SCL), Total Pi = 3.42 mM (spectrum P_i), 1 mM AMP (spectrum AMP), 0.33 ATP (spectrum ATP).

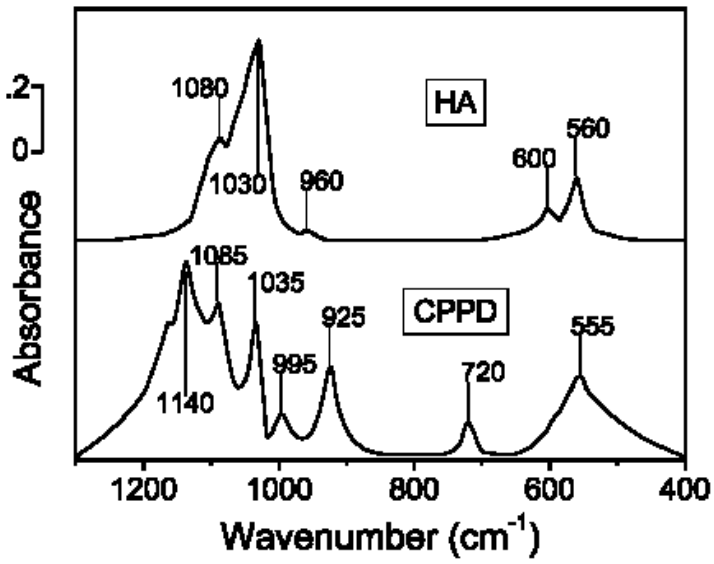

Figure 7. Infrared spectra of hydroxyapatite (HA) and calcium pyrophosphate dihydrate (CPPD) standards.

The Regulatory Effect of PP_i on Biomineralization

To identify the conditions to produce HA or other minerals, MVs were incubated in the SCL buffer with 2 mM Ca^{2+}, P_i at 1.42-3.42 mM concentration range and PP_i at 0.01-2.41 mM concentration range. P_i/PP_i ratios were calculated initially and during the induction phase of mineralization since PP_i was continuously hydrolyzed and both P_i and PP_i were involved in the mineral formation. The final P_i/PP_i ratio was determined for each initial P_i/PP_i ratio. The initial P_i/PP_i ratio (within 1.42-3.42 mM P_i and 0.01-2.41 mM PP_i) predetermined the type of mineral formed by MVs. Without PP_i, the period of induction phase was about 3 hours when MVs were incubated in the SCL buffer with 2 mM Ca^{2+} (Fig. 8A), and 0.5 hours when the SCL buffer was supplemented by 2 mM Ca^{2+} and 2 mM P_i corresponding to a total amount of 3.42 mM P_i in SCL (Fig. 8B). A higher amount of P_i decreased the induction time of mineral formation. MVs incubated in the presence of Ca^{2+} and P_i formed crystalline HA (Fig. 9, spectrum I). The induction time of mineralization increased from 3 hours to 6 hours (Fig. 8A) after addition of 0.01 mM PP_i into the SCL medium with 2 mM Ca^{2+} (since SCL medium contained 1.42 mM P_i, the initial P_i/PP_i ratio was 142 ± 47 and final P_i/PP_i ratio was 198.3 ± 65.6, Table III). Addition of 0.024 mM PP_i and 2 mM P_i in SCL (total P_i was 3.42 mM in SCL medium; initial P_i/PP_i ratio: 142 ± 47 and final P_i/PP_i ratio was 198.3 ± 65.6), increased the induction time of mineralization from 0.5 hours to 2.5 hours (Fig. 8B) and the mineral formed was crystalline HA (Fig. 9, spectrum II). At the initial P_i/PP_i ratio between infinity to 142 ± 47, the induction time increased (Table 3), but the mineral formed was always HA (Table 3). The turning point where the mineral phase contained a mixture of poorly crystalline HA and other minerals, was reached with an initial P_i/PP_i ratio of 71 ± 14.2 (Table 3). The maximal induction time of mineral formation occurred upon addition of 0.05 ± 0.01 mM PP_i in SCL with 1.42 mM total P_i concentration (18 hours, Fig. 8A) or 0.12 mM PP_i in SCL with 3.42 mM total P_i concentration (10 hours, Fig. 8B), corresponding for both to an initial P_i/PP_i ratio of 28.4 ± 5.7 (Fig. 8C) and to a final P_i/PP_i ratio of 102.9 ± 20.7 (Table 3). The minerals formed under these conditions were not HA as evidenced by the absence of characteristic HA bands at 960-961 cm^{-1}, 600-601 cm^{-1} and 560-562 cm^{-1}. Amorphous mixtures were produced (Fig. 9, spectrum III). The induction time of mineral formation decreased with the diminution of initial P_i/PP_i ratio from 28.4 ± 5.7, indicating faster mineral formation. Addition of 0.1 mM PP_i in SCL with 1.42 mM total P_i concentration (initial P_i/PP_i ratio of 14.2 ± 1.4 and final P_i/PP_i ratio of 24.5 ± 2.4) reduced the induction time of mineral formation to 9 hours. It was further reduced to 7 hours with the addition of 0.5 mM PP_i (initial P_i/PP_i ratio of 2.8 ± 0.3 and final ratio of 6.2 ± 0.7) and to 5 hours with 1 mM PP_i (initial P_i/PP_i ratio of 1.4 ± 0.1 and final ratio of 2.8 ± 0.3) (Fig. 8A). We observed also a decrease of induction time of mineral formation at the same P_i/PP_i ratio but with higher PP_i concentrations in SCL medium containing 3.42 mM P_i (Fig. 8B). Due to the higher amount of PP_i and P_i, there was a higher amount of mineral formed as evidenced by the larger turbidity and the kinetics (Fig 8B vs Fig 8A). Although the mineral formation in MVs was stimulated with higher concentrations of PP_i, the nature

of mineral deposits was different. At the initial P_i/PP_i ratios between 14.2 ± 1.4 and 2.8 ± 0.3, the mineral phase was composed of a mixture of minerals, including CPPD (Fig. 9, spectrum IV), as characterized by the appearance of the characteristic CPPD bands at 1140 cm^{-1}, 925 cm^{-1}, 725 cm^{-1} and 555 cm^{-1} (Fig. 7, spectrum: CPPD). At the initial P_i/PP_i ratio lower than 2.8 ± 0.3, the spectrum of the mineral formed by MVs resembled CPPD (Fig. 9, spectrum V). CPPD mineral was exclusively produced by MVs when the initial P_i/PP_i ratio was lower than 1.4 ± 0.1 (Fig. 9, spectrum VI). Under the same conditions, no CPPD was formed in SCL medium without MVs.

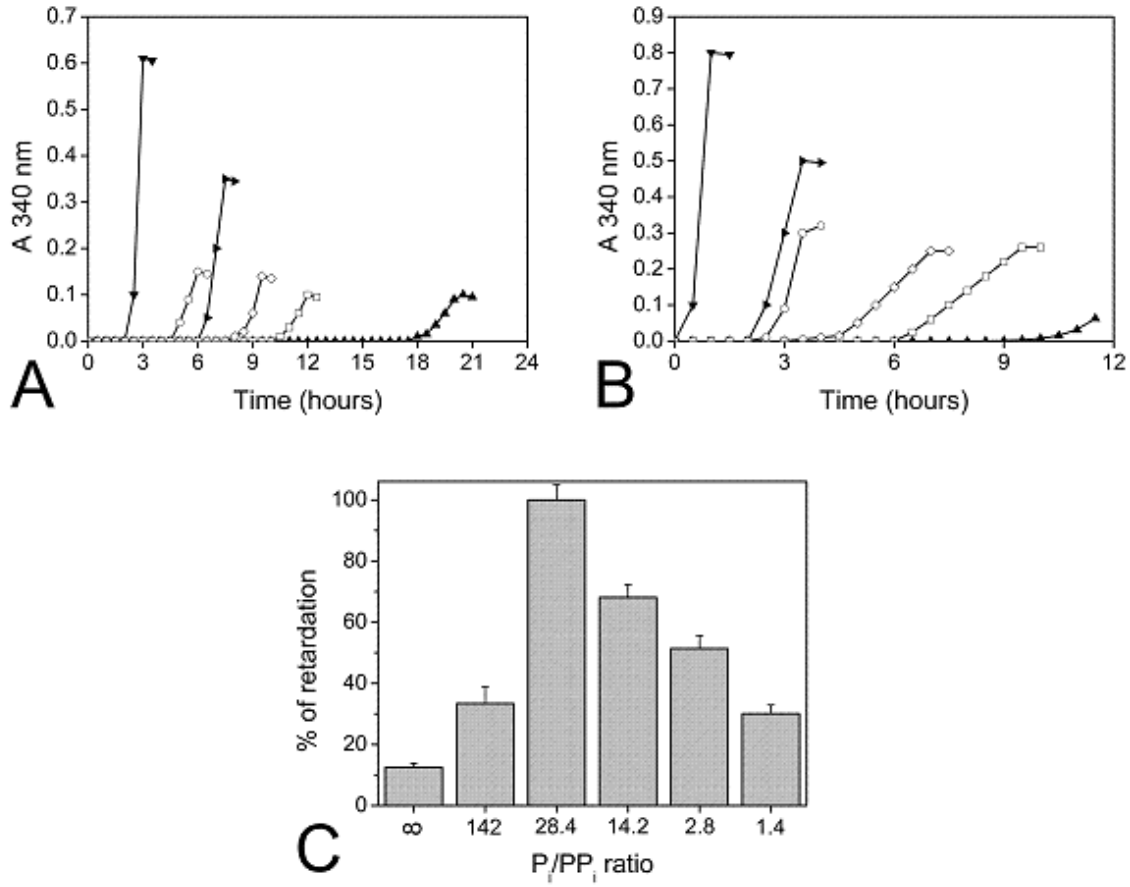

Fig. 8. Retardation of PP_i-initiated mineral formation. (A) MVs were incubated at 37 °C in SCL buffer containing 2 mM Ca^{2+}, 1.42 mM P_i and inorganic pyrophosphate (PP_i) at various concentrations: (▼) without additional PP_i, (►) 0.01 mM, (▲) 0.05 mM, (□) 0.1 mM, (◊) 0.5 mM and (○) 1 mM PP_i corresponding to an initial P_i/PP_i ratio of 142, 28.4, 14.2, 2.8, and 1.4, respectively. (B) MVs were incubated at 37 °C in SCL buffer containing 2 mM Ca^{2+}, 3.42 mM P_i and different concentrations of PP_i: (▼) without additional PP_i, (►) 0.024 mM, (▲) 0.12 mM, (□) 0.24 mM, (◊) 1.2 mM and (○) 2.41 mM PP_i, corresponding to the same P_i/PP_i ratio as in panel A. (C) All results were combined and normalized as percentages of the maximal retardation of mineralization induced by PP_i.

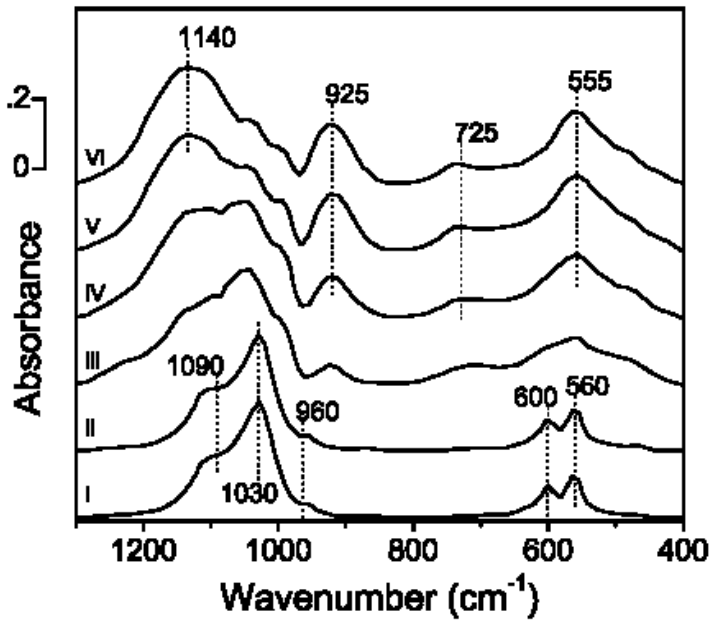

Figure 9. Infrared spectra of minerals produced by MVs at different P_i/PP_i molar ratios: (I) no PP_i, (II) 142, (III) 28.4, (IV) 14.2, (V) 2.8 and (VI) 1.4. MVs were incubated at 37 °C in SCL buffer containing 2 mM Ca^{2+}, 3.42 mM P_i and PP_i at 0, 0.024 mM, 0.12 mM, 0.24 mM, 1.2 mM or 2.41 mM.

TABLE III. The effect of the P_i/PP_i ratio on the mineralization mediated by MVs.

Initial $[P_i]/[PP_i]$	Final $[P_i]/[PP_i]$	Retardation time (%)	Minerals formed IR spectra in Fig 9
∞	∞	12.5 ± 1.4	HA (I)
142 ± 47	198.3 ± 65.6	33.4 ± 5.6	HA (II)
71 ± 14.2	138.7 ± 27.7	50.1 ± 3.5	HA + other
28.4 ± 5.7	102.9 ± 20.7	100 ± 5.0	Other (III)
14.2 ± 1.4	24.5 ± 2.4	68.1 ± 4.2	CPPD + other (IV)
2.8 ± 0.3	6.2 ± 0.7	51.4 ± 4.2	CPPD (V)
1.4 ± 0.1	2.8 ± 0.3	30.1 ± 2.8	CPPD (VI)

MVs were incubated in the SCL buffer containing 2 mM Ca^{2+}, P_i at 1.42-3.42 mM concentration range and PP_i at 0.01-2.41 mM concentration range. Initial P_i/PP_i ratios and P_i/PP_i ratios prior to the onset of calcification were calculated. The kinetics of mineralization was followed by light scattering at 340 nm and the minerals formed by MVs were identified by infrared spectroscopy (Fig. 9, the numbering of spectra corresponded to a specific P_i/PP_i ratio). Induction time was the longest (100 %) at initial $[P_i]/[PP_i]$ = 28.4 ± 5.7 and the lowest (12.5 ± 1.4) in the absence of PP_i.

DISCUSSION

Our report focused on the conditions favoring HA and CPPD minerals induced by MVs from growth plate cartilage. MVs were used to mimic pathologic calcification, since the initiation of mineral formation mediated by MVs during endochondral calcification is similar to that which appears in a variety of pathologic calcifications [6]. Although the MV model has the disadvantage that matrix and cellular issues cannot be addressed, it provides an easily quantifiable and well-characterized model to analyze the initiation of HA or CPPD formation [47]. MVs served to model arthritic crystal deposition characterized by HA or CPPD deposits in joint cartilage. In the absence of inhibitors, Ca^{2+}/P_i ratio and the Ca^{2+} x P_i product are critical factors affecting the kinetics of the biomineralization process [69]. Increasing the P_i concentration (Fig. 5) and addition of phosphomonoester substrates of TNAP, such as AMP, reduced the induction time of HA formation (Fig. 5). However, addition of ATP, another source of P_i after its hydrolysis, led to a high retardation of the induction phase of mineralization (Fig. 5) and to a mixture of poorly crystalline HA and other minerals (Fig. 3, spectrum: ATP), consistent with the findings of Zhang *et al*. [39]. The retardation was due to the inhibitory effect of ATP [68] or PP_i [41-43], on the HA formation. ATP is a source of P_i (after its hydrolysis by TNAP, ATPases and other PME enzymes) but also a source of PP_i after its hydrolysis by NPP1 and TNAP [39]. PP_i, when hydrolyzed, provides P_i for HA formation but inhibits the seeding of calcium-phosphate minerals itself. In addition, high concentrations of PP_i led to the precipitation of immature CPPD mineral. Alternatively, metastable equilibrium between Ca^{2+}, P_i and PP_i can be disturbed, inducing mineral formations without MVs. Cheng and Pritzker [70] reported that HA was formed in aqueous solution when P_i/PP_i was higher than 100, while CPPD was produced when P_i/PP_i was less than 3. MVs from growth plate cartilages are able to produce CPPD minerals [37,71]. Since osteoarthritic MVs and growth plate MVs have a similar protein machinery associated with mineralization, our data underline a mechanism of CPPD pathological deposit. Our data emphasize that not only PP_i concentration affected the nature of the formed mineral but also that the P_i/PP_i ratio is a key parameter to favor HA or CPPD formation as proposed previously [37] and is a determinant factor leading to pathological mineralization or its inhibition. Initial P_i/PP_i ratio higher than 140 led to HA deposition, mimicking conditions during endochondral bone formation or arthritic crystal deposition. When P_i/PP_i ratio was lower than 70, it inhibited the MV-induced seeding of HA, which corresponds to the conditions where mineralization is inhibited. An initial P_i/PP_i ratio lower than 2.8 led to deposits of pathological CPPD, while an initial P_i/PP_i ratio higher than 28.4 inhibited CPPD formation. The P_i/PP_i ratio could reflect somehow the overall differentiation state of chondrocytes (mature vs hypertrophic), the levels of expression of TNAP, NPP1 or other proteins affecting P_i and PP_i concentrations as well as the balance between pro- and anti- calcification factors and may serve as an indicator of the calcification process.

ACKNOWLEDGEMENTS

We thank Dr. Laurence Bessuelle for her help with electron microscopy and Dr. John Carew for correcting the English. This work was supported by a Polonium grant (05819NF), CNRS (France) and by a grant N301 025 32-1120 from Polish Ministry of Science and Higher Education.

REFERENCES

[1] Thouverey C, Bleicher F, Bandorowicz-Pikula J. Extracellular ATP and its effects on physiological and pathological mineralization. Curr Opin Orthop 2007;18:460-466.

[2] Balcerzak M, Hamade E, Zhang L, Pikula S, Azzar G, Radisson J, *et al*. The roles of annexins and alkaline phosphatase in mineralization process. Acta Biochim Pol 2003;50:1019-38.

[3] Kirsch T. Determinants of pathological mineralization. Curr Opin Rheumatol 2006;18:174-80.

[4] Van de Lest CHA, Vaandrager AB. Mechanisms of cell-mediated mineralization. Curr Opin Orthop 2007;18:434-43.

[5] Kirsch T. Physiological and pathological mineralization: a complex multifactorial process. Curr Opin Orthop 2007;18:425-27.

[6] Anderson HC. The role of matrix vesicles in physiological and pathological calcification. Curr Opin Orthop 2007;18:428-33.

[7] Karpouzas GA, Terkeltaub RA. New developments in the pathogenesis of articular cartilage calcification. Curr Rheumatol Rep 1999;1:121-27.

[8] Derfus BA, Kurtin SM, Camacho NP, Kurup I, Ryan LM. Comparison of matrix vesicles derived from normal and osteoarthritic human articular cartilage. Connect Tissue Res 1996;35:337-42.

[9] Derfus B, Kranendonk S, Camacho N, Mandel N, Kushnaryov V, Lynch K, *et al*. Human osteoarthritic cartilage matrix vesicles generate both calcium pyrophosphate dihydrate and apatite in vitro. Calcif Tissue Int 1998;63:258-62.

[10] Anderson HC. Calcific diseases. A concept. Arch Pathol Lab Med 1983;107:341-48.

[11] Reginato AM, Shapiro IM, Lash JW, Jimenez SA. Type X collagen alterations in rachitic chick epiphyseal growth cartilage. J Biol Chem 1988;263:9938-45.

[12] Hatori M, Klatte KJ, Teixeira CC, Shapiro IM. End labeling studies of fragmented DNA in the avian growth plate: evidence of apoptosis in terminally differentiated chondrocytes. J Bone Miner Res 1995;10:1960-8.

[13] Binette F, McQuaid DP, Haudenschild DR, Yaeger PC, McPherson JM, Tubo R. Expression of a stable articular cartilage phenotype without evidence of hypertrophy by adult human articular chondrocytes in vitro. J Orthop Res 1998;16:207-16.

[14] Kirsch T, Nah HD, Shapiro IM, Pacifici M. Regulated production of mineralization-competent matrix vesicles in hypertrophic chondrocytes. J Cell Biol 1997;137:1149-60.

[15] Anderson HC. Molecular biology of matrix vesicles. Clin Orthop Relat Res 1995;266-80.

[16] Anderson HC, Garimella R, Tague SE. The role of matrix vesicles in growth plate development and biomineralization. Front Biosci 2005;10:822-37.

[17] Ali SY. Analysis of matrix vesicles and their role in the calcification of epiphyseal cartilage. Fed Proc 1976;35:135-42.

[18] Paulsen F, Tillmann B. Composition of the extracellular matrix in human cricoarytenoid joint articular cartilage. Arch Histol Cytol 1999;62:149-63.

[19] Sweet MB, Thonar EJ, Immelman AR, Solomon L. Biochemical changes in progressive osteoarthrosis. Ann Rheum Dis 1977;36:387-98.

[20] Pritzker KP. Crystal-associated arthropathies: what's new in old joints. J Am Geriatr Soc 1980;28:439-45.

[21] Ali SY. Apatite-type crystal deposition in arthritic cartilage. Scan Electron Microsc 1985;4:1555-66.

[22] Anderson HC. Mechanisms of pathologic calcification. Rheum Dis Clin North Am 1988;14:303-19.

[23] Anderson HC. Matrix vesicles and calcification. Curr Rheumatol Rep 2003;5:222-6.

[24] Cheung HS, Kurup IV, Sallis JD, Ryan LM. Inhibition of calcium pyrophosphate dihydrate crystal formation in articular cartilage vesicles and cartilage by phosphocitrate. J Biol Chem 1996;271:28082-5.

[25] Derfus BA, Camacho NP, Olmez U, Kushnaryov VM, Westfall PR, Ryan LM, *et al.* Transforming growth factor beta-1 stimulates articular chondrocyte elaboration of matrix vesicles capable of greater calcium pyrophosphate precipitation. Osteoarthritis and Cartilage 2001;9:189-94.

[26] Kirsch T, Swoboda B, Nah HD. Activation of annexin II and V expression, terminal differentiation, mineralization and apoptosis in human osteoarthritic cartilage. Osteoarthritis and Cartilage 2000;8:294-302.

[27] Rees JA, Ali SY. Ultrastructural localisation of alkaline phosphatase activity in osteoarthritic human articular cartilage. Ann Rheum Dis 1988;47:747-53.

[28] Einhorn TA, Gordon SL, Siegel SA, Hummel CF, Avitable MJ, Carty RP. Matrix vesicle enzymes in human osteoarthritis. J Orthop Res 1985;3:160-69.

[29] Johnson K, Hashimoto S, Lotz M, Pritzker K, Goding J, Terkeltaub R. Up-regulated expression of the phosphodiesterase nucleotide pyrophosphatase family member PC-1 is a marker and pathogenic factor for knee meniscal cartilage matrix calcification. Arthritis Rheum 2001;44:1071-81.

[30] Nanba Y, Nishida K, Yoshikawa T, Sato T, Inoue H, Kuboki Y. Expression of osteonectin in articular cartilage of osteoarthritic knees. Acta Med Okayama 1997;51:239-43.

[31] Nakase T, Miyaji T, Tomita T, Kaneko M, Kuriyama K, Myoui A, *et al.* Localization of bone morphogenetic protein-2 in human osteoarthritic cartilage and osteophyte. Osteoarthritis and Cartilage 2003;11:278-84.

[32] Wang X, Manner PA, Horner A, Shum L, Tuan RS, Nuckolls GH. Regulation of MMP-13 expression by RUNX2 and FGF2 in osteoarthritic cartilage. Osteoarthritis and Cartilage 2004;12:963-73.

[33] Johnson KA, Hessle L, Vaingankar S, Wennberg C, Mauro S, Narisawa S, *et al*. Osteoblast tissue-nonspecific alkaline phosphatase antagonizes and regulates PC-1. Am J Physiol Regul Integr Comp Physiol 2000;279:R1365-77.

[34] Anderson HC, Harmey D, Camacho NP, Garimella R, Sipe JB, Tague S, *et al*. Sustained osteomalacia of long bones despite major improvement in other hypophosphatasia-related mineral deficits in tissue nonspecific alkaline phosphatase/nucleotide pyrophosphatase phosphodiesterase 1 double-deficient mice. Am J Pathol 2005;166:1711-20.

[35] Hessle L, Johnson KA, Anderson HC, Narisawa S, Sali A, Goding JW, *et al*. Tissue-nonspecific alkaline phosphatase and plasma cell membrane glycoprotein-1 are central antagonistic regulators of bone mineralization. Proc Natl Acad Sci USA 2002;99:9445-9.

[36] Golub EE, Boesze-Battaglia K. The role of alkaline phosphatase in mineralization. Curr Opin Orthop 2007;18:444-448.

[37] Garimella R, Bi X, Anderson HC, Camacho NP. Nature of phosphate substrate as a major determinant of mineral type formed in matrix vesicle-mediated in vitro mineralization: an FTIR imaging study. Bone 2006;38:811-7.

[38] Hamade E, Azzar G, Radisson J, Buchet R, Roux B. Chick embryo anchored alkaline phosphatase and mineralization process in vitro. Eur J Biochem 2003;270:2082-90.

[39] Zhang L, Balcerzak M, Radisson J, Thouverey C, Pikula S, Azzar G, *et al.* Phosphodiesterase activity of alkaline phosphatase in ATP-initiated Ca^{2+} and phosphate deposition in isolated chicken matrix vesicles. J Biol Chem 2005;280:37289-96.

[40] Blumenthal NC. Mechanisms of inhibition of calcification. Clin Orthop Relat Res 1989;279-89.

[41] Register TC, Wuthier RE. Effect of pyrophosphate and two diphosphonates on 45Ca and $32P_i$ uptake and mineralization by matrix vesicle-enriched fractions and by hydroxyapatite. Bone 1985;6:307-12.

[42] Tanimura A, McGregor DH, Anderson HC. Matrix vesicles in arthrosclerotic calcification. Proc Soc Exp Biol Med 1983;172:173-7.

[43] Tenenbaum HC. Levamisole and inorganic pyrophosphate inhibit beta-glycerophosphate induced mineralization of bone formed in vitro. Bone Miner 1987;3:13-26.

[44] Terkeltaub RA. Inorganic pyrophosphate generation and disposition in pathophysiology. Am J Physiol Cell Physiol 2001;281:C1-C11.

[45] Ryan LM, Rosenthal AK. Metabolism of extracellular pyrophosphate. Curr Opin Rheumatol 2003;15:311-4.

[46] Viriyavejkul P, Wilairatana V, Tanavalee A, Jaovisidha K. Comparison of characteristics of patients with and without calcium pyrophosphate dihydrate crystal deposition disease who underwent total knee replacement surgery for osteoarthritis. Osteoarthritis and Cartilage 2007;15:232-235.

[47] Gohr C. In vitro models of calcium crystal formation. Curr Opin Rheumatol 2004;16:263-7.

[48] Harmey D, Hessle L, Narisawa S, Johnson KA, Terkeltaub R, Millan JL. Concerted regulation of inorganic pyrophosphate and osteopontin by akp2, enpp1, and ank: an integrated model of the pathogenesis of mineralization disorders. Am J Pathol 2004;164:1199-209.

[49] Ho AM, Johnson MD, Kingsley DM. Role of the mouse ank gene in control of tissue calcification and arthritis. Science 2000;289:265-70.

[50] Zaka R, Williams CJ. Role of the progressive ankylosis gene in cartilage mineralization. Curr Opin Rheumatol 2006;18:181-86.

[51] Johnson K, Terkeltaub R. Upregulated ank expression in osteoarthritis can promote both chondrocyte MMP-13 expression and calcification via chondrocyte extracellular PP_i excess. Osteoarthritis and Cartilage 2004;12:321-35.

[52] Johnson K, Terkeltaub R. Inorganic pyrophosphate (PP_i) in pathologic calcification of articular cartilage. Front Biosci 2005;10:988-97.

[53] Hirose J, Ryan LM, Masuda I. Up-regulated expression of cartilage intermediate-layer protein and ANK in articular hyaline cartilage from patients with calcium pyrophosphate dihydrate crystal deposition disease. Arthritis Rheum 2002;46:3218-29.

[54] Wu LN, Yoshimori T, Genge BR, Sauer GR, Kirsch T, Ishikawa Y, *et al.*. Characterization of the nucleational core complex responsible for mineral induction by growth plate cartilage matrix vesicles. J Biol Chem 1993;268:25084-94.

[55] Balcerzak M, Radisson J, Azzar G, Farlay D, Boivin G, Pikula S, *et al*. A comparative analysis of strategies for isolation of matrix vesicles. Anal Biochem 2007;361:176-82.

[56] Laemmli UK. Cleavage of structural proteins during the assembly of the head of bacteriophage T4. Nature 1970;227:680-85.

[57] Towbin H, Staehelin T, Gordon J. Electrophoretic transfer of proteins from polyacrylamide gels to nitrocellulose sheets: procedure and some applications. Proc Natl Acad Sci USA 1979;76:4350-54.

[58] Cyboron GW, Wuthier RE. Purification and initial characterization of intrinsic membrane-bound alkaline phosphatase from chicken epiphyseal cartilage. J Biol Chem 1981;256:7262-68.

[59] Wu LN, Genge BR, Dunkelberger DG, LeGeros RZ, Concannon B, Wuthier RE. Physicochemical characterization of the nucleational core of matrix vesicles. J Biol Chem 1997;272:4404-11.

[60] Wu LN, Sauer GR, Genge BR, Valhmu WB, Wuthier RE. Effects of analogues of inorganic phosphate and sodium ion on mineralization of matrix vesicles isolated from growth plate cartilage of normal rapidly growing chickens. J Inorg Biochem 2003;94:221-35.

[61] Anderson HC, Cecil R, Sajdera SW. Calcification of rachitic rat cartilage in vitro by extracellular matrix vesicles. Am J Pathol 1975;79:237-54.

[62] Majeska RJ, Wuthier RE. Studies on matrix vesicles isolated from chick epiphyseal cartilage. Association of pyrophosphatase and ATPase activities with alkaline phosphatase. Biochim Biophys Acta 1975;391:51-60.

[63] Robison R. The Possible Significance of Hexosephosphoric Esters in Ossification. Biochem J 1923;17:286-93.

[64] McLean FM, Keller PJ, Genge BR, Walters SA, Wuthier RE. Disposition of preformed mineral in matrix vesicles. Internal localization and association with alkaline phosphatase. J Biol Chem 1987;262:10481-88.

[65] Whyte MP. Hypophosphatasia and the role of alkaline phosphatase in skeletal mineralization. Endocr Rev 1994;15:439-61.

[66] Pleshko N, Boskey, A. Mendelsohn R. Novel infrared spectroscopic method for the determination of crystallinity of hydroxyapatite minerals. Biophys J 1991;60:786-93.

[67] Sauer GR, Wuthier RE. Fourier transform infrared characterization of mineral phases formed during induction of mineralization by collagenase-released matrix vesicles in vitro. J Biol Chem 1988;263:13718-24.

[68] Boskey AL, Boyan BD, Schwartz Z. Matrix vesicles promote mineralization in a gelatin gel. Calcif Tissue Int 1997;60:309-15.

[69] Walhmu WB, Wu LN, Wuthier RE. Effects of Ca/P_i ratio, Ca^{2+} x P_i ion product, and pH of incubation fluid on accumulation of $45Ca^{2+}$ by matrix vesicles in vitro. Bone Miner 1990;8:195-209.

[70] Cheng PT, Pritzker KP. Pyrophosphate, phosphate ion interaction: effects on calcium pyrophosphate and calcium hydroxyapatite crystal formation in aqueous solutions. J Rheumatol 1983;10:769-77.

[71] Hsu HH, Camacho NP, Anderson HC. Further characterization of ATP-initiated calcification by matrix vesicles isolated from rachitic rat cartilage. Membrane perturbation by detergents and deposition of calcium pyrophosphate by rachitic matrix vesicles. Biochim Biophys Acta 1999;1416:320-32.

Matrix Vesicles Originate from Apical Membrane Microvilli of Mineralizing Osteoblast-like Saos-2 Cells

[1,2]Cyril Thouverey, [1]Agnieszka Strzelecka-Kiliszek, [1]Marcin Balcerzak, [2]René Buchet and [1]Sławomir Pikula

[1]Department of Biochemistry, Nencki Institute of Experimental Biology, Polish Academy of Sciences, PL-02093 Warsaw, Poland.

[2]Université de Lyon, Lyon, F-69003, France ; Université Lyon 1, Villeurbanne, F-69622, France ; INSA-Lyon, Villeurbanne, F-69622, France; CPE Lyon, Villeurbanne, F-69616, France; ICBMS CNRS UMR 5246, Villeurbanne, F-69622, France.

Running title: Origin of matrix vesicles

Keywords: Matrix vesicles - origin - Saos-2 cells - microvilli - mineralization

Abbreviations: AA, ascorbic acid; AnxA6, vertebrate annexins A6; AR-S, Alizarin Red-S; β-GP, β-glycerophosphate; CCD, cytochalasin D; CHOL, cholesterol; DAG, diacylglycerols; FACS, fluorescence activated cell sorter; FBS, fetal bovine serum; FFA, free fatty acids; FITC, fluorescein isothiocyanate; FTIR, Fourier transformed infrared spectroscopy; HA, hydroxyapatite; HBSS, Hank's balanced salt solution; MAG, monoacylglycerols; MVs, matrix vesicles; PA, phosphatidic acid; PAGE, polyacrylamide gel electrophoresis; PBS, phosphate-buffered saline; PC, phosphatidylcholine; PE, phosphatidylethanolamine; PHL, phalloidin, PI, phosphatidylinositol; P_i, inorganic phosphate, PP_i, inorganic pyrophosphate; PS, phosphatidylserine; SDS, sodium dodecyl sulfate; SM, sphingomyelin; TAG, triacylglycerols; TNAP, tissue non-specific alkaline phosphatase; TBS, Tris-buffered saline; TRITC, tetramethylrhodamine isothiocyanate.

ABSTRACT

In bone, mineralization is tightly regulated by osteoblasts and hypertrophic chondrocytes which release matrix vesicles (MVs) and control extracellular ionic conditions and matrix composition. MVs are the initial sites of hydroxyapatite mineral formation by concentrating Ca^{2+} and P_i ions. Despite growing knowledge about their morphologies and functions, their biogenesis is not well understood. The purpose of this work was to determine the source of MVs in osteoblast lineage, Saos-2 cells, and to check whether MV formation originated from microvilli. Microvilli were isolated from apical plasma membrane of Saos-2 cells. Their morphology, structure and function were compared with those of MVs. The role of actin network in MV release was investigated by using microfilament perturbing drugs. MVs and microvillar vesicles were found to exhibit similar morphology with trilaminar membranes and diameters of the same range as observed by electron microscopy. Both vesicles were able to induce hydroxyapatite formation. Electrophoretic profiles of microvillar vesicles were comparable to those of MVs. Both membranes displayed analogous enrichment in alkaline phosphatase, Na^+/K^+ ATPase, and annexins A2 and A6. MVs and microvillar vesicles exhibited almost the same lipid composition with higher content of cholesterol, sphingomyelin and phosphatidylserine as compared to plasma membrane. Finally, cytochalasin D, which inhibits actin polymerization, was found to stimulate the formation of MVs. Our findings were consistent with the hypothesis that MVs originated from cell microvilli and that actin filament disassembly was involved in their biogenesis.

INTRODUCTION

Bone is a complex, dynamic, highly specialized form of connective tissue that together with cartilage makes up the skeleton. Bone matrix is composed of an organic phase, containing mostly type-I collagen, providing tensile strength, and an inorganic phase, hydroxyapatite, which gives it mechanical resistance [Buckwalter and Cooper, 1987]. Osteoclasts, osteoblasts and osteocytes are the three major cell types present in bone. Plasticity of the skeleton and its ability to adapt relies on continuous modeling and remodeling that require osteoclastic resorption of bone matrix and deposition of a new mineralized matrix by osteoblasts [Marks and Popoff, 1988]. Osteocytes maintain the osseous matrix, participate in extracellular exchanges and are involved in the mechanotransduction [Marks and Popoff, 1988]. Bone mineralization occurs during the formation, development, remodeling and repair of osseous tissue [Thouverey et al., 2007, Van de Lest and Vaandrager, 2007]. Thus, osseous mineralization is initiated by two types of cells: Hypertrophic chondrocytes during endochondral ossification and osteoblasts during intramembranous and haversian ossification. The regulation of physiological mineralization is mediated at cellular and tissue levels, and requires coordination between stimulatory and inhibitory factors [Van de Lest and Vaandrager, 2007]. Osteoblasts are fusiform, cuboidal, polyhedral or spherical cells located at the surface of forming bone. These cells are polarized with a basolateral plasma membrane facing the bone marrow and an apical plasma membrane facing the forming bone [Ilvesaro et al., 1999]. Osteoblasts, as odontoblasts and hypertrophic chondrocytes, participate in the synthesis of extracellular matrix proteins and in the matrix mineralization by releasing matrix vesicles (MVs) [Anderson, 1995; Balcerzak et al., 2003]. Osteoblasts can divide, differentiate into osteocytes or die by apoptosis. Extracellular MVs (between one hundred to several hundred nanometers in diameter) initiate the mineralization of bone matrix by promoting the deposition of hydroxyapatite (HA) in their lumen [Anderson et al., 1967]. MVs create an optimal environment by accumulating Ca^{2+} and inorganic phosphate (P_i) to induce the formation of HA [Anderson, 2003]. Then, the breakdown of MV membrane releases HA crystals in the extracellular matrix where mineralization is propagated [Anderson, 1995]. Despite growing knowledge about the structure and functions of MVs, little is known about their mechanism of biogenesis, especially from osteoblasts. It has been demonstrated that MVs derive from the plasma membrane of hypertrophic chondrocytes [Rabinovitch and Anderson, 1976; Wuthier et al., 1977]. Four hypotheses have been proposed concerning the mechanisms of MV formation [Rabinovitch and Anderson, 1976]. As areas of mineralization coincide with chondrocyte apoptosis in growth plate cartilages, it was suggested that MVs derive from the rearrangement of apoptotic cell membrane [Kardos and Hubbard, 1982]. This was not confirmed by Kirsch et al. [2003] who showed that MVs and apoptotic bodies are structurally and functionally different. However, it should be noted that MV formation and apoptosis probably occur concomitantly during cell differentiation process. Indeed, only

mature (but not immature) osteoblasts mineralize their matrix, while only terminally differentiated growth-plate chondrocytes release MVs [Kirsch, 2007]. Electron microscopic observations indicated that MVs could be formed by extrusion of preformed cytoplasmic structures in the extracellular matrix [Akisaka and Shigenaga, 1983; Akisaka et al., 1988]. The findings of Rabinovitch and Anderson [1976] favored other hypotheses of subunit secretion with an extracellular assembly and, above all, the budding from cellular processes. Then, Cecil and Anderson [1978] confirmed this last hypothesis that MVs appear to bud from the tips of plasma membrane microvilli of hypertrophic chondrocytes [Anderson, 1995]. Furthermore, MVs may arise from the membrane adjacent to newly formed extracellular matrix [Morris et al., 1992]. Cell surface microvilli of hypertrophic chondrocytes were found to be the precursors of MVs and the actin network appeared to be essential for their formation [Hale et al., 1983; Hale and Wuthier, 1987]. The aim of this work was to check whether MVs originate from microvilli of osteoblast lineage, as in the case of hypertrophic chondrocytes. Several models of cell cultures have been described in the literature to monitor mineralization and MV biogenesis [Golub et al., 1982; Anderson et al., 1990; Garimella et al., 2004]. Human osteosarcoma Saos-2 cells express the entire osteoblastic differentiation program from proliferation to mineralization [Hausser and Brenner, 2004], produce a collagenous extracellular matrix [McQuillan et al., 1995] and spontaneously release mineralization-competent MVs [Fedde, 1992]. Therefore, we selected Saos-2 cell cultures as a convenient model of osteoblastic mineralization to analyze the mechanisms involved in the release of MVs into the extracellular matrix. To this end, microvilli from apical Saos-2 cell plasma membrane were purified. Their protein and lipid compositions as well as their ability to mineralize were compared with those of MVs. The role of actin network in MV formation was investigated by using two drugs which affect microfilament polymerization and depolymerization [Hale and Wuthier, 1987]. Our findings confirmed that mineralizing osteoblast-like Saos-2 cells are polarized and that microvilli from apical plasma membrane are sites of origin of MVs. Moreover, the actin network depolymerization was found to enhance MV release from Saos-2 cells.

MATERIALS AND METHODS

Cell Culture and Stimulation for Mineralization

Human osteosarcoma Saos-2 cells (ATCC HTB-85) were cultured in McCoy's 5A (ATCC) supplemented with 100 U/mL penicillin, 100 g/mL streptomycin (both from Sigma) and 15 % FBS (v:v) (Gibco). The mineralization was induced by culturing the confluent cells (7 days to reach confluence) in growth medium supplemented with 50 g/mL ascorbic acid (AA) (Sigma) and 7.5 mM β-glycerophosphate (β-GP) (Sigma) [Gillette and Nielsen-Preiss. 2004, Vaingankar et al., 2004]. Concerning drug treatments, cell cultures were grown to confluence and treated with 200 ng/mL cytochalasin D (CCD) or 1 µg/mL phalloidin (PHL) (both from Sigma). Drugs were added to the media in dimethyl sulfoxide (DMSO). Control cultures received an equivalent amount of the solvent (0.05%, v:v).

Alkaline phosphatase activity assay

Tissue non-specific alkaline phosphatase activity was measured using *p*-nitrophenyl phosphate as substrate at pH 10.4 by recording absorbance at 420 nm ($\varepsilon_{p\text{-NP}}$ is equal to 18.8 $mM^{-1}.cm^{-1}$) [Cyboron and Wuthier, 1981]. Enzyme units are µmol of *p*-nitrophenolate released per min per mg of proteins.

Immunofluorescence and Confocal Microscopy

Saos-2 cells were cultured on cover slips at 37 C in 5 % CO_2 humidified atmosphere. Cells (10^5) were washed with PD buffer (125 mM NaCl, 5 mM KCl, 10 mM $NaHCO_3$, 1 mM KH_2PO_4, 10 mM glucose, 1 mM $CaCl_2$, 1 mM $MgCl_2$, 20 mM Hepes, pH 6.9) and fixed with 3 % (w:v) paraformaldehyde in PD buffer for 20 min at room temperature [Strzelecka-Kiliszek et al., 2008]. Fixed cells were incubated in 50 mM NH_4Cl in PD buffer (10 min, room temperature) and then, permeabilized with 0.08 % (v:v) Triton X-100 in PD buffer (5 min, 4°C). After additional washing, with PD buffer and TBS (130 mM NaCl, 25 mM Tris-HCl, pH 7.5), cells were incubated with a blocking solution, 5 % FBS in TBS (v:v) for 45 min at room temperature. Then, probes were incubated with mouse monoclonal anti-AnxA6 (1:100, v:v) (Transduction Laboratories) or rabbit polyclonal anti-cofilin-1 (1:50, v:v) (Sigma), diluted in TBS containing 0.5 % FBS (v:v) and 0.05 % Tween 20 (v:v). After 1 h of incubation at room temperature, the cells were washed and incubated for 1 h at room temperature with goat anti-mouse IgG-FITC (1:200, v:v) or goat anti-rabbit IgG-TRITC (1:100) (both from Sigma). After washing, the samples were mounted in Moviol 4-88/DABCO. Z-

section images were acquired with TCS SP2 confocal microscope (Leica). Resting and stimulated cells were identified and each cell type was quantified as percentage of cell population.

Calcium Nodule Detection

Cell cultures were washed with PBS and stained with 0.5 % (w:v) Alizarin Red-S (AR-S) in PBS (pH 5.0) for 30 min at room temperature [Vaingankar et al., 2004]. After washing 4 times with PBS to remove free calcium ions, stained cultures were photographed. Then, cell cultures were destained with 10% (w:v) cetylpyridinium chloride in PBS pH 7.0 for 60 min at room temperature [Stanford et al., 1995]. AR-S concentration was determined by measuring absorbance at 562 nm.

Preparation of Microvilli and Matrix Vesicles

Both preparations were performed simultaneously with the same cell cultures according to Wu et al. [1993] for MV preparation and Jimenez et al. [2004] for microvilli preparation with slight modifications. Saos-2 cell cultures were digested with 100 U/mL collagenase Type IA (Sigma) in Hank's balanced salt solution (HBSS: 5.4 mM KCl, 0.3 mM Na_2HPO_4, 0.4 mM KH_2PO_4, 0.6 mM $MgSO_4$, 137 mM NaCl, 5.6 mM D-glucose, 2.38 mM $NaHCO_3$, pH 7.4) at 37°C for 3 hours. Then cells were pelleted by centrifugation at 600 x *g* for 15 min. Supernatant was centrifuged at 20,000 x *g* for 20 min to sediment all the cell debris, nuclei, mitochondria and lysosomes. Supernatant was centrifuged at 80,000 x *g* for 60 min yielding pellet containing MVs.

Cells were homogenized in 5 mL of sucrose buffer in the presence of protease inhibitor cocktail (Sigma). The homogenate was then centrifuged twice at 10,000 x *g* for 15 min to sediment intact cells, cell debris, nuclei, mitochondria, lysosomes. To separate the microvillar membranes from the basolateral plasma membranes, the supernatant was supplemented with 12 mM $MgCl_2$, stirred at 4 °C for 20 min to induce basolateral membrane precipitation and centrifuged twice at 2,500 x *g* for 10 min to pellet aggregates of basolateral membranes. Supernatant was centrifuged at 12,000 x *g* for 60 min to pellet microvilli. Fractions containing MVs and microvilli (8.6 % sucrose, w:v) were overlaid on a sucrose step gradient made with 45 %/ 37 %/ 25 % (w:v) sucrose and centrifuged at 90,000 x *g* for 5 hours. The alkaline phosphatase activity was measured in fractions collected from sucrose gradient. The 25 % and 37 % sucrose fractions were collected, mixed, diluted tenfold in HBSS and centrifuged at 120,000 x *g* for 60 min. The protein concentration in the fractions was determined using the Bio-Rad Protein Assay.

SDS-PAGE and Immunoblot Analysis

Proteins of each fraction were separated on 8, 10 or 12 % (w:v) SDS-polyacrylamide gels [Laemmli, 1970] and then electro-transferred (Mini-ProteanII™ Kit, Bio-Rad) onto nitrocellulose membranes (Hybond™-ECL™, Amersham Biosciences) according to Towbin et al. [1979]. Nitrocellulose membranes were blocked with 5 % (w:v) milk in TBS for 1 hour at room temperature. The nitrocellulose membranes were then incubated with primary antibodies, i.e. mouse monoclonal anti-Na^+/K^+ ATPase (1:2500) (Abcam), mouse monoclonal anti-AnxA2 (1:2500) (Transduction Laboratories), mouse monoclonal anti-AnxA6 (1:5000) (Transduction Laboratories), mouse monoclonal anti-actin (1:2000) (Transduction Laboratories) or rabbit polyclonal anti-cofilin-1 (1:2000) (Sigma) prepared in 3 % (w:v) milk in TBS supplemented with 0.05 % (v:v) Tween 20 (TTBS) at 4 °C overnight. Nitrocellulose membranes were washed several times with TTBS and then incubated with secondary antibodies, i.e. sheep anti-mouse or anti-rabbit IgG conjugated with horseradish peroxidase (1:5000) (both from Amersham Biosciences) prepared in 3 % (w:v) milk in TTBS. Finally, the membranes were washed and immunoreactive bands were visualized by using ECL reagents according to the manufacturer's instructions (Amersham Biosciences).

Electron Microscopy

Microvilli and MVs were washed in PD buffer and fixed with 3 % (w:v) paraformaldehyde/1 % (w:v) glutaraldehyde mixture in 100 mM sodium phosphate buffer (pH 7.2) for 1 hour at room temperature [Strzelecka-Kiliszek et al., 2002]. After washing, samples were postfixed with 1% (w:v) osmium tetroxide in 100 mM sodium phosphate buffer (pH 7.2) for 20 min at room temperature and then dehydrated in a graded ethanol solution series at room temperature (25 % (v:v) for 5 min, 50 % (v:v) for 10 min, 75 % (v:v) for 15 min, 90 % (v:v) for 20 min, 100 % (v:v) for 30 min). Then, samples were incubated in mixtures of LR White resin/100% ethanol at volume ratios of 1:2 and 1:1 (each 30 min, at room temperature). Finally, samples were infiltrated twice with 100 % (v:v) LR White resin (Polysciences) for 1 hour at room temperature, moved to the gelatin capsule and polymerized at 56°C for 48 hours. 700-Å-sections were cut using an ultramicrotome LKB Nova, placed on formvar-covered and carbon-labeled 300 Mesh nickel grids (Agar Scientific Ltd). The sample-covered grids were counterstained with 2.5 % (w:v) uranyl acetate in ethanol for 1-1.5 hours at room temperature. Finally, the grids were washed in 50 % ethanol, then in water and stained with lead citrate for 2 min in NaOH atmosphere at room temperature, washed in water and dried [Strzelecka-Kiliszek et al., 2002]. The samples were observed by JEM-1200EX transmission electron microscopy (JEOL).

Lipid Composition

Total lipids of samples were extracted according to Folch et al. [1957] with slight modifications. Total lipids of samples (15 µg of proteins) were extracted in chloroform:methanol (2:1, by vol.). The organic phase was collected and washed 3 times in chloroform:methanol:H_2O (3:48:47, by vol.). The lipid composition of samples was determined by thin layer chromatography (Balcerzak et al., 2007). Phospholipids were separated by a first migration up to 12 cm from the origin of plates in ethyl acetate:1-propanol:chloroform:methanol:0.25 % (w:v) KCl (25:25:25:10:9, by vol.). Plates were completely dried. Then, other lipids were separated by a second migration up to 18 cm from the origin in heptane:isopropyl ether:acetic acid (75:21:4, by vol.). After complete drying, lipids spots were visualized by incubating plates in 10 % (w:v) $CuSO_4$/8 % (v:v) H_2SO_4 for 10 min and heating at 180 °C for 20 min. Chromatograms were scanned and analyzed by densitometry using ImageJ software (NIH).

Mineralization Assay

Aliquots of MVs and each membranous fraction obtained from cell fractionation were diluted to a final concentration of 20 µg of total proteins/mL in the mineralization buffer (100 mM NaCl, 12.7 mM KCl, 0.57 mM $MgCl_2$, 1.83 mM $NaHCO_3$, 0.57 mM Na_2SO_4, 3.42 mM NaH_2PO_4, 2 mM $CaCl_2$, 5.55 mM D-glucose, 63.5 mM sucrose and 16.5 mM TES (pH 7.4). Samples were incubated at 37 °C for 6 hours. The mineral complexes were centrifuged at 3,000 x *g* for 10 min and washed several times with water. The final pellets were dried and incorporated by pressing into 100 mg of KBr. Mineral compositions were determined using a Nicolet 510M Infrared spectrometer (Nicolet) equipped with a DTGS detector; 64 interferograms were recorded at a 4 cm^{-1} optical resolution.

FACScan Analysis

Dead cells were identified by the propidium iodide staining [Krishan, 1975]; 10^6 cells were incubated in 0.25 % Trypsin (w:v)/0.03 % EDTA (w:v) (Sigma), washed twice in PBS and centrifuged at 600 x *g* for 10 min. Then cells were suspended in 2 mL propidium iodide-solution (50 g/mL propidium iodide in PBS), incubated for 5 min at room temperature and used directly for flow analysis of propidium iodide fluorescence. For evaluation of cell apoptosis by propidium iodide staining [Dressler, 1988], 10^6 cells were trypsinized and centrifuged at 2,500 x *g* for 5 min. Pellet was suspended in 0.2 mL PBS and added directly to 0.5 mL of pure cold ethanol (-20°C) to a final concentration of 70 % (v:v) and fixed overnight at -20°C. After fixation, cells were centrifuged at 1,500 x *g* for 5 min and the pellet was suspended in 0.5 mL propidium iodide-solution (50 g/mL

propidium iodide/0.1 mg/mL RNAse A/0.05 % (v:v) Triton X-100 in PBS) and incubated for 45 min at 37°C. After incubation, cells were centrifuged at 1,500 x *g* for 5 min and the pellet was suspended in 2 mL of PBS and used for flow analysis of propidium iodide fluorescence. The propidium iodide fluorescence was monitored by FACScan flow cytometer (Becton-Dickinson) using Cell Quest software (Becton-Dickinson).

RESULTS

Differentiation of Saos-2 Cell and Mineralization

Saos-2 cells cultured in McCoy's 5A medium containing 0.9 mM Ca^{2+} and 4.2 mM P_i produced apparent calcium nodules characteristic of osteoblastic mineralization as detected by AR-S staining (Fig. 1A, B). Ascorbic acid (AA) and β-glycerophosphate (β-GP) are two osteogenic factors commonly used to stimulate osteoblastic differentiation and mineralization [Gillette and Nielsen-Preiss. 2004, Vaingankar et al., 2004]. As expected, the mineral deposition was highly enhanced by the concomitant addition of 50 µg/mL AA and 7.5 mM β-GP in Saos-2 cell cultures (Fig. 1A). Resting Saos-2 cells produced within 9 days the same amount of calcium minerals as stimulated Saos-2 cells within 3 days (Fig. 1B).

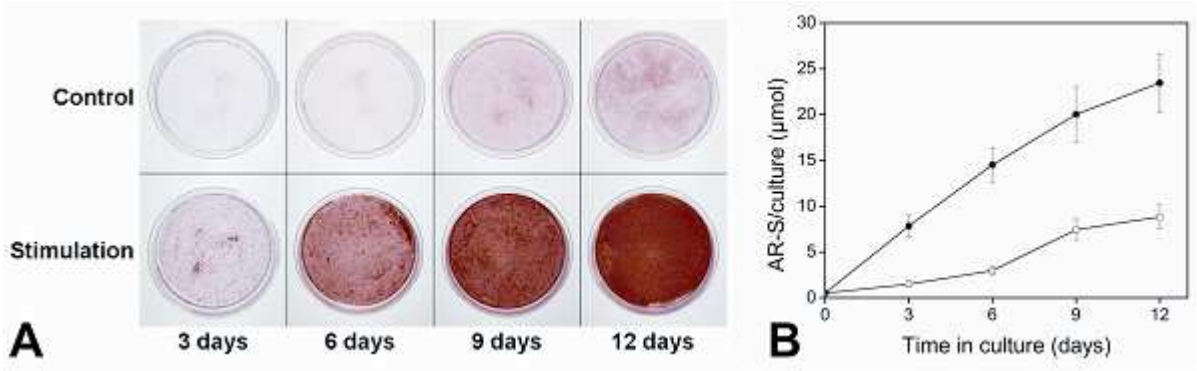

Figure 1. Mineralization by Saos-2 cells. Saos-2 cells were incubated at the indicated time under normal conditions or stimulated with 50 µg/mL ascorbic acid (AA) and 7.5 mM β-glycerophosphate (β-GP). (A) Non-stimulated and stimulated cell cultures were stained with AR-S to detect calcium nodules and photographed. (B) AR-S was solubilized in control (□) and stimulated (●) cell cultures by cetylpyridinium chloride and quantified at 562 nm (Results are mean ± SD, n=3).

To evaluate the Saos-2 cell differentiation induced by AA and β-GP, cellular specific TNAP activity, MV biogenesis, AnxA6 localization and cellular morphology were compared between untreated and treated cells. TNAP is a metalloenzyme which provides P_i from various phosphorylated substrates during mineralization. Following the treatment with AA and β-GP, TNAP activity of Saos-2 cells increased with culture time in comparison to untreated cells (Fig. 2). AnxA6 belongs to a large family of Ca^{2+}- and lipid-binding proteins which are involved in Ca^{2+} homeostasis in bone cells and in extracellular MVs. Immunocytochemistry revealed that most of the resting Saos-2 cells exhibited a fusiform or fibrobast-like shape with a characteristic nuclear exclusion of AnxA6 (Fig. 3A, control), consistent with a cytoplasmic and membrane localization. However, a few cells were retracted, became round and displayed a cytoplasmic location of AnxA6 and an enrichment of AnxA6 in plasma membrane-bound vesicles (Fig. 3A, control). Some Saos-2 cells exhibiting this phenotype increased in

the presence of AA and β-GP (Fig. 3A, stimulation) in a time-dependent manner (Fig. 3C), suggesting a differentiated state favoring mineralization. From the previous findings of Hale and Wuthier [1987] on hypertrophic chondrocytes, we hypothesized that Saos-2 cell apical microvilli facing the bone forming side are the precursors of MVs.

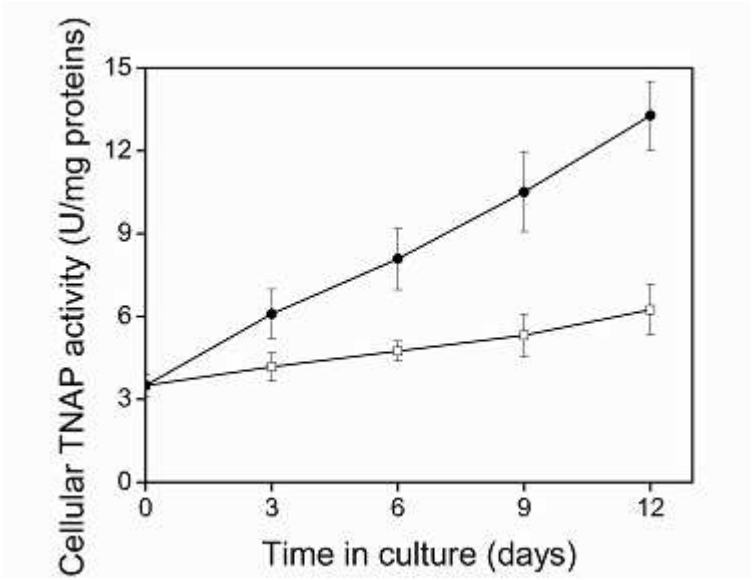

Figure 2. Tissue non-specific alkaline phosphatase activity in Saos-2 cells. Saos-2 cells were grown under normal conditions (control) or were stimulated with 50 µg/mL AA and 7.5 mM β-GP for different incubation times. Tissue non-specific alkaline phosphatase activities of control (□) and stimulated (●) cells were measured every 3 days and are expressed as U/mg cellular protein (Results are mean ± SD, n=3).

Saos-2 Cell Microvilli as Precursors of Matrix Vesicles

Apical microvilli were isolated from Saos-2 cells according to the method of Jimenez et al. [2004] used to isolate microvilli from human placental syncytiotrophoblast. It consisted of the Mg^{2+}-induced precipitation in which non-microvillar membranes were aggregated and could be separated from vesicular microvilli by a low-speed centrifugation. Morphology of microvilli and MVs were compared by electron microscopy. MVs were identified as closed, spherical vesicle structures delimited by a characteristic trilaminar membrane [Fedde, 1992], with a diameter ranging from 100 to 500 nm (Fig. 4A, B). Microvilli were found to rearrange in round vesicle-like structures during their preparation (Fig. 4C, D). These microvillar vesicles of 100-300 nm diameter range were delimited by a trilaminar membrane (Fig. 4C, D), showing a morphology similar to that of MVs. The ability of MVs, microvilli and other membranous fractions from Saos-2 cells to mineralize was checked by incubating the samples in mineralization buffer at 37 °C. After 6 hours of incubation, the samples were centrifuged and the resulting pellets were analyzed by infrared spectroscopy. MVs and microvillar rearranged vesicles were both able to induce the formation of hydroxyapatite (HA) under these conditions as probed by infrared spectroscopy (Fig. 5). The amount of HA minerals formed by microvilli (Fig. 5,

bottom trace) was lower than the amount produced by MVs (Fig. 5, middle trace). In contrast, no other fractions from Saos-2 cells produced HA.

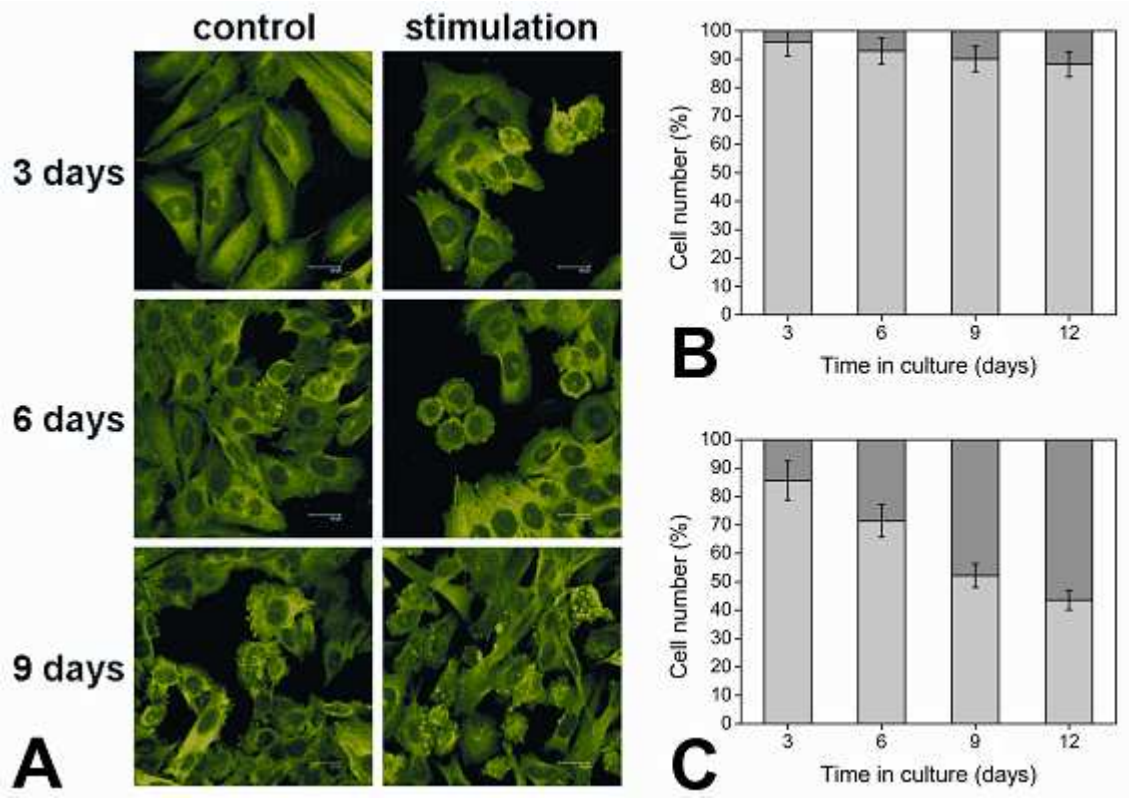

Figure 3. Cellular morphology and annexin A6 distribution in Saos-2 cells. Saos-2 cells were grown under normal conditions (control) or stimulated (stimulation) with 50 µg/mL AA and 7.5 mM β-GP for different incubation times directly on cover slips. AnxA6 was stained by immunocytochemistry and detected by confocal microscopy in control and stimulated Saos-2 cells cultured for 12 days. Two phenotypes were observed - resting cells and differentiated cells - and quantified in control (B) and stimulated (C) cell cultures every 3 days and are presented as percentage of cell population (control cells in light gray, differentiated cells in dark gray). (Results are mean ± SD, n=3).

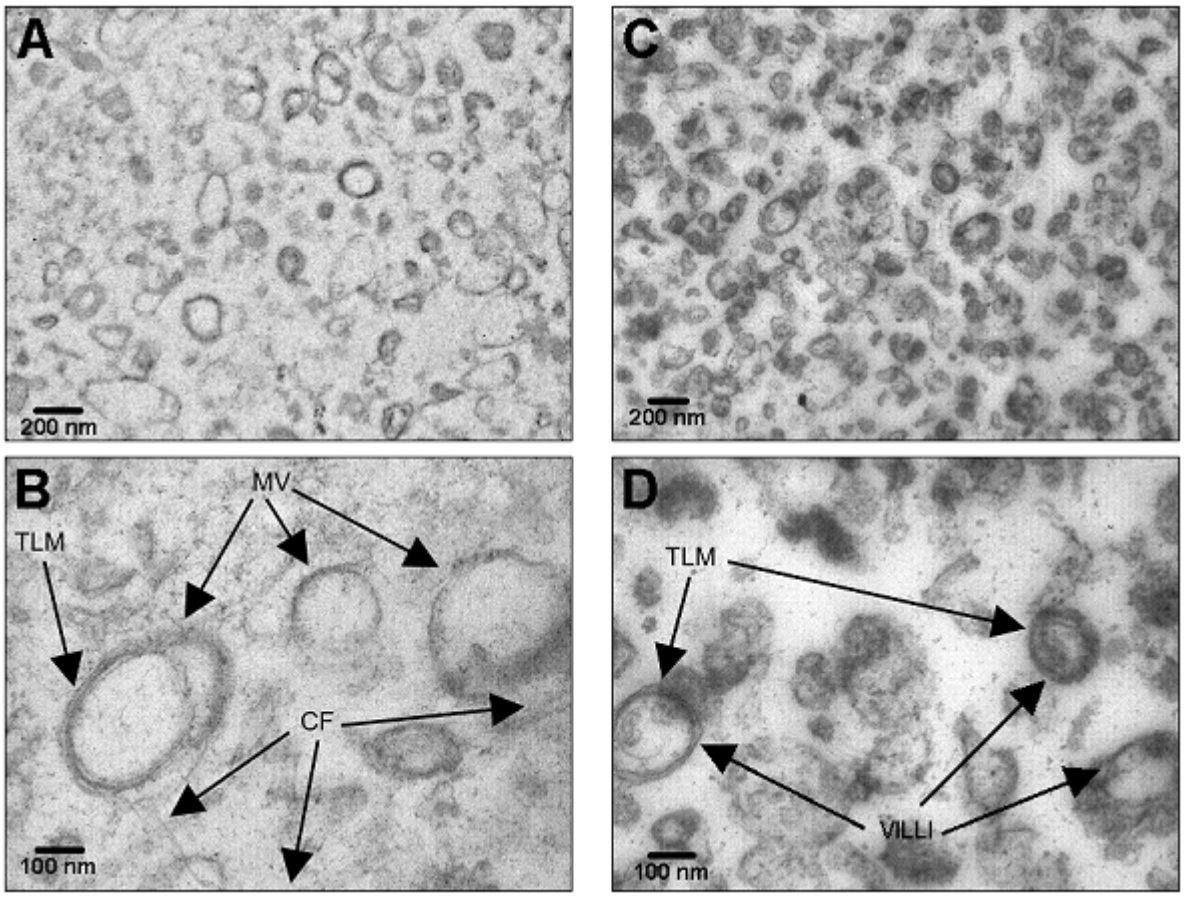

Figure 4. Ultrastructural morphology of matrix vesicles and microvilli. MV, matrix vesicle (A, B); VILLI, microvilli (C, D); trilaminar membranes were evidenced (TLM); CF stands for collagen fibrils. (Magnifications: A and C, x 20,000; B and D, x 50,000).

Saos-2 Cell Microvilli and Matrix Vesicles Exhibited Similar Protein and Lipid Composition

The lipid composition of MVs was compared with that of Saos-2 cell basolateral membranes and microvilli. The lipid content of MVs and that of microvilli were almost identical (Table I). Expressed as apparent percentage of total lipids, MVs and microvilli were enriched in cholesterol and contained less triacylglycerols and monoacylglycerols than basolateral membrane fraction (Table I). Free cholesterol consisted of about 46.7 % and 45.9 % of total MV and microvillar lipids, respectively (Table I). The phospholipid composition of MVs and microvilli were nearly identical with ~36 % of phosphatidylethanolamine (PE), ~26.5 % of phosphatidylcholine (PC), ~3.5 % of phosphatidic acid, ~7 % of phosphatidylinositol, ~16.5 % of phosphatidylserine (PS) and ~11 % of sphingomyelin (SM) (Table II). The amounts of PE and PC in MVs and microvilli were lower than those in basolateral membranes, whereas the amounts of PS and SM were higher in MVs and microvilli than those in basolateral membranes (Table II). Thus, MVs and microvilli obtained from Saos-2 cell cultures indicated enriched contents in cholesterol, PS and SM as in the case of MV produced by epiphyseal cartilage cells [Wuthier, 1975] or by hypertrophic chondrocytes [Glaser and Conrad, 1981].

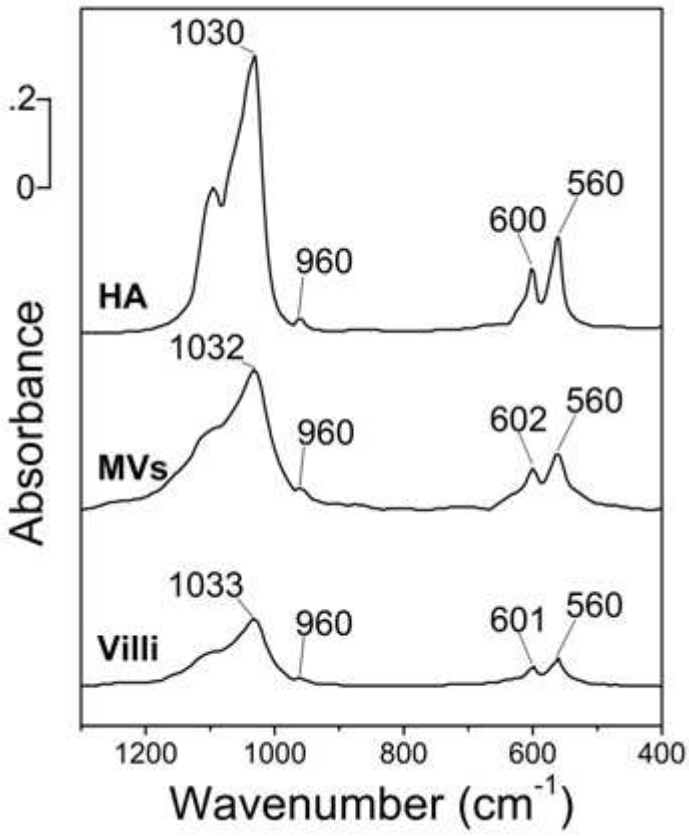

Figure 5. Infrared spectra of minerals formed by matrix vesicles and microvilli. MVs and microvilli from Saos-2 cells were incubated at 37 °C in mineralization buffer for 6 hours, then the minerals formed were collected, washed and analyzed by infrared spectroscopy. Infrared spectrum of hydroxyapatite as control (HA); Infrared spectrum of minerals formed by matrix vesicles (MVs) and by microvilli (Villi). Infrared spectra of minerals indicated that the minerals formed by MVs and microvilli were hydroxyapatite. (Typical infrared spectra among two independent measurements).

The protein profile of MV was also compared with that of the other membranous fractions obtained from Saos-2 cells (Fig. 6A). The distribution of MV proteins (Fig. 6A, lane 6) closely resembled that of microvillar proteins (Fig. 6A, lane 4) but was different from that of other fractions (Fig. 6A, lanes 1, 2, 3 and 5). MV and microvillar protein profiles exhibited similar major bands with apparent molecular weights of: 115, 85, 72, 50, 45, 38, 36, 34, 33, 30 and 24 kDa (Fig. 6A, lanes 4 and 6). The immunodetection of Na^+/K^+ ATPase, AnxA6 and AnxA2 (Fig. 6B) indicated that they were enriched and TNAP activity was higher (Fig. 6C) in microvilli and MVs as compared to the other fractions. Thus, microvilli and MVs exhibited similar lipid and protein compositions.

TABLE I. Lipid composition of basolateral membrane, microvilli and matrix vesicles.

	BLM	Microvilli	MVs
	% of total lipids		
TAG	24.4 ± 1.6	14.8 ± 2.4	14.3 ± 1.2
FFA	23.7 ± 1.9	23.6 ± 2.2	22.1 ± 1
CHOL	27.5 ± 1.5	45.9 ± 3.6	46.7 ± 3.2
DAG	10.2 ± 1.2	10.2 ± 0.8	10 ± 0.9
MAG	14.2 ± 1	5.5 ± 0.6	6.8 ± 0.9

BLM, basolateral membranes; Microvilli (from apical membranes); MVs, matrix vesicles; TAG, triacylglycerols; FFA, free fatty acids; CHOL, cholesterol; DAG, diacylglycerols; MAG, monoacylglycerols. Chromatogram scans were analyzed by densitometry using ImageJ software. Values are expressed as apparent percentages (intensity of the lipid to intensity of all lipids). (Results are mean ± SD, n=3).

TABLE II. Phospholipid composition of basolateral membrane, microvilli and matrix vesicles.

	BLM	Microvilli	MVs
	% of total phospholipids		
PE	38.1 ± 2.6	35.9 ± 2.5	35.8 ± 1.9
PA	5.1 ± 1.1	3.4 ± 0.3	3.5 ± 0.6
PI	9.9 ± 0.9	7.4 ± 1.5	6.7 ± 0.3
PS	9.9 ± 0.4	16.4 ± 1.2	16.3 ± 1.3
PC	32.6 ± 1.8	26.9 ± 2.2	26.2 ± 1
SM	4.4 ± 0.6	9.9 ± 0.9	11.5 ± 1

BLM, basolateral membranes; Microvilli (from apical membranes); MVs, matrix vesicles; PE, phosphatidylethanolamine; PA, phosphatidic acid; PI, phosphatidylinositol; PS, phosphatidylserine; PC, phosphatidylcholine; SM, sphingomyeline. Chromatogram scans were analyzed by densitometry using ImageJ software. Values are expressed as apparent percentages (intensity of the lipid to intensity of all phospholipids). (Results are mean ± SD, n=3).

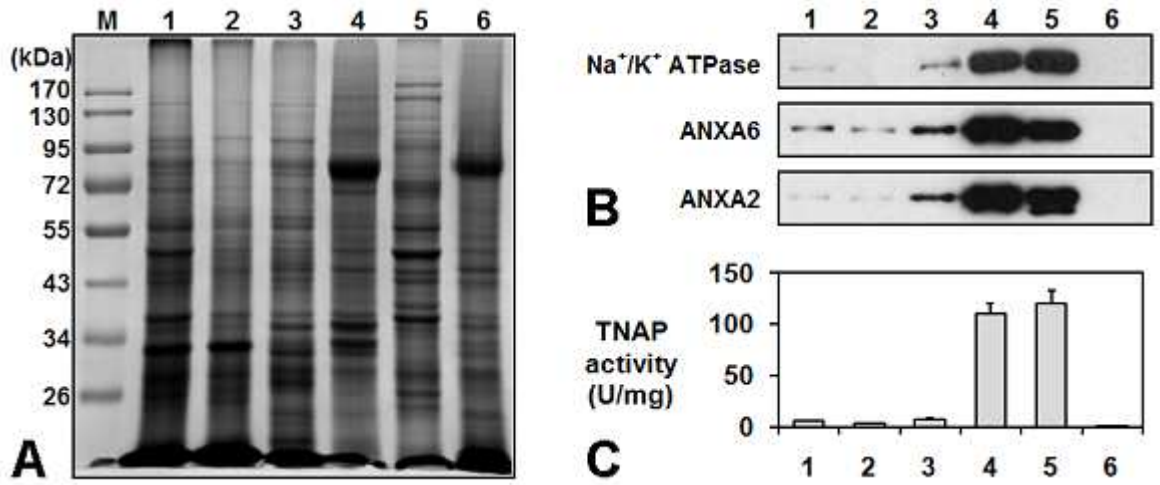

Figure 6. Protein profiles of mineralizing Saos-2 cells, cell fractions and matrix vesicles. (A) Protein profiles analyzed by 10 % SDS- PAGE followed by Coomassie brilliant blue staining of intact Saos-2 cells (lane 1); cell debris, nuclei, mitochondria, lysosomes (lane 2); basolateral membranes (lane 3); microvilli (lane 4); microsomal and cytoplasmic fractions (lane 5); and MVs (lane 6) (Typical gel among five independent measurements). (B) Detection of Na^+/K^+ ATPase, AnxA6 and AnxA2 by Western Blotting and (C) alkaline phosphatase activity in intact Saos-2 cells (lane 1); cell debris, nuclei, mitochondria, lysosomes (lane 2); basolateral membranes (lane 3); microvilli (lane 4); MVs (lane 5); and final supernatant (lane 6). (Typical Western Blot among five independent measurements), (Results are mean ± SD, n=10).

Role of Actin Depolymerization in Matrix Vesicle Release from Saos-2 cells

It has been reported that the release of MVs from cultured epiphyseal chondrocytes was correlated with changes in cellular actin distribution [Hale et al., 1983]. Therefore, we assessed the role of the actin network in MV formation by osteoblast-like Saos-2 cells. Cofilin-1 controls reversibly actin polymerization and depolymerization in a pH-sensitive manner [Pope et al., 2004]. The actin-binding protein co-localized with AnxA6 in control Saos-2 cells (Fig. 7A, control) and especially at the periphery of stimulated Saos-2 cells (Fig. 7A, stimulation). Moreover, the immunodetection of cofilin-1 and actin revealed their presence in both MV and microvillar fractions (Fig. 7B). This suggested that actin microfilaments are involved in MV biogenesis. Therefore, we investigated whether actin polymerization or depolymerization could affect MV formation by monitoring the release of MVs from Saos-2 cells treated with actin-perturbing drugs: cytochalasin D or phalloidin which are known to inhibit microfilament assembly or disassembly, respectively [Hale and Wuthier, 1987]. In parallel, we examined effects of combined AA and β-GP with cytochalasin D or phalloidin on cell viability (Fig. 8A) and cell apoptosis (Fig. 8B) by FACScan using propidium iodide staining. Six days of stimulation with AA and β-GP decreased the cell viability from 70 to 55 % (Fig. 8A). The rate of apoptosis in the case of stimulated cells was about 40 %, i.e. twice as high as for control cells (Fig. 8B). Furthermore, the stimulation of Saos-2 cells using these two osteogenic factors led to an increased release of MVs as

shown in Figure 9. These findings suggested that AA and β-GP induced terminal differentiation of Saos-2 cells were able to mineralize and this is consistent with the fact that mineralization is accompanied by osteoblast apoptosis [Anderson, 1995]. The cell viability of stimulated cells treated with phalloidin was not affected (Fig. 8A) whereas the treatment with cytochalasin D increased cell apoptosis from 40 % to ~75 % (Fig. 8B). Phalloidin, which stabilizes actin microfilament, did not affect significantly the production of MVs from treated stimulated Saos-2 cells while cytochalasin D, which inhibits the actin microfilament formation, enhanced MV formation (Fig. 9). The protein profiles of MVs from Saos-2 cells treated with or without cytochalasin D or phalloidin were identical, except for high levels of actin in MVs obtained from cells treated with phalloidin (results not shown). This demonstrates that the mechanism of MV formation from Saos-2 cells involved actin microfilament depolymerization.

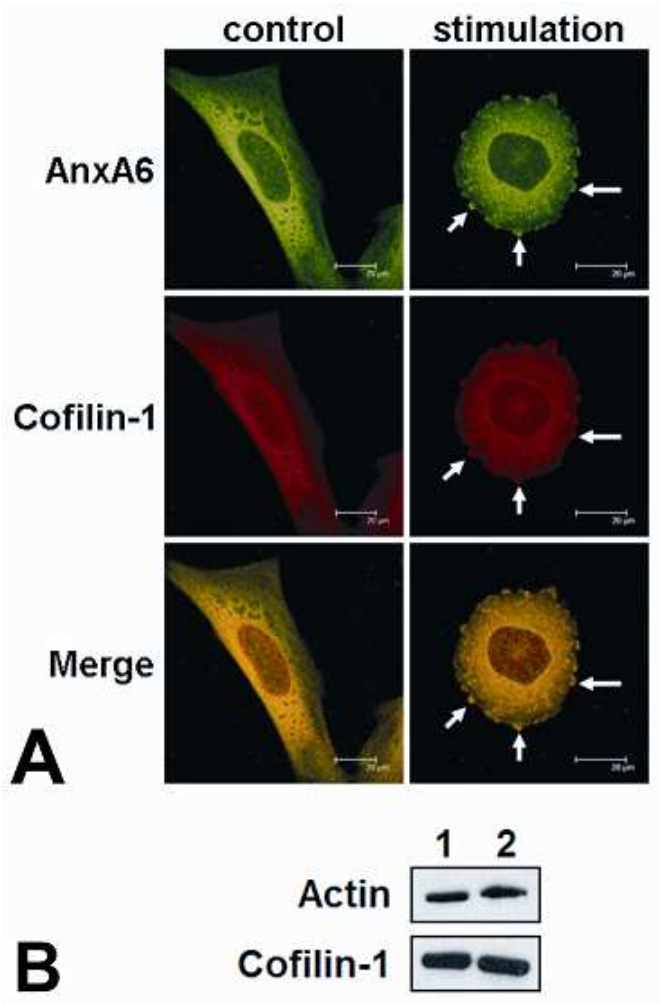

Figure 7. Localization of AnxA6 and cofilin-1 in Saos-2 cells. Saos-2 cells were cultured under normal conditions or stimulated with 50 µg/mL AA and 7.5 mM β-GP for 6 days directly on cover slips. (A) AnxA6 (green) and cofilin-1 (red) were stained by immunocytochemistry and detected by confocal microscopy in control and stimulated Saos-2 cells. Merge pictures (yellow) evidenced co-localization of AnxA6 and cofilin-1. Plasma membrane extrusions of stimulated Saos-2 cells are indicated with white arrows. (B) Detection of actin and cofilin-1 by Western Blotting in microvilli (lane 1) and MVs (lane 2). (Results are mean ± SD, n=3).

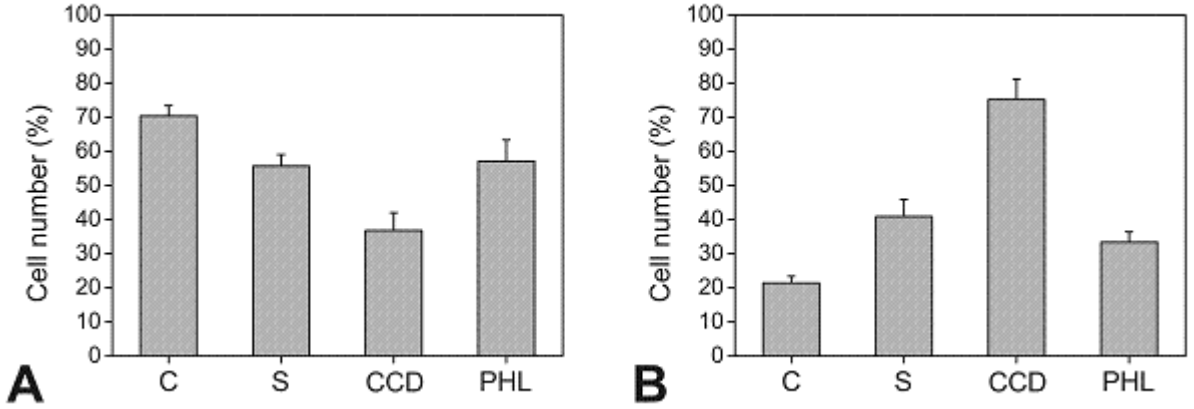

Figure 8. Cell viability and apoptosis of Saos-2 cells. Saos-2 cells were maintained under normal conditions (C), stimulated (S) with 50 µg/mL AA and 7.5 mM β-GP or stimulated and treated with cytochalasin D (CCD) or phalloidin (PHL) for 6 days. Cell viability (A) and cell apoptosis (B) were determined by propidium iodide staining and FACScan analysis and are presented as percentage of cell population. (Results are mean ± SD, n=3).

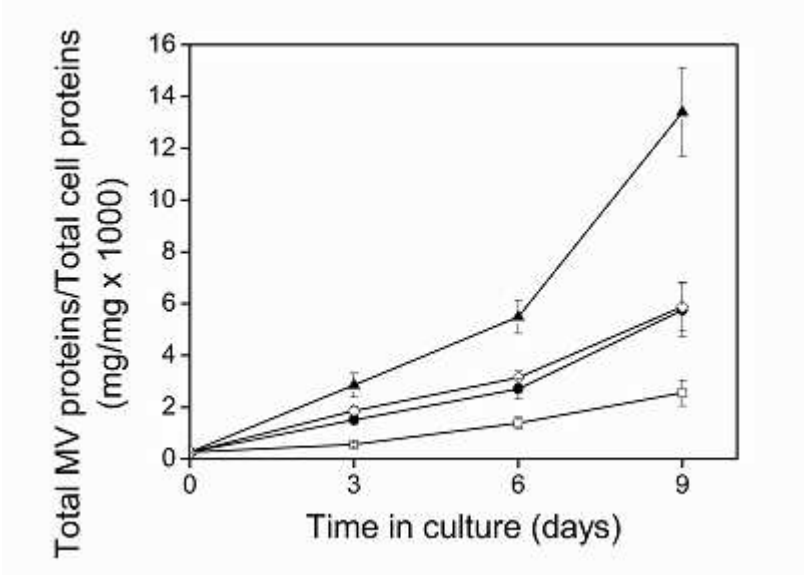

Figure 9. Matrix vesicle formation from Saos-2 cells. Saos-2 cells were maintained under normal conditions (□), stimulated (●) with 50 µg/mL AA and 7.5 mM β-GP or stimulated and treated with cytochalasin D (▲) or phalloidin (◊) for different incubation times. MV release from Saos-2 cells was monitored as a ratio of total MV protein/total cellular protein. (Results are mean ± SD, n=3).

DISCUSSION

Ascorbic Acid and β-Glycerophosphate Induce Saos-2 Cell Differentiation and Release of MVs

Human osteosarcoma Saos-2 cells served as a model of pro-mineralizing cells, permitting us to determine the site of MV origin and the mechanisms leading to their release in the extracellular matrix. Osteoblast-mediated osteogenesis is divided into three main phases: 1) cell proliferation, 2) extracellular matrix deposition and maturation, and 3) mineralization [Owen et al., 1990; Manduca et al., 1997]. Saos-2 cells express the entire osteoblastic differentiation sequence from proliferation to mineralization [Hausser and Brenner, 2004]. They produce a collagenous extracellular matrix [McQuillan et al., 1995] and spontaneously release mineralization-competent MVs [Fedde, 1992]. AA and β-GP are commonly employed to stimulate osteoblastic differentiation and mineralization [Ecarot-Charrier et al., 1983; Nefussi et al., 1985; Quarles et al., 1992; Gillette and Nielsen-Preiss. 2004, Vaingankar et al., 2004]. In the present work, we used AA and β-GP simultaneously to stimulate Saos-2 cell-mediated mineralization (Fig. 1) and this was associated with changes in Saos-2 cell differentiation: TNAP activity was enhanced (Fig. 2), AnxA6 was enriched in the plasma membrane extensions (Fig. 3A) and Saos-2 cell became spherical (Fig. 3A). These findings are consistent with earlier reports on osteoblast differentiation induced by concomitant addition of AA and β-GP [Ecarot-Charrier et al., 1983; Nefussi et al., 1985; Quarles et al., 1992; Gillette and Nielsen-Preiss. 2004, Vaingankar et al., 2004]. AA is an exogenous osteogenic factor that stimulates the sequential differentiation of osteoblasts [Harada et al., 1991; Franceschi and Iyer, 1992; Quarles et al., 1992]. It has been shown that AA enhanced osteoblast proliferation which is mediated through its stimulatory effect on the collagen synthesis [Harada et al., 1991]. Franceschi and Iyer [1992] demonstrated that AA induced a temporal osteoblastic differentiation of MC3T3-E1 cells in culture: 1) The collagen synthesis and deposition is stimulated by the increase of type I procollagen expression and processing of procollagens to collagens. 2) During the mineralization phase, TNAP expression and activity are enhanced, and osteocalcin synthesis is induced. 3) These changes of marker gene expression were shown to be accompanied by changes of osteoblast shape: from fusiform to cuboidal shape [Quarles et al., 1992]. β-GP displays synergic action with AA to stimulate collagen accumulation and TNAP activity [Quarles et al., 1992]. It is also required for matrix mineralization by providing P_i after its hydrolysis by TNAP [Nefussi et al., 1985; Bellows et al., 1991; Anagnostou et al., 1996]. Moreover, P_i released from β-GP hydrolysis can act as a messenger for osteoblast differentiation [Conrads et al., 2005]. In addition to these effects of AA and β-GP, we found that they also stimulated the release of MVs from mineralizing Saos-2 cells (Fig. 9), which contributed to the increase of matrix mineralization. The stimulation with AA and β-GP induced a parallel significant increase of Saos-2 cell apoptosis (Fig. 8B). This was consistent with the fact that the differentiation state of mineralizing

Saos-2 cells was terminal and that cells died by apoptosis. Since local enrichment of AnxA6 in the plasma membrane could signal the origin of MVs, we decided to determine whether apical microvilli of Saos-2 cells were the precursors of MVs in the plasma membrane.

Matrix Vesicles Are Formed From Saos-2 Cell Microvilli

A well-established method for the purification of microvilli from human placental syncytiotrophoblast [Jimenez et al., 2004] served to purify microvilli from osteoblast-like Saos-2 cells. This method was very effective as revealed by the high enrichment of TNAP activity, a microvillar marker enzyme (Fig. 6C). The MV fraction was obtained simultaneously from cell cultures by collagenase digestion and several differential centrifugation steps. Microvilli and MVs were both enriched in TNAP activity in the same range (Fig. 6C). During the preparation, microvilli formed vesicles as observed by electron microscopy (Fig. 4C, D), exhibiting identical spherical shapes with the same diameter ranges and analogous trilaminar membranous layers as in the case of MVs (Fig. 4A, B). Microvilli and MVs from Saos-2 cell cultures were able to form HA within 6 hours in the presence of Ca^{2+} ions and P_i, while other subcellular membranous fractions did not (Fig. 5). This functional similarity could originate from structural similarity. Therefore, the lipid and protein compositions of MVs and microvilli were compared. MVs were enriched in several proteins associated with mineralization (Fig. 6B, lane 5): annexins (AnxA2 and AnxA6) which are involved in Ca^{2+} homeostasis by mediating Ca^{2+} influx into MVs [Kirsch et al., 2000, Wang and Kirsch, 2002; Wang et al., 2005]; Na^+/K^+ ATPase [Hsu and Anderson, 1996] and TNAP [Anderson, 2004], implicated in the P_i homeostasis. Microvilli were also enriched in these proteins (Fig. 6B, lane 4). In addition, protein profiles of MVs and microvilli were similar (Fig. 6A, lanes 4 and 6). Phospholipid composition of MVs was identified for the first time by Wuthier [1975]. Negatively charged PS and annexins act as nucleators of Ca^{2+} and P_i [Wu et al., 1993; 1996; Genge et al., 2007; Genge et al., 2008]. Our MVs and microvilli exhibited a significant higher enrichment in PS than in basolateral membrane of Saos-2 cells (Table II). The apparent lipid composition of MVs isolated from Saos-2 cell cultures was not exactly the same as MVs isolated from growth plate cartilage [Wuthier, 1975] or hypertrophic chondrocyte cultures [Hale and Wuthier, 1987], but showed similar characteristics such as enriched contents in PS, SM and cholesterol (Tables I and II). The lipid and phospholipid compositions of isolated MVs and microvilli were very similar (Tables I and II). These findings are consistent with those reported by Hale and Wuthier [1987] showing that hypertrophic chondrocyte microvilli were the precursors of MVs. We found that cofilin-1, an actin binding protein, was co-localized with AnxA6, especially in plasma membrane extrusions in the case of stimulated cells, and that cofilin-1 as well as actin were both present in microvilli and MVs (Fig. 7). Second, cytochalasin D, an inhibitor of actin microfilament polymerization, stimulated MV formation by Saos-2 cells but not phalloidin which

stabilized actin polymerization (Fig. 9). Our findings indicated that actin depolymerization was involved in mineralization-competent MV formation and that the morphological and structural characteristics of MVs were similar to those of apical microvilli suggesting that MVs derived from apical microvilli of mineralizing Saos-2 cells. This was also previously observed in the case of hypertrophic chondrocytes and it was concluded that MVs derived from microvilli [Hale and Wuthier, 1987]. Taken together, these findings suggest that the microvillar origin of MV is common in various cell types such as osteoblast-like cells and hypertrophic chondrocytes. Pathological calcification is a process that has similarities with bone formation [Kirsch, 2007; van de Lest and Vaandrager, 2007]. Therefore, it is tempting to propose that formation of MVs under physiological conditions may follow the same mechanisms that trigger the vesicular release from microvillar regions of other cells under pathological conditions leading to ectopic mineralization.

ACKNOWLEDGEMENTS

We thank Dr. John Carew for correcting the English. This work was supported by a grant N301 025 32-1120 from Polish Ministry of Science and Higher Education, by a Polonium grant (05819NF), by CNRS (France), and by the Rhône-Alpes region.

REFERENCES

Akisaka T, Shigenaga Y. 1983. Ultrastructure of growing epiphyseal cartilage processed by rapid freezing and freeze-substitution. J Electron Microsc 32:305-320.

Akisaka T, Kawaguchi H, Subita GP, Shigenaga Y, Gay CV. 1988. Ultrastructure of matrix vesicles in chick growth plate as revealed by quick freezing and freeze substitution. Calcif Tissue Int 42:383-393.

Anagnostou F, Plas C, Nefussi JR, Forest N. 1996. Role of beta-GP-derived P_i in mineralization via ecto-alkaline phosphatase in cultured fetal calvaria cells. J Cell Biochem 62:262-274.

Anderson HC. 1967. Electron microscopic studies of induced cartilage development and calcification. J Cell Biol 35:81-101.

Anderson HC, Stechschulte DJ, Collins DE, Jacobs DH, Morris DC, Hsu HHT, Redford PA, Zeiger S. 1990. Matrix vesicle biogenesis in vitro by rachitic and normal rat chondrocytes. Am J Pathol 136:391-398.

Anderson HC. 1995. Molecular biology of matrix vesicles. Clin Orthop Relat Res 314:266-280.

Anderson HC. 2003. Matrix vesicles and calcification. Curr Rheumatol Rep 5:222-226.

Anderson HC, Sipe JB, Hessle L, Dhanyamraju R, Atti E, Camacho NP, Millán JL. 2004. Impaired calcification around matrix vesicles of growth plate and bone in alkaline phosphatase-deficient mice. Am J Pathol 164:841-847.

Balcerzak M, Hamade E, Zhang L, Pikula S, Azzar G, Radisson J, Bandorowicz-Pikula J, Buchet R. 2003. The roles of annexins and alkaline phosphatase in mineralization process. Acta Biochim Pol 50:1019-1038.

Balcerzak M, Pikula S, Buchet R. 2007. Phosphorylation-dependent phospholipase D activity of matrix vesicles. FEBS Lett 580:5676-5680.

Bellows CG, Aubin JE, Heersche JN. 1991. Initiation and progression of mineralization of bone nodules formed in vitro: the role of alkaline phosphatase and organic phosphate. Bone Miner 14:27-40.

Buckwalter JA, Cooper RR. 1987. Bone structure and function. Instr Course Lect 36:27-28.

Cecil RN, Anderson HC. 1978. Freeze-fracture studies of matrix vesicle calcification in epiphyseal growth plate. Metab Bone Dis 1:89-97.

Conrads KA, Yi M, Simpson KA, Lucas DA, Camalier CE, Yu LR, Veenstra TD, Stephens RM, Conrads TP, Beck GR Jr. 2005. A combined proteome and microarray investigation of inorganic phosphate-induced pre-osteoblast cells. Mol Cell Proteomics 4:1284-1296.

Cyboron GW, Wuthier RE. 1981. Purification and initial characterization of intrinsic membrane-bound alkaline phosphatase from chicken epiphyseal cartilage. J Biol Chem 256:7262-7268.

Dressler LG. 1988. DNA flow cytometry and prognostic factors in 1331 frozen breast cancer specimens. Cancer 61:420-427.

Ecarot-Charrier B, Glorieux FH, Van Der Rest M, Pereira G. 1983. Osteoblasts isolated from mouse calvaria initiate matrix mineralization in culture. J Cell Biol 96:639-643.

Fedde KN. 1992. Human osteosarcoma cells spontaneously release matrix-vesicle-like structures with the capacity to mineralize. Bone Miner 17:145-151.

Folch J, Lees M, Sloane Stanley GH. 1957. A simple method for the isolation and purification of total lipids from animal tissues. J Biol Chem 226:497-509.

Franceschi RT, Iyer BS. 1992. Relationship between collagen synthesis and expression of the osteoblast phenotype in MC3T3-E1 cells. J Bone Miner Res 7:235-246.

Garimella R, Bi X, Camacho N, Sipe JB, Anderson HC. 2004. Primary culture of rat growth plate chondrocytes: an in vitro model of growth plate histotype, matrix vesicle biogenesis and mineralization. Bone 34:961-970.

Genge BR, Wu LN, Wuthier RE. 2007. In vitro modeling of matrix vesicle nucleation: synergistic stimulation of mineral formation by annexin A5 and phosphatidylserine. J Biol Chem 282:26035-26045.

Genge BR, Wu LN, Wuthier RE. 2008. Mineralization of biomimetic models of the matrix vesicle nucleation core: Effect of lipid composition and modulation by cartilage collagens J Biol Chem Feb 4 [Epub ahead of print].

Gillette JM, Nielsen-Preiss SM. 2004. The role of annexin 2 in osteoblastic mineralization. J Cell Sci 117:441-449.

Glaser JH, Conrad HE. 1981. Formation of matrix vesicles by cultured chick embryo chondrocytes. J Biol Chem 256:12607-12611.

Golub EE, Schattschneider SC, Berthold P, Burke A, Shapiro IM. 1983. Induction of chondrocyte vesiculation in vitro. J Biol Chem 258:616-621.

Hale JE, Chin JE, Ishikawa Y, Paradiso PR, Wuthier RE. 1983. Correlation between distribution of cytoskeletal proteins and release of alkaline phosphatase-rich vesicles by epiphyseal chondrocytes in primary culture. Cell Motil 3:501-512.

Hale JE, Wuthier RE. 1987. The mechanism of matrix vesicle formation. Studies on the composition of chondrocyte microvilli and on the effects of microfilament-perturbing agents on cellular vesiculation. J Biol Chem 262:1916-1925.

Harada S, Matsumoto T, Ogata E. 1991. Role of ascorbic acid in the regulation of proliferation in osteoblast-like MC3T3-E1 cells. J Bone Miner Res 6:903-908.

Hausser HJ, Brenner RE. 2004. Low doses and high doses of heparin have different effects on osteoblast-like Saos-2 cells in vitro. J Cell Biochem 91:1062-1073.

Hsu HHT, Anderson HC. 1996. Evidence of the presence of a specific ATPase responsible for ATP-initiated calcification by matrix vesicles isolated from cartilage and bone. J Biol Chem 271:26383-26388.

Ilvesaro J, Metsikkö K, Väänänen K, Tuukkanen J. 1999. Polarity of osteoblasts and osteoblast-like UMR-108 cells. J Bone Miner Res 14:1338-1344.

Jimenez V, Henriquez M, Llanos P, Riquelme G. 2004. Isolation and purification of human placental plasma membranes from normal and pre-eclamptic pregnancies. a comparative study. Placenta. 25:422-437.

Kardos TB, Hubbard MJ. 1982. Are matrix vesicles apoptotic bodies? Prog Clin Biol Res 101:45-60.

Kirsch T, Harisson G, Golub EE, Nah HD. 2000. The roles of annexins and types II and X collagen in matrix vesicle-mediated mineralization of growth plate cartilage. J Biol Chem 275:35577-35583.

Kirsch T, Wang W, Pfander D. 2003. Functional differencies between growth plate apoptotic bodies and matrix vesicles. J Bone Miner Res 18:1872-1881.

Kirsch T. 2007. Physiological and pathological mineralization: a complex multifactorial process. Curr Opin Orthop 18:434-443.

Krishan A. 1975. Rapid flow cytometric analysis of mammalian cell cycle by propidium iodide staining. J Cell Biol 66:188-193.

Laemmli UK. 1970. Cleavage of structural proteins during the assembly of the head of bacteriophage T4. Nature 227:680-685.

Manduca P, Palermo C, Caruso C, Brizzolara A, Sanguineti C, Filanti C, Zicca A. 1997. Rat tibial osteoblasts III: Propagation in vitro is accompanied by enhancement of osteoblast phenotype. Bone 21:31-39.

Marks SC, Popoff SN. 1988. Bone cell biology: the regulation of development, structure and function in the skeleton. Am J Anat 183:1-44.

McQuillan DJ, Richardson MD, Bateman JF. 1995. Matrix deposition by a calcifying human osteogenic sarcoma cell line (Saos-2). Bone 16:415-426.

Morris DC, Masuhara K, Takaoka K, Ono K, Anderson HC. 1992. Immunolocalization of alkaline phosphatase in osteoblasts and matrix vesicles of human fetal bone. Bone Miner 19:287-298.

Nefussi JR, Boy-Lefevre ML, Boulekbache H, Forest N. 1985. Mineralization in vitro of matrix formed by osteoblasts isolated by collagenase digestion. Differentiation 29:160-168.

Owen TA, Aronow M, Shalhoub V, Barone LM, Wilming L, Tassinari MS, Kennedy MB, Pockwinse S, Lian JB, Stein GS. 1990. Progressive development of the rat osteoblast phenotype in vitro: reciprocal relationships in expression of genes associated with osteoblast proliferation and differentiation during formation of the bone extracellular matrix. J Cell Physiol 143:420-430.

Pope BJ, Zierler-Gould KM, Kühne R, Weeds AG, Ball LJ. 2004. Solution structure of human cofilin: actin binding, pH sensitivity, and relationship to actin-depolymerizing factor. J Biol Chem 279:4840-4848.

Quarles LD, Yohay DA, Lever LW, Caton R, Wenstrup RJ. 1992. Distinct proliferative and differentiated stages of murine MC3T3-E1 cells in culture: an in vitro model of osteoblast development. J Bone Miner Res 7:683-692.

Rabinovitch AL, Anderson HC. 1976. Biogenesis of matrix vesicles in cartilage growth plates. Fed Proc 35:112-116.

Stanford CM, Jacobson PA, Eanes ED, Lembke LA, Midura RJ. 1995. Rapidly forming apatitic mineral in an osteoblastic cell line (UMR 106-01 BSP). J Biol Chem 270:9420-9428.

Strzelecka-Kiliszek A, Buszewska ME, Podszywalow-Bartnicka P, Pikula S, Otulak K, Buchet R, Bandorowicz-Pikula J. 2008. Calcium- and pH-dependent localization of annexin A6 isoforms in Balb/3T3 fibroblasts reflecting their potential participation in vesicular transport. J Cell Biochem. Epub ahead of print.

Strzelecka-Kiliszek A, Kwiatkowska K, Sobota A. 2002. Lyn and Syk kinases are sequentially engaged in phagocytosis mediated by FcR. J Immunol 169:6787-6794.

Thouverey C, Bleicher F, Bandorowicz-Pikula J. 2007. Extracellular ATP and its effects on physiological and pathological mineralization. Curr Opin Orthop 18:460-466.

Towbin H, Staehelin T, Gordon J. 1979. Electrophoretic transfer of proteins from polyacrylamide gels to nitrocellulose sheets: procedure and some applications. Proc Natl Acad Sci USA 76:4350-4354.

Vaingankar SM, Fitzpatrick TA, Johnson K, Goding JW, Maurice M, Terkeltaub R. 2004. Subcellular targeting and function of osteoblast nucleotide pyrophosphatase phosphodiesterase 1. Am J Physiol Cell Physiol 286:C1177-1187.

Van de Lest CHA, Vaandrager AB. 2007. Mechanisms of cell-mediated mineralization. Curr Opin Orthop 18:434-443.

Wang W, Kirsch T. 2002. Retinoic acid stimulates annexin-mediated growth plate chondrocyte mineralization. J Cell Biol 157:1061-1069.

Wang W, Xu J, Kirsch T. 2005. Annexin V and terminal differentiation of growth plate chondrocytes. Exp Cell Res 305:156-165.

Wu LN, Yoshimori T, Genge BR, Sauer GR, Kirsch T, Ishikawa Y, Wuthier RE. 1993. Characterization of the nucleational core complex responsible for mineral induction by growth plate cartilage matrix vesicles. J Biol Chem 268:25084-25094.

Wu LN, Genge BR, Sauer GR, Wuthier RE. 1996. Characterization and reconstitution of the nucleational complex responsible for mineral formation by growth plate cartilage matrix vesicles. Connect Tissue Res 35:309-315.

Wuthier RE. 1975. Lipid composition of isolated epiphyseal cartilage cells, membranes and matrix vesicles. Biochim Biophys Acta 409:128-143.

Wuthier RE, Majeska RJ, Collins GM. 1977. Biosynthesis of matrix vesicles in epiphyseal cartilage. I. In vivo incorporation of 32P orthophosphate into phospholipids of chondrocyte, membrane, and matrix vesicle fractions. Calcif Tissue Res 23:135-139.

Proteomic Characterization of the Origin and Biogenesis of Calcifying Matrix Vesicles from Osteoblast-like Saos-2 cells.

[1,2]Cyril Thouverey, [3]Agata Malinowska, [1]Marcin Balcerzak, [1]Agnieszka Strzelecka-Kiliszek, [2]René Buchet and [1]Sławomir Pikuła

[1]Department of Biochemistry, Nencki Institute of Experimental Biology, Polish Academy of Sciences, PL-02093 Warsaw, Poland.

[2]Université de Lyon, Lyon, F-69003, France; Université Lyon 1, Villeurbanne, F-69622, France; INSA-Lyon, Villeurbanne, F-69622, France; CPE Lyon, Villeurbanne, F-69616, France; ICBMS CNRS UMR 5246, Villeurbanne, F-69622, France.

[3]Department of Biophysics, Institute of Biochemistry and Biophysics, Polish Academy of Sciences, PL-02093 Warsaw, Poland.

Running title: Proteomic of Saos-2 Microvilli and Matrix Vesicles

Keywords: Biogenesis, mass spectrometry, matrix vesicles, microvilli, mineralization, proteomic.

Abbreviations: AA, ascorbic acid; AnxAs, vertebrate annexins; Arf, ADP-ribosylation factor; AR-S, Alizarin Red-S; ATPase, adenosine triphosphatase; β-GP, β-glycerophosphate; ER, endoplasmic reticulum; ESI, electrospray ionization; FBS, fetal bovine serum; FPR, false positive rate; HA, hydroxyapatite; HBSS, Hank's balanced salt solution; MMP, matrix metalloprotease; MS/MS, tandem mass spectrometry; MVs, matrix vesicles; NPP1, ectonucleotide pyrophosphatase phosphodiesterase 1; PAGE, polyacrylamide gel electrophoresis; PBS, phosphate-buffered saline; P_i, inorganic phosphate, PP_i, inorganic pyrophosphate; PS, phosphatidylserine; SDS, sodium dodecyl sulfate; TBS, Tris-buffered saline; TNAP, tissue non-specific alkaline phosphatase.

ABSTRACT

Mineralization-competent cells, hypertrophic chondrocytes, osteoblasts and odontoblasts, initiate the mineralization process by releasing matrix vesicles (MVs) from their specialized areas of plasma membrane. These extracellular organelles are involved in the initial step of mineralization by promoting the formation of hydroxyapatite in their lumen. Despite growing knowledge about the morphology and the functions of MVs, their biogenesis is not well understood. It has been suggested that MVs could originate from cell microvilli. To ascertain the origin of biogenesis of MVs, we compared MV proteome released from Saos-2 cells with that of microvilli isolated from the apical plasma membrane of Saos-2 cells. 576 gene products in MVs and 869 gene products in microvilli were identified by tandem mass spectrometry. 85 % of MV proteins (487 gene products) were identical to those of microvilli. Lipid raft markers were present among common MV and microvillar proteins: GPI-anchored (TNAP, CD59), myristoylated (MARCKS), palmitoylated (stomatin), flotillin 1/2, AnxA2, AnxA6, V-ATPase and β-actin, indicating that MVs originate from apical microvillar lipid rafts. The presence of protein-markers (valosin-containing protein, SNAP α) and vesicular trafficking proteins (Niemann-Pick C1, sortin nexin 4/6, Rab7) revealed an endoplasmic reticular origin of MVs. Finally, the release of MVs from microvilli may be driven by the concomitant actions of actin-depolymerizing proteins (gelsolin, cofilin 1) and contractile motor proteins (myosin).

INTRODUCTION

Hypertrophic chondrocytes from embryonic or growth plate cartilages, osteoblasts from bones and odontoblasts from teeth initiate the mineralization process by releasing matrix vesicles (MVs) from specialized areas of plasma membranes [1-5]. These extracellular organelles are involved in the initial phase of mineralization by promoting the formation of hydroxyapatite (HA) in their lumen [6]. Ion channels and transporters present in MV membrane act for Ca^{2+} [7-9] and inorganic phosphate (P_i) uptakes into these organelles [7,10]. By accumulating Ca^{2+} and P_i, MVs create an optimal environment to induce the formation of HA [1-3]. The second phase of mineralization starts with the release of HA crystals from MVs and the propagation of mineral formation in the extracellular matrix [2]. MVs have a protein machinery essential to initiate and regulate the first phase of mineralization.

Recently, the whole proteomes of MVs isolated from chicken embryo growth plate cartilage [11] and from pre-osteoblast MC3T3-E1 cell cultures [12] have been described. Among identified proteins, several annexins (AnxA1, AnxA2, AnxA4-A7 and AnxA11) are involved in Ca^{2+} homeostasis by mediating Ca^{2+} influx into MVs [7-9]. PHOSPHO1 [13], 5'-nucleotidase [14], ion-motive ATPases [14,15], tissue non-specific alkaline phosphatase (TNAP) [16,17], are implicated in the P_i homeostasis, while ectonucleotide pyrophosphatase phosphodiesterase 1 (NPP1) is responsible for the production of inorganic pyrophosphate (PP_i) [18], a potent inhibitor of HA growth [19]. It has been proposed that NPP1 and TNAP have antagonistic effects [20-23] on mineral formation due to their opposing activities: either production of PP_i by NPP1 or its hydrolysis by TNAP. P_i transport into MVs may be performed by sodium-dependent P_i transporter (a member of the type III Glvr-1gene family) [24-26] or by alkaline pH-specific P_i transporter not strictly sodium-dependent [10,27]. Anionic phospholipids, including phosphatidylserine (PS), are enriched in the inner leaflet of MV membranes and serve with annexins and probably other Ca^{2+}-binding proteins [12,28] as a nucleation site for mineral formation due to their Ca^{2+}-binding properties [29-31].

Extracellular matrix proteins such as collagens [8,9,32,33] and proteoglycans [34,35], interact with the external surface of MVs [11,12]. These interactions between extracellular matrix components and MVs are necessary to control the mineral growth and its directional expansion [1,2]. Furthermore, several enzymes such as matrix metalloproteases (MMP-2, MMP-9, MMP-13) [36], proteoglycanases [37,38], carboxypeptidase M [11] and aminopeptidases [12] are present at the outer surface of MVs. They catalyze degradation of the extracellular matrix, hydrolyze mineralization inhibitory proteins and increase the access of MVs to extracellular ions. Numerous protein kinases and G proteins traditionally involved in signal transduction were detected in MVs [11,12,39]. Actin [40,41] as well as actinins, filamins, gelsolin and myristoylated alanine-rich C kinase substrate (MARCKS) [11,12] were

major cytoskeletal proteins identified in MVs. Finally, phospholipase A2 [42], phospholipase D [43], lactate dehydrogenase [44], carbonic anhydrase II [45] have been detected in MVs.

Despite growing knowledge about the structure and functions of MVs, little is known about their mechanism of biogenesis, especially from osteoblasts. MV formation occurs by polarized budding and pinching off of vesicles from specific regions of the plasma membrane of mineralization-competent cells [1,46,47]. Osteoblasts are polarized cells with an apical plasma membrane facing to the forming bone where MVs are released [48]. The apical side of mineralizing osteoblasts exhibits numerous cytoplasmic projections [49], similar to those observed on hypertrophic chondrocytes. Electron microscopic observations indicated that MVs are formed by budding from the tip of cytoplasmic extensions of mineralizing cells [46]. Several proteins such as TNAP [50], AnxA5 [51,52], calbindin D9k [28] were found to be enriched in both cell cytoplasmic protrusions and extracellular MVs. Hale and Wuthier demonstrated that MVs could originate from cell surface microvilli of hypertrophic chondrocytes as indicated by similar lipid compositions and high enrichment in TNAP activity [53].

Microvilli are 1-µm-length and 80-nm-diameter extensions from the apical plasma membrane of cells. These cylindrical-shaped projections enclose cytoplasm and actin microfilaments, but little or no cellular organelles [54-56]. In addition to actin, villin [55-57], actinin [55,56,58], vinculin [59], radixin, moesin, and MARCKS [55] are specific cytoskeletal components of microvilli from various cell types, and are also found in calcifying MVs [11,12]. Typical markers of apical microvilli such as alkaline phosphatase [50,55,60-62], 5'-nucleotidase [55], Na^+/K^+-ATPase [55,56], galectins [61], aminopeptidase N [61,62], AnxA2 [55,63,64], AnxA5 [51,52,55], AnxA6 [55,64] are also present in MVs. Microvilli from various cellular origins [61,62] and MVs [65,66] exhibit similar lipid composition with lipid rafts having high contents in cholesterol and sphingomyeline. Several mechanisms of vesicle formation from microvilli were described in the literature. For example, it has been suggested that the contraction of the spectrin-actin network of erythrocytes could form vesicles at the cell surface [67]. Membrane vesiculation has been also observed from intestinal [68] or kidney proximal tubule microvilli [69].

Summarizing, existing data in the literature suggest that calcifying MVs could originate from apical microvilli of mineralization-competent cells. Therefore, the purpose of this work was to compare the proteome of MVs with that of microvilli isolated from mineralizing osteoblast-like Saos-2 cells. We identified 576 MV and 869 microvillar gene products by LC ESI-MS/MS. Among MV proteins, 487 of them (85 %) were common with microvilli.

EXPERIMENTAL PROCEDURES

Cell Culture

Human osteosarcoma Saos-2 cells (ATCC HTB-85) were cultured in McCoy's 5A (ATCC) supplemented with 100 U/mL penicillin, 100 μg/mL streptomycin (both from Sigma) and 15 % FBS (v:v) (Gibco). The mineralization was induced by culturing the confluent cells (7 days to reach confluence) in growth medium supplemented with 50 μg/mL ascorbic acid (AA) (Sigma) and 7.5 mM β-glycerophosphate (β-GP) (Sigma) [70,71].

Calcium Nodule Detection

Cell cultures were washed with PBS and stained with 0.5 % (w:v) Alizarin Red-S (AR-S) in PBS (pH 5.0) for 30 min at room temperature [71]. After washing 4 times with PBS to remove free calcium ions, stained cultures were photographed or visualized under fluorescence microscope Axio Observer.Z1 (Zeiss) using transmitted light and phase contrast filter. Then, cell cultures were destained with 10% (w:v) cetylpyridinium chloride in PBS pH 7.0 for 60 min at room temperature [72]. AR-S concentration was determined by measuring absorbance at 562 nm.

Preparation of Microvilli and Matrix Vesicles

Both preparations were performed simultaneously with the same cell cultures according to Wu et al. [29] for MV preparation and Jimenez et al. [60] for microvilli preparation with slight modifications. Saos-2 cell cultures were digested with 100 U/mL collagenase Type IA (Sigma) in the Hank's balanced salt solution (HBSS: 5.4 mM KCl, 0.3 mM Na_2HPO_4, 0.4 mM KH_2PO_4, 0.6 mM $MgSO_4$, 137 mM NaCl, 5.6 mM D-glucose, 2.38 mM $NaHCO_3$, pH 7.4) at 37 °C for 3 hours. Then cells were centrifuged (600 x *g*, 15 min) yielding pellet 1. The supernatant was centrifuged (20,000 x *g*, 20 min) to sediment all the cell debris, nuclei, mitochondria, lysosomes as the pellet 2. The second supernatant was subjected to an ultracentrifugation (80,000 x *g*, 60 min) yielding pellet 3 containing MVs. Pellet 1 containing intact cells was homogenized in 5 mL of sucrose buffer in the presence of protease inhibitor cocktail (Sigma). The homogenate was then centrifuged twice at 10,000 x *g* for 15 min to sediment intact cells, cell debris, nuclei, mitochondria, lysosomes (pellet A). To separate the microvillar membranes from the basolateral plasma membranes, the supernatant A was supplemented with 12 mM $MgCl_2$, stirred at 4 °C for 20 min to induce basolateral membrane precipitation and centrifuged twice at 2,500 x *g* for 10 min to pellet aggregates of basolateral membranes (pellet B). The

supernatant was centrifuged at 12,000 x *g* for 60 min to pellet microvilli (pellet C). The last supernatant contained microsomal and cytosolic fractions. Fractions with MVs and microvilli (8.6 % sucrose, w:v) were overlaid on a sucrose step gradient made with 45 %/ 37 %/ 25 % (w:v) sucrose and centrifuged at 90,000 x *g* for 5 hours. The alkaline phosphatase activity was measured in fractions collected from sucrose gradient. The 25 % and 37 % sucrose fractions were collected, mixed, diluted ten fold in HBSS and centrifuged at 120,000 x *g* for 60 min. The protein concentration in the fractions was determined using the Bradford assay kit (Bio-Rad).

Electron Microscopy

Stimulated Saos-2 cells, microvilli and MVs were washed in PD buffer (125 mM NaCl, 5 mM KCl, 10 mM $NaHCO_3$, 1 mM KH_2PO_4, 10 mM glucose, 1 mM $CaCl_2$, 1 mM $MgCl_2$, 20 mM Hepes, pH 6.9) and fixed with 3 % (w:v) paraformaldehyde/1 % (w:v) glutaraldehyde mixture in 100 mM sodium phosphate buffer (pH 7.2) for 1 hour at room temperature [73]. After washing, samples were post-fixed with 1% (w:v) osmium tetroxide in 100 mM sodium phosphate buffer (pH 7.2) for 20 min at room temperature and then dehydrated in a graded ethanol solution series at room temperature (25 % (v:v) for 5 min, 50 % (v:v) for 10 min, 75 % (v:v) for 15 min, 90 % (v:v) for 20 min, 100 % (v:v) for 30 min). Then, samples were incubated in mixtures of LR White resin/100% ethanol at volume ratios of 1:2 and 1:1 (each 30 min, at room temperature). Finally, samples were infiltrated twice with 100 % (v:v) LR White resin (Polysciences) for 1 hour at room temperature, moved to the gelatin capsule and polymerized at 56°C for 48 hours. 700-A-sections were cut using an ultramicrotome LKB Nova, placed on formvar-covered and carbon-labeled 300 Mesh nickel grids (Agar Scientific LtD). The sample-covered grids were counterstained with 2.5 % (w:v) uranyl acetate in ethanol for 1-1.5 hours at room temperature. Finally, the grids were washed in 50 % ethanol, then in water and stained with lead citrate for 2 min in NaOH atmosphere at room temperature, washed in water and dried [73]. The samples were observed by the mean of a JEM-1200EX transmission electron microscopy (JEOL).

Assay of Marker Enzyme Activities

Succinate dehydrogenase activity was assayed at 37 °C in 0.5 mL-volumes of phosphate buffer containing 0.05 % (w:v) nitroblue tetrazolium, 0.2 % (v:v) Triton X-100, 20 mM succinate sodium, pH 7.4 by recording absorbance at 630 nm. Enzyme units are ΔA_{630} per hour per mg of proteins. NADH oxidase activity was determined at 37 °C in 1 mL-volumes containing 0.14 mM NADH, 1.3 mM potassium ferricyanide, 10 mM Tris-HCl, pH 7.5 by recording absorbance at 340 nm (ε_{NADH} is equal to 6.22 $mM^{-1}.cm^{-1}$) [74]. Enzyme units are µmol of NADH oxidized per hour per mg of proteins. Acid phosphatase activity was assayed at 37 °C using *p*-nitrophenyl phosphate as substrate in

piperazine glycyl-glycine buffer at pH 5 with 0.2 % Triton X-100 (v:v) [74]. Enzyme units are ΔA_{420} per hour per mg of proteins. Leucine aminopeptidase activity was determined at 37 °C using L-leucine-*p*-nitroanilide as substrate in phosphate buffer at pH 7.4 by recording absorbance at 410 nm (ε_{p}-nitroanilide is equal to 8.8 $mM^{-1}.cm^{-1}$) [74]. Enzyme units are µmol of *p*-nitroanilide released per hour per mg of proteins. Tissue non-specific alkaline phosphatase activity was measured using *p*-nitrophenyl phosphate as substrate at pH 10.4 by recording absorbance at 420 nm ($\varepsilon_{p\text{-NP}}$ is equal to 18.8 $mM^{-1}.cm^{-1}$) [75]. Enzyme units are µmol of *p*-nitrophenolate released per min per mg of proteins.

Mineralization Assay

Aliquots of MVs were diluted to a final concentration of 20 µg of total proteins/mL in the mineralization buffer (100 mM NaCl, 12.7 mM KCl, 0.57 mM $MgCl_2$, 1.83 mM $NaHCO_3$, 0.57 mM Na_2SO_4, 3.42 mM NaH_2PO_4, 2 mM $CaCl_2$, 5.55 mM D-glucose, 63.5 mM sucrose and 16.5 mM TES (pH 7.4). Samples were incubated at 37 °C for 6 hours. The mineral complexes were centrifuged at 3,000 x *g* for 10 min and washed several times with water. The final pellets were dried and incorporated by pressing into 100 mg of KBr. Mineral compositions were determined using a Nicolet 510M Infrared spectrometer (Nicolet); 64 interferograms were recorded at a 4 cm^{-1} optical resolution.

Tandem Mass Spectrometry Analysis of Protein Digests

MV and microvillar proteins were prepared according two methods. First, they were boiled in Laemmli gel loading buffer at 100 °C for 5 min, separated on one dimensional SDS-(10 %, w/v) polyacrylamide gels, and stained with Coomassie Brillant Blue (Sigma) (Fig. 1). 11 bands were cut from each gels (Fig. 1) and submitted to a standard in-gel tryptic digestion. Second, MV and microvillar protein samples were directly digested and alkylated in solution without prior SDS-PAGE step, to ensure that all proteins, including low molecular weight and hydrophobic proteins, were analyzed. Both samples were supplemented with 10 ng/µL trypsin (Promega) in 25 mM ammonium hydrocarbonate (pH 8.5), and incubated overnight at 37 °C. Tryptic solutions were incubated with 10 mM DTT for 30 min at 56 °C to reduce cysteins, and then alkylated with 50 mM iodoacetamide for 45 min in the darkness at room temperature. The reaction was stopped with the addition of 1 % TFA (v/v) and stored at 4 °C. Tryptic peptide mixtures were applied to a RP-18 precolumn (LC Packings) using a 0.1 % (v/v) TFA solution as the mobile phase, and transferred to a nano-HPLC RP-18 column (LC Packings). Peptide mixtures were separated using an ACN gradient (0-50 % ACN in 30 min) in the presence of 0.05 % (v/v) formic acid at a flow rate of 150 nL/min. The column was connected to the Finningan Nanospray ion source of a LTQ-FTICR mass spectrometer (Thermo) working in the regime of data-dependent MS to MS/MS switch.

Database Searching

Mass spectra obtained in both experiments were searched against the latest version of no redundant protein database from the National Center of Biotechnology Information (NCBI), using the engine 8-processor on-site licensed MASCOT software (http://www.matrixscience.com). Search parameters were set as following: taxonomy: human; enzyme: trypsin; fixed modifications: carbamidomethylation (C); variable modifications: carbamidomethylation (K), oxidation (M); protein mass: unrestricted; peptide mass tolerance: ± 40 ppm; MS/MS fragment ion mass tolerance: ± 0.8 Da; max missed cleavages: 1. To confirm the statistical validity of accepted protein hits, the false positive rate (FPR) values were calculated. All mass spectra were searched against a NCBI randomized database and the FPR was computed by dividing the number of accepted queries from the randomized search by the number of accepted from the standard search, and multiplying the result by 100 %. MASCOT peptide score values were accepted for a given search only if the FPR value corresponding to this score value was not higher than 1%, otherwise the hits were discarded. MASCOT scores with values of 50 and 54 correspond to FPR values of 1.08 and 1.03 in experiments performed with sample solution and gel slices, respectively. Only protein hits characterized by at least one high-scoring peptide were validated. All identified proteins were searched against the Human Protein Reference Database (http://www.hprd.org) to determine their classification, molecular weight, number of transmembrane domains, post-translational modifications and subcellular localization.

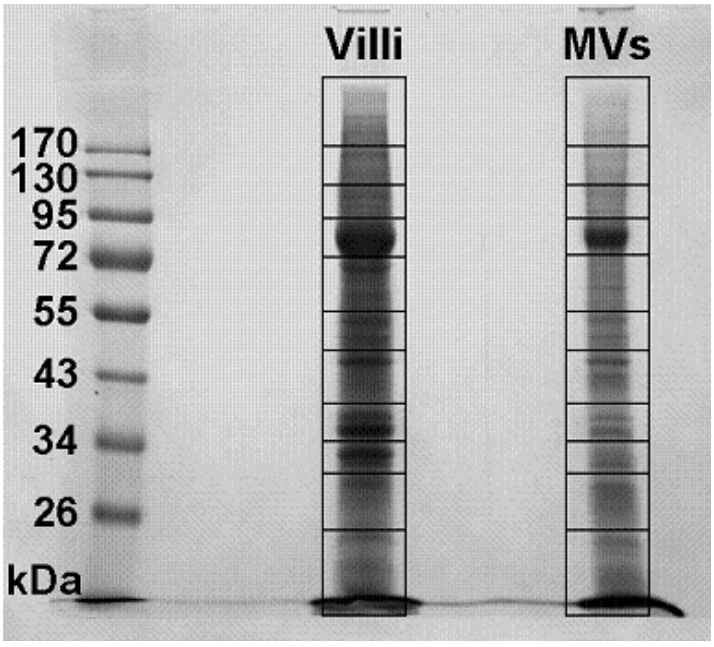

Figure 1. Protein profiles of Saos-2 cell microvilli and MVs. Protein profiles analyzed by 10 % SDS- PAGE followed by Coomassie brilliant blue staining of microvilli (Villi) and matrix vesicles (MVs). 11 gel slices were cut for in-gel tryptic digestion and protein identification by tandem mass spectrometry.

RESULTS

Saos-2 Cell-Mediated Mineralization

Saos-2 cells cultured in McCoy's 5A medium containing 0.9 mM Ca^{2+} and 4.2 mM P_i produced apparent calcium nodules characteristic of osteoblastic mineralization as detected by AR-S staining (Fig. 2). Ascorbic acid (AA) and β-glycerophosphate (β-GP) are two osteogenic factors commonly used to stimulate osteoblastic differentiation and mineralization [70,71]. As expected, the mineral deposition was highly enhanced by the concomitant addition of 50 µg/mL AA and 7.5 mM β-GP in Saos-2 cell cultures (Fig. 2). Stimulated Saos-2 cells produced 6 times more calcium minerals than resting Saos-2 cells within 6 days (Fig. 2C). MVs purified from stimulated Saos-2 cell cultures were able to form hydroxyapatite minerals after 6 hours of incubation in a mineralization buffer containing 2 mM Ca^{2+} and 3.42 mM P_i (Fig. 3).

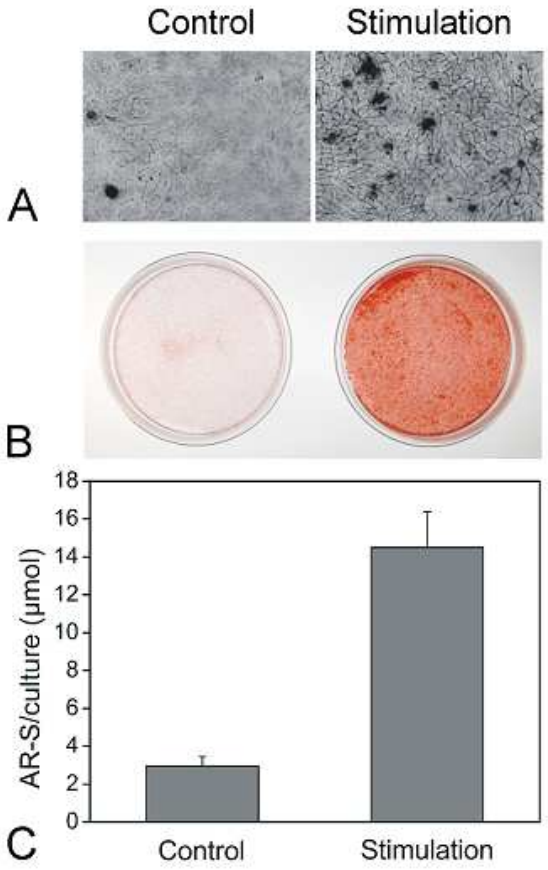

Figure 2. Mineralization by Saos-2 cells. (A) Saos-2 cells were incubated for twelve days in the absence (control) or presence of 50 µg/mL ascorbic acid and 7.5 mM β-glycerophosphate (stimulation), stained with AR-S to detect calcium nodules and visualized under fluorescence microscope Axio Observer.Z1 (Zeiss) using transmitted light and phase contrast filter. (B) Saos-2 cells were maintained six days under normal conditions or stimulated, stained with AR-S and photographed. (C) AR-S was solubilized in control and stimulated cell cultures by cetylpyridinium chloride and quantified at 562 nm (Results are mean ± SD, n=3).

Morphological and Biochemical Characterization of Apical Microvilli and Matrix Vesicles

Apical microvilli and MVs were simultaneously purified from mineralizing Saos-2 cells and their morphologies were compared. MVs were identified as closed, spherical vesicle structures delimited by a characteristic trilaminar membrane [39], with a diameter ranging from 100 to 400 nm (Fig. 4A). In some cases, it was possible to observe needle-like electron-dense mineral deposits inside the MVs (Fig. 4B), showing their ability to mineralize. Another membrane-delimited structures (400 to 800 nm of diameter) containing multiple 100-nm-diameter vesicles were present (Fig. 4C). Microvilli were found to rearrange in vesicle-like structures during their preparation (Fig. 4D). These microvillar vesicles were delimited by a trilaminar membrane and had a diameter between 100 and 300 nm (Fig. 4D), showing a similar morphology as compared to MVs. Different marker-enzyme activities were measured during the preparation of microvilli and MVs to evaluate the purity of the samples (Table I). Around 81 % of the total succinate dehydrogenase activity, an inner mitochondrial membrane marker, 72 % of the total NADH oxidase activity, a mitochondrial and endoplasmic reticulum marker, and 79 % of the total acid phosphatase activity, a lysosome marker, were found in the pellet A containing these organelles (Table I). In contrast, these activities were very low (less than 0.7 %) or even non-detected in the fractions of microvilli and MVs, indicating relatively pure fractions of microvilli and MVs (Table I). Moreover, the leucine aminopeptidase activity, a microvillar marker enzyme, and the TNAP activity, a MV marker enzyme, were highly enriched in microvilli and MVs (Table I).

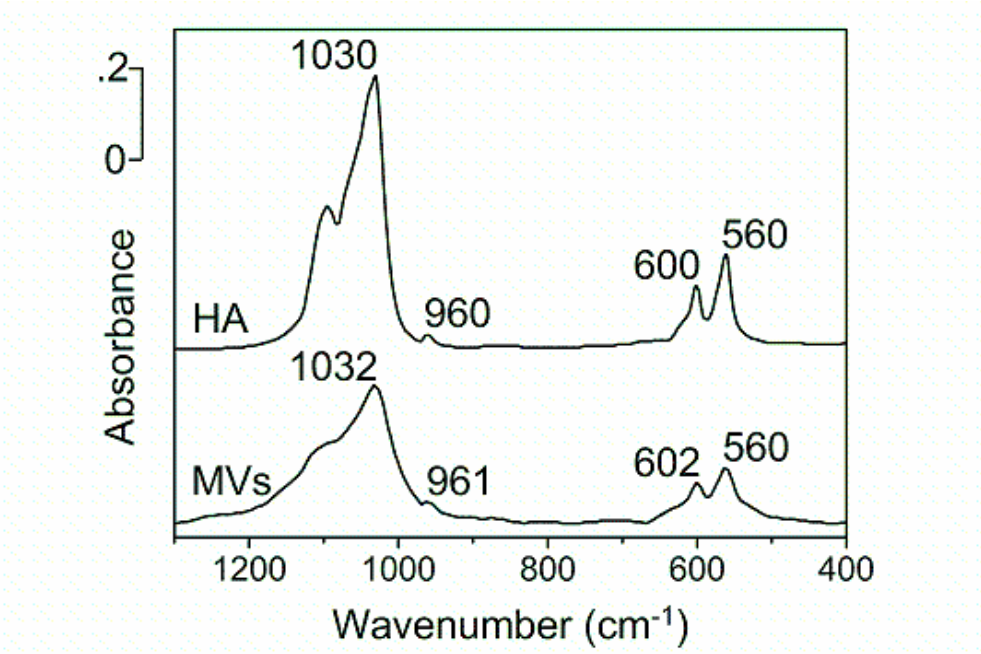

Figure 3. Infrared spectra of minerals formed by MVs. MVs cells were incubated at 37 °C in mineralization buffer for 6 hours, then the minerals formed were collected, washed and analyzed by infrared spectroscopy. Infrared spectrum of hydroxyapatite as control (HA); Infrared spectrum of minerals formed by matrix vesicles (MVs). Infrared spectra of mineral indicated that the mineral formed by MVs was hydroxyapatite. (Typical infrared spectrum among three independent measurements).

TABLE I. Evaluation of the purity of microvilli and matrix vesicles.

		Digest	Pellet A	Pellet B	Microvilli	Supernatant C	Pellet 2	MVs	Supernatant
Proteins	mg	30.44 ± 0.13	12.25 ± 0.79	2.42 ± 0.64	0.45 ± 0.09	5.83 ± 1.13	2.17 ± 0.24	0.71 ± 0.18	7.72 ± 1.71
	%	100	40.2 ± 2.6	8 ± 2.1	1.5 ± 0.3	19.1 ± 3.7	7.1 ± 0.8	2.3 ± 0.6	25.3 ± 5.6
Succinate dehydrogenase	U/mg	2.12 ± 0.14	4.25 ± 0.79	2.33 ± 0.4	ND	ND	2.08 ± 0.21	ND	ND
	%	100	80.7 ± 15	8.7 ± 1.5	-	-	7 ± 0.7	-	-
	E	1	2	1.1	-	-	1	-	-
NADH oxidase	U/mg	13.51 ± 1.18	24.37 ± 4.07	20.09 ± 5.80	5.61 ± 0.96	8.08 ± 2.16	7.23 ± 1.08	1.9 ± 0.6	ND
	%	100	72.6 ± 12.1	11.8 ± 3.4	0.6 ± 0.1	11.5 ± 3.1	3.8 ± 0.6	0.3 ± 0.1	-
	E	1	1.8	1.5	0.4	0.6	0.5	0.1	-
Acid phosphatase	U/mg	2.26 ± 0.19	4.44 ± 0.29	2.6 ± 0.6	1.14 ± 0.15	ND	4.04 ± 0.82	0.67 ± 0.02	ND
	%	100	79 ± 5.2	8.7 ± 2.1	0.7 ± 0.1	-	12.7 ± 2.6	0.7 ± 0.1	-
	E	1	2	1.2	0.5	-	1.8	0.3	-
Leucine aminopeptidase	U/mg	1.04 ± 0.12	0.74 ± 0.13	1.23 ± 0.15	6.82 ± 0.77	0.82 ± 0.2	2.13 ± 0.25	5.3 ± 0.85	0.46 ± 0.1
	%	100	28.5 ± 5	9.4 ± 1.2	9.7 ± 1.1	15 ± 3.7	14.6 ± 1.7	11.8 ± 1.9	11.3 ± 2.4
	E	1	0.7	1.2	6.6	0.8	2	5.1	0.5
Alkaline phosphatase	U/mg	8.41 ± 0.42	3.2 ± 0.24	7.13 ± 0.7	110 ± 6	2.14 ± 0.41	14.06 ± 2.4	121 ± 13.3	1.22 ± 0.98
	%	100	15 ± 1.2	6.7 ± 0.7	19.3 ± 1.1	4.9 ± 1.9	11.9 ± 2	33.4 ± 3.7	3.7 ± 3
	E	1	0.4	0.9	13.1	0.3	1.7	14.4	0.1

Succinate dehydrogenase (marker of the inner mitochondrial membrane), NADH oxidase (both mitochondial membranes and endoplasmic reticulum), acid phosphatase (lysosomes), leucine aminopeptidase (apical plasma membranes) and alkaline phosphatase (apical plasma membranes and matrix vesicles) activities were measured in all fractions obtained during the simultaneous isolation of microvilli and matrix vesicles from Saos-2 cell cultures. The names of fractions and enzyme units are given in the Experimental Procedures section. (ND: non-detected).

Identification of Saos-2 Microvillar Proteins

Apical microvilli were isolated from Saos-2 cells according to the well-established method of Jimenez et al. [60] for the isolation of microvilli from human placental syncytiotrophoblast. It consisted of the Mg^{2+}-induced precipitation in which non-microvillar membranes were aggregated and could be separated from vesicular microvilli by a low-speed centrifugation. The mass spectrometry analysis of peptides obtained by in-gel and in-sample trypsin digestions resulted in the identification of 869 proteins. The identified protein profile of the Saos-2 cell apical microvilli can be divided into different functional categories: cytoskeletal proteins, cell adhesion proteins, membrane trafficking proteins, enzymes, proteases, calcium binding proteins, extracellular matrix components, transmembrane proteins, transporters, cell surface receptors, regulatory proteins, immune system proteins, chaperones, ubiquitin proteasome system proteins, proteins involved in protein metabolism, nucleic acid metabolism, unknown, and others. Several proteins identified in the Saos-2 microvilli were previously found in the microvilli from other cell types [55,56,76-77] such as β-actin, ezrin, actinin α1 and α4, moesin, radixin, gelsolin, plastin 1 and 3, dynein and MARCKS which are specific cytoskeletal components of microvilli; Ras-related proteins Rab1B and Rab7, ADP-ribosylation factor

(Arf) 1 and 4, and 14-3-3 family members which are involved in signal transduction; annexins (AnxA1, AnxA2, AnxA4-6, AnxA11); proteins such as alkaline phosphatase, 5'-nucleotidase, Na^+/K^+-ATPase, phosphoglycerate kinase 1, enolase 1, glyceraldehyde-3-phosphate dehydrogenase, 4F2 cell surface antigen, basigin, galectins, integrin α5, transferrin receptor protein 1 and lactate dehydrogenase.

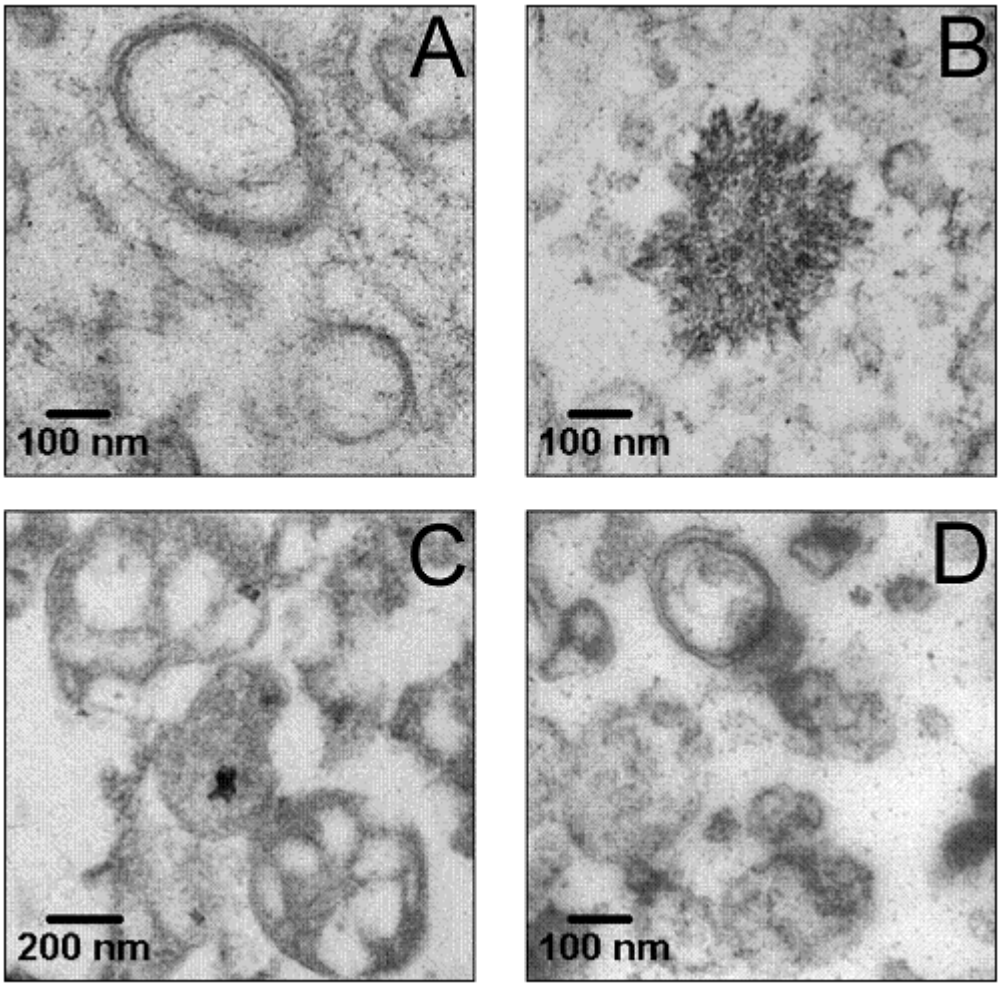

Figure 4. Electron microscopic view of intact cell microvilli, isolated microvilli, matrix vesicles and multivesicular bodies. MV, matrix vesicle (A,B); MVB, multivesicular bodies (C); Villi, microvilli (D). (Magnifications: A, B, D, x 50,000; C, x 30,000).

Identification of Matrix Vesicle Proteins

The MS analysis of peptides resulting from the in-gel and in-sample tryptin digestions identified 576 gene products (supplemental Table 1) with a score equal or higher than the value corresponding to a FPR ≤ 1 % for a given experiment. The peptide score, the number of peptide matches as well as the number of transmembrane domain and the type of post-translational modifications of each identified

proteins are given in table II and supplemental table 1. Several identified proteins are usually resident in other cellular organelles such as nucleus (ATP-dependent DNA helicase II, 70 kDa subunit), mitochondrion (ATP synthase, H+ transporting, mitochondrial F1 complex, α subunit 1), endoplasmic reticulum (lanosterol synthase), Golgi apparatus (Golgi-Associated protein 1) and lysosomes (lysosome-associated membrane glycoprotein 1), however these proteins can be also found in cytoplasm and plasma membrane. The protein profile of MVs can be divided into various functional categories (Fig. 5; numbers in brackets indicate members of each family identified): cytoskeletal proteins (43), cell adhesion proteins (13), membrane trafficking proteins (65), extracellular matrix components (6), proteases (13), enzymes (83), calcium binding proteins (15), transmembrane proteins (18), transporters (36), cell surface receptors (20), signal transduction proteins (58), immune system proteins (10), chaperones (22), ubiquitin proteasome system proteins (28), proteins involved in protein metabolism (67), nucleic acid metabolism (36), unknown (32), and others (11). Among them, several are known to be implicated in MV mineralization: TNAP, NPP1, Na^+/K^+-ATPase, Ca^{2+}-ATPase, PHOSPHO1, AnxA2, AnxA5, AnxA6, β-actin, lactate dehydrogenase B, and chondroitin sulfate proteoglycan 2.

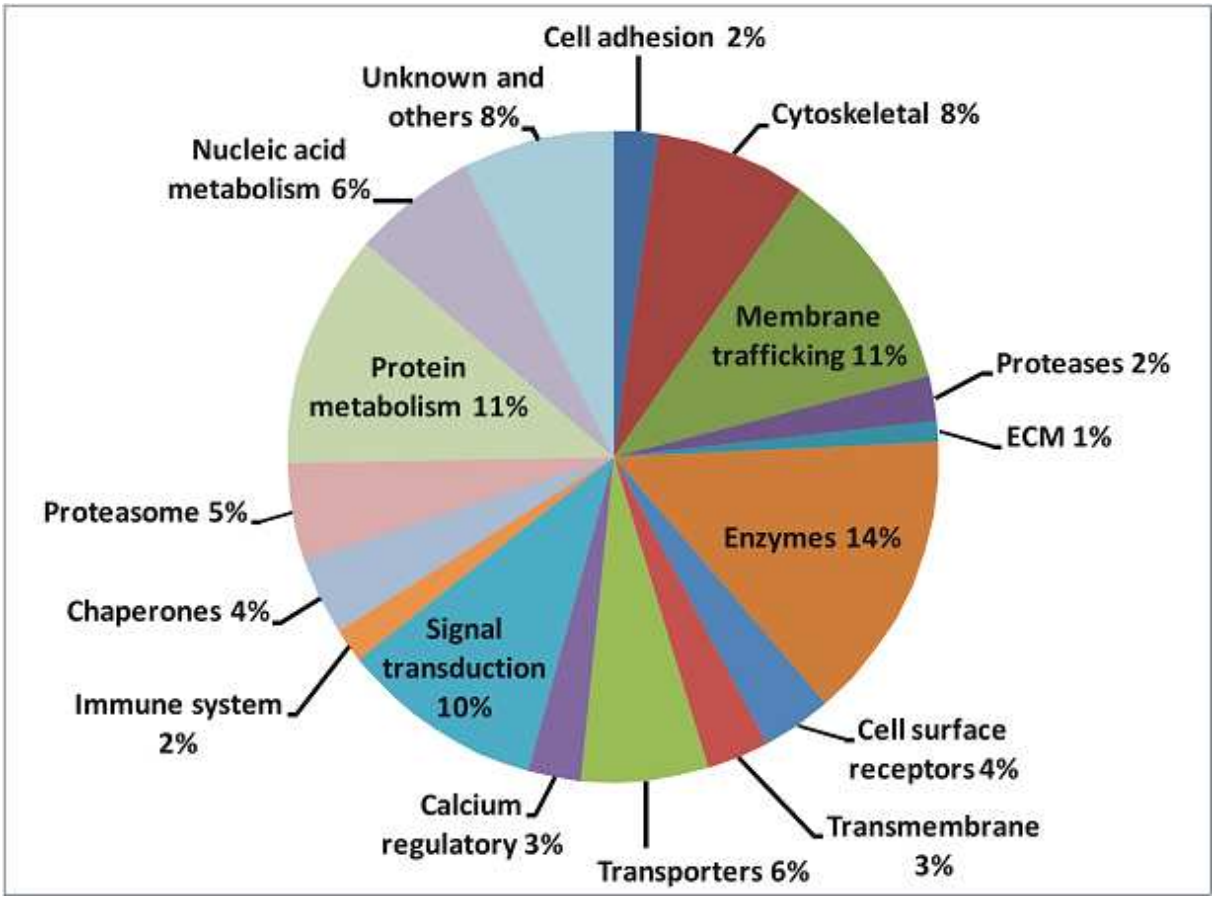

Figure 5. Functional classification of 576 proteins identified in MVs.

TABLE II. Examples of proteins identified in matrix vesicles and Saos-2 cell apical microvilli.

GI number	Protein name	MW (Da)	CRMVs[a]	Microvilli[b]	TM/PTM[c]
Cell adhesion proteins					
gi|4503131	Catenin β1	85496	126.0 (5)	306.0 (6)	
gi|5031699	Flotillin 1	47355	85.0 (1)	516.0 (7)	
gi|5174557	Milk fat globule-EGF factor 8 protein	43123	197.0 (6)	63.0 (2)	
Cytoskeletal proteins					
gi|119602166	Dynein cytoplasmic heavy chain 1	532406	250.0 (6)	2091.0 (35)	
gi|16753233	Talin 1	269667	406.0 (11)	1301.0 (23)	
gi|12667788	Myosin heavy polypeptide 9 non-muscle	226532	2775.0 (46)	2730.0 (51)	
gi|55960300	Gelsolin	85697	103.0 (1)	96.0 (1)	Myristoylation
gi|46249758	Ezrin	69413	163.0 (2)	156.0 (2)	
gi|4505257	Moesin	67820	297.0 (12)	498.0 (7)	
gi|14389309	Tubulin α6	49895	437.0 (9)	724.0 (12)	
gi|4501885	β-actin	41737	765.0 (16)	1067.0 (23)	
gi|5031635	Cofilin 1	18502	289.0 (3)	354.0 (5)	
Extracellular matrix proteins					
gi|119616317	Chondroitin sulfate proteoglycan 2	372819	62.0 (2)	-	
gi|4503053	Hyaluronan and proteoglycan link protein 1	40165	484.0 (9)	129.0 (1)	
gi|19923989	Collagen triple helix repeat-containing 1	26224	135.0 (2)	-	
Cell surface receptors					
gi|4504747	Integrin α3	118755	462.0 (12)	243.0 (9)	1 TM
gi|62089374	Integrin αV	116038	390.0 (14)	522.0 (13)	1 TM
gi|9716092	Sortilin	92067	124.0 (3)	179.0 (2)	1 TM
gi|20146101	Basigin	42200	136.0 (7)	263.0 (6)	1 TM
Proteases					
gi|4507657	Tripeptidyl peptidase II	138449	751.0 (18)	561.0 (7)	
gi|2039383	ADAM 17	93021	99.0 (1)	-	1 TM
gi|116256327	Membrane metallo-endopeptidase	85514	363.0 (12)	694.0 (12)	1 TM
Enzymes					
gi|67476453	Fatty acid synthase	273426	495.0 (17)	1051.0 (29)	
gi|119568427	Ectonucleotide pyrophosphatase/phosphodiesterase 1	99930	74.0 (1)	384.0 (5)	1 TM
gi|182871	Glucose-6-phosphate dehydrogenase	88892	167.0 (3)	-	
gi|89954531	Sphingomyelin phosphodiesterase 3	71081	172.0 (5)	325.0 (5)	2 TM
gi|4557425	Ectonucleoside triphosphate diphosphohydrolase 3	59133	75.0 (1)	61.0 (2)	1 TM
gi|35505	Pyruvate kinase 3	58062	454.0 (11)	589.0 (14)	
gi|116734717	Tissue non-specific alkaline phosphatase	57305	2723.0 (48)	2858.0 (67)	GPI
gi|4503571	Enolase 1	47169	720.0 (21)	1102.0 (24)	
gi|4557032	Lactate dehydrogenase B	36638	327.0 (9)	232.0 (5)	
gi|5031857	Lactate dehydrogenase A	36689	232.0 (4)	-	
gi|5174539	Cytosolic malate dehydrogenase	36426	158.0 (5)	447.0 (7)	
gi|11056044	Inorganic pyrophosphatase 1	32660	150.0 (4)	84.0 (1)	
gi|30425420	PHOSPHO1	29713	80.0 (1)	138.0 (2)	
gi|4505591	Peroxiredoxin 1	22110	151.0 (5)	120.0 (4)	
Transmembrane proteins					
gi|6731237	Myoferlin	234708	339.0 (9)	738.0 (17)	1 TM
gi|119588731	Transmembrane protein 16E	107187	193.0 (4)	180.0 (3)	8 TM
gi|42556032	Prominin 1	97202	162.0 (4)	-	4 TM
gi|181184	Stomatin	31731	292.0 (7)	505.0 (8)	1 TM; Palmitoylation

TABLE II. Continued.

GI number	Protein name	MW (Da)	CRMVs[a]	Microvilli[b]	TM/PTM[c]
Transporters/Channels					
gi|134288865	SLC4A7 (sodium bicarbonate cotransporter)	136044	140.0 (3)	177.0 (3)	11 TM
gi|1705852	Voltage-dependent calcium channel α2/δ1	123183	188.0 (5)	227.0 (5)	
gi|21361181	Na^+/K^+ ATPase α1	112896	990.0 (31)	1577.0 (38)	10 TM
gi|384062	SLC24A3 ($Na^+/K^+/Ca^{2+}$ exchanger)	71992	85.0 (1)	-	10 TM
gi|61744475	4F2 antigen	71123	522.0 (14)	739.0 (16)	1 TM
gi|12652633	SLC1A5 (Neutral amino acid transporter)	56598	304.0 (10)	544.0 (10)	9 TM
gi|25188179	Voltage-dependent anion channel 3	30659	85.0 (2)	294.0 (5)	
gi|14251209	Chloride intracellular channel 1	26923	166.0 (3)	114.0 (1)	
Calcium binding proteins					
gi|71773329	Annexin A6	75873	873.0 (27)	1064.0 (22)	
gi|1703322	Annexin A11	54390	105.0 (1)	466.0 (9)	
gi|55584155	Annexin A7	52739	249.0 (8)	379.0 (13)	
gi|18645167	Annexin A2	40411	753.0 (18)	803.0 (20)	
gi|4502101	Annexin A1	38714	593.0 (15)	1390.0 (23)	
gi|1703319	Annexin A4	36085	417.0 (11)	612.0 (13)	
gi|809185	Annexin A5	35937	710.0 (16)	2148.0 (26)	
gi|4507207	Sorcin	21676	197.0 (4)	167.0 (4)	
Membrane trafficking proteins					
gi|1708865	LDL receptor-related protein 1	504605	439.0 (10)	956.0 (14)	1 TM
gi|4758012	Clathrin heavy chain 1	191614	1224.0 (33)	1746.0 (47)	
gi|4557803	Niemann Pick C1 protein	142148	81.0 (1)	242.0 (4)	12 TM
gi|4758032	Coatomer protein complex β2	102487	55.0 (1)	183.0 (6)	
gi|119598698	Clathrin adaptor complex AP50	49389	100.0 (2)	-	
gi|13375926	Vacuolar protein sorting 37B	31307	194.0 (4)	-	
gi|98986464	Transmembrane trafficking protein	24976	154.0 (3)	198.0 (3)	1 TM
gi|73536235	Rab14	23897	168.0 (3)	220.0 (4)	
gi|34147513	Rab7	23490	301.0 (8)	491.0 (9)	Prenylation
gi|1374813	SNAP 23	23354	55.0 (1)	118.0 (1)	Palmitoylation
gi|33695095	Rab10	22469	246.0 (4)	329.0 (4)	
gi|4502201	ADP-ribosylation factor 1	20697	197.0 (4)	294.0 (5)	Myristoylation
Signaling proteins					
gi|249616	Insulin-like growth factor I receptor	154793	174.0 (3)	169.0 (2)	1 TM
gi|47938093	Protein tyrosine kinase 7	118391	204.0 (3)	293.0 (5)	1 TM
gi|62088530	Protein kinase Cα	76764	111.0 (4)	312.0 (6)	
gi|24111250	GTP binding protein, α13	44049	269.0 (5)	218.0 (8)	Palmitoylation
gi|4504041	GTP binding protein G (i) α2	40451	381.0 (8)	751.0 (16)	
gi|306785	GTP binding protein β1	37377	159.0 (2)	449.0 (8)	
gi|82407948	14-3-3 protein γ	28303	222.0 (2)	369.0 (3)	
gi|4507953	14-3-3 protein ζ	27745	319.0 (5)	582.0 (7)	
gi|2914478	Rac1	23467	74.0 (1)	91.0 (1)	
gi|4826962	Rac3	21379	139.0 (3)	332.0 (6)	
gi|15451856	Caveolin 1	20472	91.0 (2)	-	1 TM; Palmitoylation
Immune system proteins					
gi|1633574	MHC class I antigen A2	40841	231.0 (6)	352.0 (6)	1 TM
gi|4502693	CD9 antigen	25416	87.0 (1)	-	4 TM
gi|19923362	Thy-1 cell surface antigen	17935	119.0 (1)	85.0 (2)	GPI

TABLE II. Continued.

GI number	Protein name	MW (Da)	CRMVs[a]	Microvilli[b]	TM/PTM[c]
Chaperones					
gi|306891	Heat shock 90 kDa protein β1	83264	437.0 (12)	1111.0 (23)	
gi|5729877	Heat shock 70 kDa protein 8	70898	907.0 (16)	932.0 (13)	
gi|14124984	Chaperonin containing TCP1 γ	60534	282.0 (8)	696.0 (15)	
gi|36796	T-complex polypeptide 1	60343	443.0 (13)	522.0 (6)	
Ubiquitin proteasome system proteins					
gi|23510338	Ubiquitin-activating enzyme E1	117849	511.0 (12)	877.0 (15)	
gi|4506675	Ribophorin I	68569	88.0 (2)	174.0 (3)	1 TM
gi|22538467	Proteasome subunit β4	29204	354.0 (6)	246.0 (5)	
gi|5453990	Proteasome activator subunit 1	28602	118.0 (2)	257.0 (3)	
gi|4506183	Proteasome subunit α3	28433	143.0 (3)	-	
gi|123296530	Proteosome subunit β9	23264	105.0 (2)	211.0 (3)	
Protein metabolism					
gi|4503483	Eukaryotic translation elongation factor 2	95338	201.0 (4)	222.0 (3)	
gi|124219	Eukaryotic translation initiation factor 4B	69151	127.0 (2)	112.0 (2)	
gi|55665593	Eukaryotic translation elongation factor 1 α-like 3	50141	318.0 (10)	235.0 (8)	
gi|16579885	Ribosomal protein L4	47697	211.0 (7)	243.0 (6)	
gi|15718687	Ribosomal protein S3	26688	725.0 (15)	287.0 (9)	
gi|4506743	Ribosomal protein S8	24205	186.0 (6)	372.0 (5)	
gi|4506617	Ribosomal protein L17	21397	212.0 (4)	270.0 (4)	
gi|4506681	Ribosomal protein S11	18431	347.0 (5)	205.0 (5)	
gi|292435	Ribosomal protein L26	17258	162.0 (4)	128.0 (3)	
gi|4506701	Ribosomal protein S23	15808	232.0 (3)	63.0 (1)	
gi|4506633	Ribosomal protein L31	14632	147.0 (2)	-	
Nucleic acid metabolism					
gi|6006515	Spliceosome-associated protein 130	135577	317.0 (5)	193.0 (4)	
gi|55956788	Nucleolin	76614	194.0 (2)	451.0 (9)	
gi|4503841	ATP-dependent DNA helicase II, 70 kDa subunit	69843	858.0 (19)	487.0 (7)	
gi|12653493	Brain abundant membrane attached signal protein 1	22693	303.0 (10)	247.0 (6)	Myristoylation
gi|386772	Histone H3	15388	433.0 (7)	-	
Others					
gi|61743954	AHNAK nucleoprotein	629099	67.0 (1)	1586.0 (33)	
gi|119620171	Dysferlin	237294	814.0 (14)	1075.0 (18)	1 TM
gi|46812315	Macroglobulin α2	163292	79.0 (2)	-	
gi|13375569	Hp95	96023	432.0 (9)	536.0 (6)	
gi|16757970	Niban protein	79855	98.0 (3)	184.0 (2)	
gi|2697005	Proliferation-associated protein 2G4	43787	66.0 (2)	106.0 (2)	
gi|55669748	Golgi-Associated protein 1	17218	105.0 (1)	167.0 (2)	
gi|5174764	Metallothionein 2A	6042	64.0 (1)	-	

[a] Highest score for given protein identified in MVs during a single experiment (number of individual peptides identified in all experiments).

[b] Highest score for given protein identified in Saos-2 microvilli during a single experiment (number of individual peptides identified in all experiments).

[c] TM, transmembrane domains; PTM, postranslational modifications.

DISCUSSION

Matrix Vesicle Proteome

MVs purified from mineralizing Saos-2 cell cultures were not significantly contaminated by other organelles as shown in Table I. TNAP activity, a known marker of MVs, amounted 121 ± 13.3 U/mg of MV proteins in our fraction. Ultrastructure of MVs viewed by electron microscopy was very similar to that previously described by Anderson et al. [79] and Balcerzak et al. [80]. Moreover, MVs were able to initiate HA formation *in vitro* (Fig. 3). Among 576 identified proteins in MV fraction, several markers of MVs are associated with mineralization, e.g. TNAP, NPP1, Na^+/K^+-ATPase, AnxA2, AnxA5, AnxA6 and chondroitin sulfate proteoglycan 2 (Table II).

Furthermore, a large amount of proteins identified by MS/MS in our samples were also identified in MVs isolated from chicken embryo growth plate cartilage [11] and from pre-osteoblast MC3T3-E1 cell cultures [12]. For example, syndecan 2, membrane metalloendopeptidase, AnxA1, AnxA4, integrin β1, integrin α5, CD9 antigen, chloride intracellular channel 4, voltage-dependent anion channel 2, solute carrier family 29 member 1, syntenin, 14-3-3 family members, protein kinase Cα, copine III, actinin α1 and 4, plastin 3, gelsolin, MARCKS, milk fat globule-EGF factor 8, eukaryotic translation elongation factor 2, macroglobulin α2 were common proteins characterized in these three proteomes (Table II and supplemental Table 1) [11,12]. Although the three types of MVs are morphologically and functionally similar, their proteomes exhibit differences. This can be explained by the fact that these three types of MVs originated from different species (chicken [11], mouse [12], human), cell types (hypertrophic chondrocytes [11], pre-osteoblasts [12], osteosarcoma osteoblast-like cells) and biological materials (tissue [11] and cell-cultures).

The proteomic analysis revealed also the presence of new MV proteins involved in the mineralization process. For example, SLC24A3 (solute carrier family 24 member 3), a $Na^+/K^+/Ca^{2+}$ exchanger, and voltage-dependent Ca^{2+} channel are new candidates for Ca^{2+} uptake and homeostasis in MVs (Table II). PP_i is a key regulatory substrate for mineralization since it is a source of P_i to sustain mineralization when hydrolyzed [20-23] but also a potent inhibitor of hydroxyapatite mineral growth [19]. In the present work, we identified two novel proteins that could be involved in its homeostasis (Table II): 1) An ectonucleoside triphosphate diphosphohydrolase 3 which could hydrolyze extracellular nucleotides producing PP_i, and 2) an inorganic pyrophosphatase 1 which hydrolyzes PP_i. Hydroxyapatite formation leads to the release of H^+, thus acidic pH inhibits mineral deposition. Intravesicular pH is crucial for mineralization and could be regulated by SLC4A7, a bicarbonate transporter (Table II), whose presence has been previously speculated by Sauer and al. [81]. A sphingomyelin phosphodiesterase 3 (Table II), is a transmembrane enzyme with an intravesicular

active site catalyzing the hydrolysis of sphingomyelin to form ceramide and phosphocholine [82]. Then, phosphocholine becomes a substrate of the luminal PHOSPHO1 (Table II) which provides P_i from its hydrolysis [13]. Therefore, this protein may contribute to mineralization by providing P_i indirectly and regulating the lipid composition of the MV membrane.

Moreover, the interactions between the extracellular matrix and MVs are required to control mineral propagation and localization. We identified several integrins in MVs that form heterodimeric surface receptors for extracellular matrix components (Table II and supplemental Table 1). For example, αV/β5 integrin receptor may interact with fibronectin, vitronectin, MMP-2, osteopontin, osteomodullin, while α5/β1 and α3/β1 integrin receptors may bind fibronectin, laminin and collagen [83]. Several metalloproteases such as ADAM 10, ADAM 17 and membrane metalloendopeptidase and aminopeptidases including tripeptidyl peptidase II, leucyl cystinyl aminopeptidase, leucine aminopeptidase, and aspartyl aminopeptidase, were found in MVs (Table II and Supplemental Table 1). Moreover, basigin, a MMP stimulator, and collagen triple helix repeat-containing 1 (Table II), a negative regulator of collagen matrix deposition, may act for matrix degradation, a necessary event in MV-mediated mineralization [36]. Finally, sortilin, a transmembrane surface receptor which may promote matrix mineralization by scavenging extracellular lipoprotein lipase [84], was identified (Table II).

Microvillar Lipid Rafts as Precursors of Matrix Vesicles

Among the 869 proteins identified in Saos-2 cell microvilli, 487 were common with those of MVs (supplemental Table 1). Therefore, 85 % of MV proteins were present in microvilli. Furthermore, a large number of proteins identified in MVs are marker proteins for microvilli, e.g. enzymes such as alkaline phosphatase, phosphoglycerate kinase 1, enolase 1, glyceraldehyde-3-phosphate dehydrogenase, lactate dehydrogenase and membrane metalloendopeptidase; transporters as 4F2 antigen (SLC3A2), SLC16A1, SLC44A1, SLC1A5, Na^+/K^+-ATPase, plasma membrane Ca^{2+}-ATPase type 4, chloride intracellular channel 1; annexins including AnxA1, AnxA2, AnxA4, AnxA5, AnxA6, AnxA7, AnxA11; signal transduction proteins like Ras-related proteins Rab1A, Rab1B, Rab5C and Rab7, Arf1, 4 and 6, and 14-3-3 family members; other proteins (basigin, integrin α5, transferrin receptor protein 1); and cytoskeletal components (Table II, Supplemental Table 1). These findings confirmed that apical cell surface microvilli are the precursors of MVs in mineralization-competent cells as reported by Hale and Wuthier [53].

The lipid composition of MV membrane is characterized by a high content in cholesterol, sphingomyelin and PS [65,66]. This suggests that MVs originate from cholesterol- and sphingomyelin-rich lipid rafts. Among common proteins in both MVs and Saos-2 cell microvilli, the

MS/MS analysis revealed the presence of glycosylphosphatidylinositol-anchored (GPI-anchored) proteins (TNAP, Thy-1 cell surface antigen, CD59 antigen), myristoylated proteins (brain abundant membrane attached protein 1, Arf 1, MARCKS, gelsolin, calcium binding protein p22, XRP2 protein) and palmitoylated proteins (transferring receptor, CD36 antigen, GTP binding protein α13, stomatin, SNAP 23, H-Ras) (Table II and supplemental Table 1). Proteins harboring GPI-anchor, myristoylation and palmitoylation target specifically to sphingolipid- and cholesterol-enriched rafts [85]. Other proteins found in MVs and microvilli in the present work are raft or raft-associated proteins such as flotillin 1 and 2, AnxA2, AnxA6, V-ATPase, G proteins, β-actin, integrins, LDL receptor-related protein 1 [85,86]. Taken together, these data suggest that MVs originate from Saos-2 cell microvillar lipid rafts.

Endoplasmic Reticular Origin of Matrix Vesicles

Several identified MV proteins are known to be residents of the ER (transmembrane protein 16E, oligosaccharyltransferase, thioredoxin domain containing 4) and the Golgi apparatus (Rab2B, Golgi-associated protein 1) (Table II and supplemental Table 1). Valosin-containing protein is an ATPase that mediates the ATP-dependent vesicle budding from the ER [87] and SNAP α is required for vesicular transport between the ER and the Golgi apparatus [88]. The coatomer protein complex mediates protein transport from the ER, via the Golgi apparatus up to the trans-Golgi network [89]. Cop-coated vesicle membrane protein p24 is a member of the p24 transmembrane protein family which is implicated in the budding of coatomer-coated and other species of coated vesicles and collecting cargo molecules into budding vesicles [90]. Arf1 and 4 belong to an abundant and highly conserved low molecular weight GTP-binding protein family that modulates vesicle budding from the Golgi apparatus and uncoating through controlled GTP hydrolysis [91]. These proteins are required for the intra-Golgi vesicle transport. This suggests that precursors of lipid rafts from which MVs will originate, are already formed in the ER and then transit through the Golgi apparatus. Finally, the coatomer protein complex mediates the budding of vesicles to be directed to the plasma membrane via a constitutive secretory pathway.

Several identified MV proteins are involved in vesicular fatty acid, cholesterol and phospholipid trafficking (CD36 antigen, Niemann-Pick C1, copine III, LDL receptor-related protein 1) as well as in vesicular protein trafficking (transmembrane protein trafficking, sorting nexin 4 and 6, vacuolar protein sorting 37B, Rab1B, Rab5C, Rab7, Rab8B, Rab10, Rab14) (Table II and supplemental Table 1). Rab7, a small GTPase belonging to the Rab family, is a key protein which regulates vesicular transport to specific areas of the plasma membrane by recruiting motor proteins [92]. Myosin 1B and 1C found in MVs and microvilli (supplemental Table 1) are motor proteins involved in vesicular

transport. However, most intracellular transport occurs via the microtubule network and only two dynein motor isoforms are involved in vesicular transport by using microtubules [92]. One of them, a cytoplasmic dynein heavy chain 1 was identified in MVs and microvilli, as well as tubulin α6 and β (Table II and supplemental Table 1). Therefore, preformed lipid rafts, from which MVs will be released, are targeted and fused to the plasma membrane via the essential protein machinery comprising AnxA1, AnxA2, AnxA4, AnxA7 and SNAP 23 (Table II). SNAP 23 is a component of the high affinity receptor (SNARE machinery) involved in apical membrane fusion [93].

Mechanisms of Matrix Vesicle Release

Microvilli are plasma membrane projections enclosing cytoplasm and actin microfilaments without cellular organelles [54-56], except free ribosomes [94]. Several specific cytoskeletal components of apical microvilli were identified in MVs in addition to actin such as ezrin, moesin, radixin, gelsolin, vinculin, plastin 1 and 3, actinin α1 and α4, and MARCKS. Ezrin, radixin and moesin belonging to the ERM family, are involved in connections of actin-based network to the plasma membrane and participate to the formation of microvilli as well as vinculin and talin 1 [95]. Arp2/3 complex (formed by actin-related protein 2 and 3) and filamin A (Table II) regulate actin polymerization and branched actin network formation [96]. Plastin 1 and 3 are actin bundling proteins that stabilize actin microfilament and thus, participate to the maintenance of microvilli [97]. Rac1 and 3 are small plasma membrane-associated GTPases that control cellular responses such as the formation of actin-based protrusions [98]. These proteins found in both MVs and microvilli, may participate in the formation and maintenance of microvilli.

Several observations indicated that MVs are formed by budding from the tip of cytoplasmic protrusions of mineralizing cells [1,46,47]. Furthermore, cytochalasin D, an inhibitor of actin microfilament assembly, was shown to stimulate MV release from hypertrophic chondrocyte microvilli [53]. These findings are supported by our observations revealing the occurrence in MVs and microvilli of modulators of actin polymerization/depolymerization (Table II and supplemental Table 1). Gelsolin is a calcium-regulated actin-modulating protein that prevents actin polymerization by end-blocking and severs actin microfilaments already formed when intracellular concentration of Ca^{2+} increases [99]. Cofilin 1 is a pH-sensitive actin-depolymerizing and severing protein [100]. These two proteins could be involved in actin network retractation leading to plasma membrane curvature and MV budding and this process may be regulated by Ca^{2+} and pH. In addition, a myosin complex comprising two myosin heavy chain 9, two myosin alkali light chain 6 and two myosin regulatory light chain MRCL3 (Table II and supplemental Table 1) could play a role in cytokinesis leading to MV release.

Alternative Mechanism of Matrix Vesicle Release

Among proteins of special interest, milk fat globule-EGF factor 8 (MFG-E8) was present in MVs and microvilli (Table II). MFG-E8 is peripheral membrane glycoprotein that interacts with integrins or PS-enriched cell surfaces in a receptor-independent manner [101]. Interestingly, this protein was found to localize in vesicles secreted from various cell types: mammary epithelial cell line, kidney cell line [101], epididymal cells [102], spleen-derived dendritic cell line [103]. It was demonstrated that its overexpression lead to the increase of vesicle formation [103]. This suggests that MFG-E8 may favor the budding of microvilli. In addition, MFG-E8 was also found in distinct small vesicles so-called exosomes derived from the same types of cells. These previous investigations indicated a different mechanism of biogenesis involving internalization of plasma membrane areas. The components of a clathrin-associated adaptor complex 2 (α1, β1 and μ subunits) as well as a clathrin heavy chain 1 and a clathrin light chain A were found in MVs and microvilli (Table II). The adaptor complex 2 is responsible for the recruitment of clathrin which is the major constituent of clathrin-coated pits and vesicles formed during endocytosis of the plasma membrane [104,105]. Therefore, microvillar lipid rafts from which MVs originate may be internalized in response to environmental stimuli. This supports the observations stating that a second pool of MVs aggregates under the plasma membrane before their extracellular release into a membranous sac [12]. This second type of MVs could correspond to the multivesicular bodies (Fig. 4) previously described by Yang and al. in zebrafish bones [106].

Conclusion

In this report, we characterized the proteome of MVs isolated from human osteosarcoma mineralization-competent Saos-2 cell-cultures. A large number of proteins associated with the mineralization process were previously identified in MVs originating from various cell types and species. We found new proteins that regulate PP_i and P_i homeostasis (ectonucleoside triphosphate diphosphohydrolase 3, inorganic pyrophosphatase 1), Ca^{2+} influx (SLC24A3, $Na^+/K^+/Ca^{2+}$ exchanger, and voltage-dependent Ca^{2+} channel) or intravesicular pH (SLC4A7, a bicarbonate transporter). The comparison of the MV proteome with that of microvilli showed 85 % of homology and the common presence of raft markers indicated that MVs are released from apical microvillar lipid rafts. Vesicular trafficking and cargo proteins pointed out the endoplasmic reticular origin of MVs and a mechanism of MV protein enrichment. Finally, the occurrence of certain cytoskeletal (gelsolin, cofilin 1) and motor proteins (a myosin complex) provided new insights about the mechanism of MV formation and release.

ACKNOWLEDGEMENTS

We thank Dr. John Carew for correcting the English. This work was supported by a grant N301 025 32-1120 from Polish Ministry of Science and Higher Education, by a Polonium grant (05819NF), by CNRS (France), and by the Rhône-Alpes region.

REFERENCES

[1] Anderson HC. Molecular biology of matrix vesicles. Clin Orthop Relat Res 1995;266-80.

[2] Anderson HC. Matrix vesicles and calcification. Curr Rheumatol Rep 2003;5:222-6.

[3] Anderson HC, Garimella R, Tague SE. The role of matrix vesicles in growth plate development and biomineralization. Front Biosci 2005;10:822-37.

[4] Anderson HC. The role of matrix vesicles in physiological and pathological calcification. Curr Opin Orthop 2007;18:428-33.

[5] Kirsch T, Nah HD, Shapiro IM, Pacifici M. Regulated production of mineralization-competent matrix vesicles in hypertrophic chondrocytes. J Cell Biol 1997;137:1149-60.

[6] Ali SY. Analysis of matrix vesicles and their role in the calcification of epiphyseal cartilage. Fed Proc 1976;35:135-42.

[7] Balcerzak M, Hamade E, Zhang L, Pikula S, Azzar G, Radisson J, Bandorowicz-Pikula J, Buchet R. The roles of annexins and alkaline phosphatase in mineralization process. Acta Biochim Pol 2003;50:1019-38.

[8] Kirsch T, Ishikawa Y, Mwale F, Wuthier RE. Roles of the nucleational core complex and collagens (types II and X) in calcification of growth plate cartilage matrix vesicles. J Biol Chem 1994;269:20103-9.

[9] Kirsch T, Harisson G, Golub EE, Nah HD. The roles of annexins and types II and X collagen in matrix vesicle-mediated mineralization of growth plate cartilage. J Biol Chem 2000;275:35577-83.

[10] Wu LN, Sauer GR, Genge BR, Valhmu WB, Wuthier RE. Effects of analogues of inorganic phosphate and sodium ion on mineralization of matrix vesicles isolated from growth plate cartilage of normal rapidly growing chickens. J Inorg Biochem 2003;94:221-35.

[11] Balcerzak M, Malinowska A, Thouverey C, Sekrecka A, Dadlez M, Buchet R, Pikula S. Proteome analysis of matrix vesicles isolated from femurs of chicken embryo. Proteomics 2008;8:192-205.

[12] Xiao Z, Camalier CE, Nagashima K, Chan KC, Lucas DA, de la Cruz MJ, Gignac M, Lockett S, Issaq HJ, Veenstra TD, Conrads TP, Beck GR Jr. Analysis of the extracellular matrix vesicle proteome in mineralizing osteoblasts. J Cell Physiol 2007;210:325-35.

[13] Stewart AJ, Roberts SJ, Seawright E, Davey MG, Fleming RH, Farquharson C. The presence of PHOSPHO1 in matrix vesicles and its developmental expression prior to skeletal mineralization. Bone 2006;39:1000-7.

[14] Einhorn TA, Gordon SL, Siegel SA, Hummel CF, Avitable MJ, Carty RP. Matrix vesicle enzymes in human osteoarthritis. J Orthop Res 1985;3:160-9.

[15] Hsu HHT, Anderson HC. Evidence of the presence of a specific ATPase responsible for ATP-initiated calcification by matrix vesicles isolated from cartilage and bone. J Biol Chem 1996;271:26383-88.

[16] Anderson HC, Sipe JB, Hessle L, Dhanyamraju R, Atti E, Camacho NP, Millán JL. Impaired calcification around matrix vesicles of growth plate and bone in alkaline phosphatase-deficient mice. Am J Pathol 2004;164:841-7.

[17] Register TC, McLean FM, Low MG, Wuthier RE. Roles of alkaline phosphatase and labile internal mineral in matrix vesicle-mediated calcification. J Biol Chem 1986;261:9354-60.

[18] Johnson K, Moffa A, Chen Y, Pritzker K, Goding J, Terkeltaub R. Matrix vesicle plasma cell membrane glycoprotein-1 regulates mineralization by murine osteoblastic MC3T3 cells. J Bone Miner Res 1999;14:883-92.

[19] Register TC, Wuthier RE. Effect of pyrophosphate and two diphosphonates on 45Ca and $32P_i$ uptake and mineralization by matrix vesicle-enriched fractions and by hydroxyapatite. Bone 1985;6:307-12.

[20] Johnson KA, Hessle L, Vaingankar S, Wennberg C, Mauro S, Narisawa S, Goding JW, Sano K, Millan JL, Terkeltaub R. Osteoblast tissue-nonspecific alkaline phosphatase antagonizes and regulates PC-1. Am J Physiol Regul Integr Comp Physiol 2000;279:R1365-77.

[21] Anderson HC, Harmey D, Camacho NP, Garimella R, Sipe JB, Tague S, Bi X, Johnson K, Terkeltaub R, Millán JL.. Sustained osteomalacia of long bones despite major improvement in other hypophosphatasia-related mineral deficits in tissue nonspecific alkaline phosphatase/nucleotide pyrophosphatase phosphodiesterase 1 double-deficient mice. Am J Pathol 2005;166:1711-20.

[22] Hessle L, Johnson KA, Anderson HC, Narisawa S, Sali A, Goding JW, Terkeltaub R, Millan JL. Tissue-nonspecific alkaline phosphatase and plasma cell membrane glycoprotein-1 are central antagonistic regulators of bone mineralization. Proc Natl Acad Sci USA 2002;99:9445-9.

[23] Golub EE, Boesze-Battaglia K. The role of alkaline phosphatase in mineralization. Curr Opin Orthop 2007;18:444-8.

[24] Montessuit C, Caverzasio J, Bonjour JP. Characterization of a Pi transport system in cartilage matrix vesicles. Potential role in the calcification process. J Biol Chem 1991;266:17791-7.

[25] Montessuit C, Bonjour JP, Caverzasio J. Expression and regulation of Na-dependent P(i) transport in matrix vesicles produced by osteoblast-like cells. J Bone Miner Res 1995;10:625-31.

[26] Guicheux J, Palmer G, Shukunami C, Hiraki Y, Bonjour JP, Caverzasio J. A novel in vitro culture system for analysis of functional role of phosphate transport in endochondral ossification. Bone 2000;27:69-74.

[27] Wu LN, Guo Y, Genge BR, Ishikawa Y, Wuthier RE. Transport of inorganic phosphate in primary cultures of chondrocytes isolated from the tibial growth plate of normal adolescent chickens. J Cell Biochem 2002;86:475-89.

[28] Balmain N, Hotton D, Cuisinier-Gleizes P, Mathieu H. Immunoreactive calbindin D9k in bone matrix vesicles. Histochemistry 1991;95:459-69.

[29] Wu LN, Yoshimori T, Genge BR, Sauer GR, Kirsch T, Ishikawa Y, Wuthier RE. Characterization of the nucleational core complex responsible for mineral induction by growth plate cartilage matrix vesicles. J Biol Chem 1993;268:25084-94.

[30] Genge BR, Wu LN, Wuthier RE. In vitro modeling of matrix vesicle nucleation: synergistic stimulation of mineral formation by annexin A5 and phosphatidylserine. J Biol Chem 2007;282:26035-45.

[31] Genge BR, Wu LN, Wuthier RE. Analysis and molecular modeling of the formation, structure, and activity of the phosphatidylserine-calcium-phosphate complex associated with biomineralization. J Biol Chem 2008;283:3827-38.

[32] Wu LN, Sauer GR, Genge BR, Wuthier RE. Induction of mineral deposition by primary cultures of chicken growth plate chondrocytes in ascorbate-containing media. Evidence of an association between matrix vesicles and collagen. J Biol Chem 1989;264:21346-55.

[33] Kirsch T, Wuthier RE. Stimulation of calcification of growth plate cartilage matrix vesicles by binding to type II and X collagens. J Biol Chem 1994;269:11462-9.

[34] Takagi M, Sasaki T, Kagami A, Komiyama K. Ultrastructural demonstration of increased sulfated proteoglycans and calcium associated with chondrocyte cytoplasmic processes and matrix vesicles in rat growth plate cartilage. J Histochem Cytochem 1989;37:1025-33.

[35] Wu LN, Genge BR, Wuthier RE. Association between proteoglycans and matrix vesicles in the extracellular matrix of growth plate cartilage. J Biol Chem 1991;266:1187-94.

[36] D'Angelo M, Billings PC, Pacifici M, Leboy PS, Kirsch T. Authentic matrix vesicles contain active metalloproteases (MMP). a role for matrix vesicle-associated MMP-13 in activation of transforming growth factor-beta. J Biol Chem 2001;276:11347-53.

[37] Dean DD, Schwartz Z, Muniz OE, Gomez R, Swain LD, Howell DS, Boyan BD. Matrix vesicles are enriched in metalloproteinases that degrade proteoglycans. Calcif Tissue Int 1992;50:342-9.

[38] Dean DD, Schwartz Z, Bonewald L, Muniz OE, Morales S, Gomez R, Brooks BP, Qiao M, Howell DS, Boyan BD. Matrix vesicles produced by osteoblast-like cells in culture become significantly enriched in proteoglycan-degrading metalloproteinases after addition of beta-glycerophosphate and ascorbic acid. Calcif Tissue Int 1994;54:399-408.

[39] Fedde KN. Human osteosarcoma cells spontaneously release matrix-vesicle-like structures with the capacity to mineralize. Bone Miner 1992;17:145-51.

[40] Muhlrad A, Bab I, Deutsch D, Sela J. Occurrence of actin-like protein in extracellular matrix vesicles. Calcif Tissue Int 1982;34:376-81.

[41] Muhlrad A, Setton A, Sela J, Bab I, Deutsch D. Biochemical characterization of matrix vesicles from bone and cartilage. Metab Bone Dis 1984;5:93-9.

[42] Wu LN, Genge BR, Kang MW, Arsenault AL, Wuthier RE. Changes in phospholipid extractability and composition accompany mineralization of chicken growth plate cartilage matrix vesicles. J Biol Chem 2002;277:5126-33.

[43] Balcerzak M, Pikula S, Buchet R. Phosphorylation-dependent phospholipase D activity of matrix vesicles. FEBS Lett 2006;580:5676-80.

[44] Hosokawa R, Uchida Y, fujiwara S, Noguchi T. Lactate dehydrogenase isoenzymes are present in matrix vesicles. J Biol Chem 1988;263:10045-7.

[45] Stechschulte DJ Jr, Morris DC, Silverton SF, Anderson HC, Väänänen HK. Presence and specific concentration of carbonic anhydrase II in matrix vesicles. Bone Miner 1992;17:187-91.

[46] Cecil RN, Anderson HC. Freeze-fracture studies of matrix vesicle calcification in epiphyseal growth plate. Metab Bone Dis 1978;1:89-97.

[47] Borg TK, Runyan RB, Wuthier RE. Correlation of freeze-fracture and scanning electron microscopy of epiphyseal chondrocytes. Calcif Tissue Res 1978;26:237-41.

[48] Ilvesaro J, Metsikkö K, Väänänen K, Tuukkanen J. Polarity of osteoblasts and osteoblast-like UMR-108 cells. J Bone Miner Res 1999;14:1338-1344.

[49] Kadis B, Goodson JM, Offenbacher S, Bruns JW, Seibert S. Characterization of osteoblast-like cells from fetal rat calvaria. J Dent Res 1980;59:2006-13.

[50] Volpin G, Rees JA, Ali SY, Bentley G. Distribution of alkaline phosphatase activity in experimentally produced callus in rats. J Bone Joint Surg Br 1986;68:629-34.

[51] von der Mark K, Mollenhauer J. Annexin V interactions with collagen. Cell Mol Life Sci 1997;53:539-45.

[52] Turnay J, Olmo N, Lizarbe MA, von der Mark K. Changes in the expression of annexin A5 gene during in vitro chondrocyte differentiation: influence of cell attachment. J Cell Biochem 2001;84:132-42.

[53] Hale JE, Wuthier RE. The mechanism of matrix vesicle formation. Studies on the composition of chondrocyte microvilli and on the effects of microfilament-perturbing agents on cellular vesiculation. J Biol Chem 1987;262:1916-25.

[54] Mooseker MS, Tilney LG. Organization of an actin filament-membrane complex. Filament polarity and membrane attachment in the microvilli of intestinal epithelial cells. J Cell Biol 1975;67:725-43.

[55] Paradela A, Bravo SB, Henríquez M, Riquelme G, Gavilanes F, González-Ros JM, Albar JP. Proteomic analysis of apical microvillous membranes of syncytiotrophoblast cells reveals a high degree of similarity with lipid rafts. J Proteome Res 2005;4:2435-41.

[56] Babusiak M, Man P, Petrak J, Vyoral D. Native proteomic analysis of protein complexes in murine intestinal brush border membranes. Proteomics 2007;7:121-9.

[57] Craig SW, Powell LD. Regulation of actin polymerization by villin, a 95,000 dalton cytoskeletal component of intestinal brush borders. Cell 1980;22:739-46.

[58] Booth AG, Kenny AJ. Proteins of the kidney microvillus membrane. Identification of subunits after sodium dodecylsullphate/polyacrylamide-gel electrophoresis. Biochem J 1976;159:395-407.

[59] Geiger B, Tokuyasu KT, Dutton AH, Singer SJ. Vinculin, an intracellular protein localized at specialized sites where microfilament bundles terminate at cell membranes. Proc Natl Acad Sci USA 1980;77:4127-31.

[60] Jimenez V, Henriquez M, Llanos P, Riquelme G. Isolation and purification of human placental plasma membranes from normal and pre-eclamptic pregnancies. A comparative study. Placenta 2004;25:422-37.

[61] Braccia A, Villani M, Immerdal L, Niels-Christiansen LL, Nystrøm BT, Hansen GH, Danielsen EM. Microvillar membrane microdomains exist at physiological temperature. Role of galectin-4 as lipid raft stabilizer revealed by "superrafts". J Biol Chem 2003;278:15679-84.

[62] Hansen GH, Pedersen ED, Immerdal L, Niels-Christiansen LL, Danielsen EM. Anti-glycosyl antibodies in lipid rafts of the enterocyte brush border: a possible host defense against pathogens. Am J Physiol Gastrointest Liver Physiol 2005;289:G1100-7.

[63] Kaczan-Bourgois D, Salles JP, Hullin F, Fauvel J, Moisand A, Duga-Neulat I, Berrebi A, Campistron G, Chap H. Increased content of annexin II (p36) and p11 in human placenta brush-border membrane vesicles during syncytiotrophoblast maturation and differentiation. Placenta 1996;17:669-76.

[64] Massey-Harroche D, Mayran N, Maroux S. Polarized localizations of annexins I, II, VI and XIII in epithelial cells of intestinal, hepatic and pancreatic tissues. J Cell Sci 1998;111:3007-15.

[65] Wuthier RE. Lipid composition of isolated epiphyseal cartilage cells, membranes and matrix vesicles. Biochim Biophys Acta 1975;409:128-43.

[66] Glaser JH, Conrad HE. Formation of matrix vesicles by cultured chick embryo chondrocytes. J Biol Chem 1981;256:12607-11.

[67] Elgsaeter A, Shotton DM, Branton D. Intramembrane particle aggregation in erythrocyte ghosts. II. The influence of spectrin aggregation. Biochim Biophys Acta 1976;426:101-22.

[68] Burgess DR, Prum BE. Reevaluation of brush border motility: calcium induces core filament solution and microvillar vesiculation. J Cell Biol 1982;94:97-107.

[69] Booth AG, Kenny J. A morphometric and biochemical investigation of the vesiculation of kidney microvilli. J Cell Sci 1976;21:449-63.

[70] Gillette JM, Nielsen-Preiss SM. The role of annexin 2 in osteoblastic mineralization. J Cell Sci 2004;117:441-9.

[71] Vaingankar SM, Fitzpatrick TA, Johnson K, Goding JW, Maurice M, Terkeltaub R. Subcellular targeting and function of osteoblast nucleotide pyrophosphatase phosphodiesterase 1. Am J Physiol Cell Physiol 2004;286:C1177-87.

[72] Stanford CM, Jacobson PA, Eanes ED, Lembke LA, Midura RJ. Rapidly forming apatitic mineral in an osteoblastic cell line (UMR 106-01 BSP). J Biol Chem 1995;270:9420-8.

[73] Strzelecka-Kiliszek A, Kwiatkowska K, Sobota A. Lyn and Syk kinases are sequentially engaged in phagocytosis mediated by FcR. J Immunol 2002;169:6787-94.

[74] Lever JE. Expression of a differentiated transport function in apical membrane vesicles isolated from an established kidney epithelial cell line. J Biol Chem 1982;257:8680-6.

[75] Cyboron GW, Wuthier RE. Purification and initial characterization of intrinsic membrane-bound alkaline phosphatase from chicken epiphyseal cartilage. J Biol Chem 1981;256:7262-8.

[76] Donowitz M, Singh S, Salahuddin FF, Hogema BM, Chen Y, Gucek M, Cole RN, Ham A, Zachos NC, Kovbasnjuk O, Lapierre LA, Broere N, Goldenring J, deJonge H, Li X. Proteome of murine jejunal brush border membrane vesicles. J Proteome Res 2007;6:4068-79.

[77] Cutillas PR, Biber J, Marks J, Jacob R, Stieger B, Cramer R, Waterfield M, Burlingame AL, Unwin RJ. Proteomic analysis of plasma membrane vesicles isolated from the rat renal cortex. Proteomics 2005;5:101-12.

[78] Bonilha VL, Bhattacharya SK, West KA, Sun J, Crabb JW, Rayborn ME, Hollyfield JG. Proteomic characterization of isolated retinal pigment epithelium microvilli. Mol Cell Proteomics. 2004;3:1119-27.

[79] Anderson HC, Cecil R, Sajdera SW. Calcification of rachitic rat cartilage in vitro by extracellular matrix vesicles. Am J Pathol 1975;79:237-54.

[80] Balcerzak M, Radisson J, Azzar G, Farlay D, Boivin G, Pikula S, Buchet R. A comparative analysis of strategies for isolation of matrix vesicles. Anal Biochem 2007;361:176-82.

[81] Sauer GR, Genge BR, Wu LN, Donachy JE. A facilitative role for carbonic anhydrase activity in matrix vesicle mineralization. Bone Miner 1994;26:69-79.

[82] Levade T, Jaffrézou JP. Signalling sphingomyelinases: which, where, how and why? Biochim Biophys Acta 1999;1438:1-17.

[83] van der Flier A, Sonnenberg A. Function and interactions of integrins. Cell Tissue Res 2001;305:285-98.

[84] Maeda S, Nobukuni T, Shimo-Onoda K, Hayashi K, Yone K, Komiya S, Inoue I. Sortilin is upregulated during osteoblastic differentiation of mesenchymal stem cells and promotes extracellular matrix mineralization. J Cell Physiol 2002;193:73-9.

[85] Lucero HA, Robbins PW. Lipid rafts-protein association and the regulation of protein activity. Arch Biochem Biophys 2004;426:208-24.

[86] Foster LJ, De Hoog CL, Mann M. Unbiased quantitative proteomics of lipid rafts reveals high specificity for signaling factors. Proc Natl Acad Sci USA 2003;100:5813-8.

[87] Zhang L, Ashendel CL, Becker GW, Morré DJ. Isolation and characterization of the principal ATPase associated with transitional endoplasmic reticulum of rat liver. J Cell Biol 1994;127:1871-83.

[88] Peter F, Wong SH, Subramaniam VN, Tang BL, Hong W. Alpha-SNAP but not gamma-SNAP is required for ER-Golgi transport after vesicle budding and the Rab1-requiring step but before the EGTA-sensitive step. J Cell Sci 1998;111:2625-33.

[89] Peter F, Plutner H, Zhu H, Kreis TE, Balch WE. Beta-COP is essential for transport of protein from the endoplasmic reticulum to the Golgi in vitro. J Cell Biol 1993;122:1155-67.

[90] Carney GE, Bowen NJ. p24 proteins, intracellular trafficking, and behavior: Drosophila melanogaster provides insights and opportunities. Biol Cell 2004;96:271-8.

[91] Serafini T, Orci L, Amherdt M, Brunner M, Kahn RA, Rothman JE. ADP-ribosylation factor is a subunit of the coat of Golgi-derived COP-coated vesicles: a novel role for a GTP-binding protein. Cell 1991;67:239-53.

[92] Jordens I, Marsman M, Kuijl C, Neefjes J. Rab proteins, connecting transport and vesicle fusion. Traffic 2005;6:1070-7.

[93] Low SH, Chapin SJ, Wimmer C, Whiteheart SW, Kömüves LG, Mostov KE, Weimbs T. The SNARE machinery is involved in apical plasma membrane trafficking in MDCK cells. J Cell Biol 1998;141:1503-13.

[94] Dixon SJ, Pitaru S, Bhargava U, Aubin JE. Membrane blebbing is associated with Ca2+-activated hyperpolarizations induced by serum and alpha 2-macroglobulin. J Cell Physiol 1987;132:473-82.

[95] Kotani H, Takaishi K, Sasaki T, Takai Y. Rho regulates association of both the ERM family and vinculin with the plasma membrane in MDCK cells. Oncogene 1997;14:1705-13.

[96] Flanagan LA, Chou J, Falet H, Neujahr R, Hartwig JH, Stossel TP. Filamin A, the Arp2/3 complex, and the morphology and function of cortical actin filaments in human melanoma cells. J Cell Biol 2001;155:511-7.

[97] Fath KR, Burgess DR. Microvillus assembly. Not actin alone. Curr Biol 1995;5:591-3.

[98] Aspenström P, Fransson A, Saras J. Rho GTPases have diverse effects on the organization of the actin filament system. Biochem J 2004;377:327-37.

[99] Janmey PA, Chaponnier C, Lind SE, Zaner KS, Stossel TP, Yin HL. Interactions of gelsolin and gelsolin-actin complexes with actin. Effects of calcium on actin nucleation, filament severing, and end blocking. Biochemistry 1985;24:3714-23.

[100] Pope BJ, Zierler-Gould KM, Kühne R, Weeds AG, Ball LJ. Solution structure of human cofilin: actin binding, pH sensitivity, and relationship to actin-depolymerizing factor. J Biol Chem 2004;279:4840-8.

[101] Oshima K, Aoki N, Kato T, Kitajima K, Matsuda T. Secretion of a peripheral membrane protein, MFG-E8, as a complex with membrane vesicles. Eur J Biochem 2002;269:1209-18.

[102] Gatti JL, Métayer S, Belghazi M, Dacheux F, Dacheux JL. Identification, proteomic profiling, and origin of ram epididymal fluid exosome-like vesicles. Biol Reprod 2005;72:1452-65.

[103] Théry C, Boussac M, Véron P, Ricciardi-Castagnoli P, Raposo G, Garin J, Amigorena S. Proteomic analysis of dendritic cell-derived exosomes: a secreted subcellular compartment distinct from apoptotic vesicles. J Immunol 2001;166:7309-18.

[104] Page LJ, Robinson MS. Targeting signals and subunit interactions in coated vesicle adaptor complexes. J Cell Biol 1995;131:619-30.

[105] Pearse BM. Clathrin: a unique protein associated with intracellular transfer of membrane by coated vesicles. Proc Natl Acad Sci USA 1976;73:1255-9.

[106] Yang L, Zhang Y, Cui FZ. Two types of mineral-related matrix vesicles in the bone mineralization of zebrafish. Biomed Mater 2007;2:21-5.

CHAPTER IV

CONCLUSIONS AND PERSPECTIVES

1. Regulatory effect of PP_i on matrix vesicle-induced mineralization.

MVs isolated from 17-day-old chicken embryo growth plate cartilage were used as a model of *in situ* mineralization to study regulatory properties of substrates, molecular machinery involved in the initial steps of mineralization and conditions that may lead to the pathological mineralization. We observed and confirmed the previously described features concerning mineral deposition induced by MVs. Rapid HA mineral deposition occurred in synthetic cartilage lymph (SCL) that mimics cartilage extracellular fluids, in the presence of MVs, underlying their role in catalyzing mineral formation [15]. An increase in P_i concentration in SCL containing already 2 mM Ca^{2+} and MVs led to an augmentation in the rate of MV-initiated crystalline HA formation, confirming that Ca^{2+}/P_i ratio and the Ca^{2+} x P_i product are critical factors affecting the kinetics of the biomineralization process [133]. Moreover, addition of monophosphoester substrates, such as AMP, accelerated HA deposition. Hydrolysis of AMP, a monophosphoester substrate of 5'-nucleotidase and TNAP present in MVs, yielded P_i which led to mature crystalline HA. However, hydrolysis of ATP, a source of P_i (after its hydrolysis by TNAP, ATPases and other PME enzymes) and also a source of PP_i (after its hydrolysis by NPP1 and TNAP) [111] inhibited mineral formation and led finally to a mixture of poorly crystalline HA and other phosphate minerals. The retardation was due to the inhibitory effect of ATP [134] or PP_i [50], on the HA formation. PP_i had a dual effect on mineralization. At low concentrations, it acted as a potent inhibitor of HA deposition but could be hydrolyzed and provide P_i for HA formation. We confirmed the fundamental role of MV-TNAP in mineralization being able to hydrolyze PP_i. PP_i hydrolysis at physiological pH (up to 96 %) was mostly due to MV-TNAP.

Having demonstrated that MVs are functional, the main purpose of this work was to determine whether or not P_i/PP_i ratio could be a determinant factor regulating pathological MV-induced calcification or its inhibition. Several calcified diseases were characterized by the deposit of HA or CPPD minerals. In osteoarthritic cartilage, articular chondrocytes underwent terminal differentiation similar to that in growth plate. They acquired the property to release mineralizing MVs. These MVs were found to be enriched in 5'-nucleotidase, TNAP, ATPases and NPP1 [45]. This could explain their ability to deposit HA minerals in degenerative joints. MVs were used to mimic pathological calcification, since the initiation of mineral formation mediated by MVs during endochondral calcification was similar to that which appeared in a variety of pathologic calcification [135]. Although MV model had the disadvantage that matrix and cellular issues could not be addressed, it provided an easily quantifiable and well-characterized system to analyze the initiation of HA or CPPD formation [136]. We found that formation of HA was optimal when the P_i/PP_i molar ratio was above 140, but was completely inhibited when the ratio decreased below 70. The retardation of any mineral formation was maximal at P_i/PP_i ratio around 30. CPPD was exclusively produced by MVs when the ratio was below 6, but its production was inhibited for a ratio exceeding 25. Our data emphasized that not only PP_i concentration affected the nature of the formed mineral but the P_i/PP_i ratio was a key

parameter to favor HA or CPPD formation and was a determinant factor leading to pathological mineralization or its inhibition. Since osteoarthritic MVs and growth plate MVs have all the protein machinery associated with mineralization, our data underlined a mechanism of pathological mineral deposit. Therefore, the P_i/PP_i ratio could reflect the differentiation state of chondrocytes (articular versus hypertrophic), the levels of expression of TNAP, NPP1 or other proteins affecting P_i and PP_i concentrations as well as the balance between pro- and anti- calcification factors and may serve as an indicator of the calcification process.

Since ATP is released by chondrocytes during stress conditions, it seems to be a preferential substrate in pathological mineralization. The conditions leading to pathological calcification initiated by ATP need to be investigated. Chondrocyte terminal differentiation is one of the determinant factors promoting extracellular matrix degradation and pathological calcification in osteoarthritic cartilages. The terminal differentiation could be a response to inflammatory molecules such cytokines and interleukins. However, these mechanisms are not well understood and remain to be elucidated, especially via the release of extracellular ATP. The prevention of terminal differentiation of articular chondrocytes would be an effective therapeutic strategy. Moreover, the comparison of non calcifying articular MV versus calcifying osteoarthritic MV proteomes could contribute to design new therapeutic targets to prevent pathological mineralization, such as enzymes affecting P_i and PP_i concentrations, Ca^{2+} and P_i transporter. Another therapeutic strategy could be developed against the mechanisms controlling MV biogenesis and release.

2. Origin, biogenesis and functions of matrix vesicles.

Although it has been demonstrated that growth plate MVs are released from chondrocyte microvilli and that actin microfilaments may be involved in MV formation [37,38], the mechanisms of MV formation from osteoblasts are not well established. Human osteosarcoma Saos-2 cells undergo the entire osteoblastic differentiation sequence from proliferation to mineralization and spontaneously release mineralizing MVs. Therefore, we selected Saos-2 cell cultures as a convenient model of osteoblastic mineralization to analyze the mechanisms involved in the release of MVs into the extracellular matrix. To verify the hypothesis that microvilli are the precursors of MVs, two different approaches were used to determine the origin, biogenesis and functions of MVs.

Firstly, different subcellular fractions from mineralizing Saos-2 cells including, basolateral membranes and apical membranes (microvilli) were purified and their protein and lipid profiles were compared as well as their abilities to mineralize to those of MVs released by these cells. The role of actin, the major cytoskeletal component of microvilli, in MV formation was investigated by employing two drugs affecting microfilament polymerization and depolymerization and monitoring

MV release. We found that MVs exhibited more similarities with apical microvilli than with other subcellular fractions including basolateral membranes. MVs and microvillar vesicles were similar in morphology and both were able to produce HA when incubated in a mineralization buffer. Protein profiles of microvilli and of MVs were similar and both were enriched in usual proteins implicated in mineralization such as TNAP, Na^+/K^+ ATPase, AnxA2 and AnxA6. Their lipid compositions were similar with characteristic enrichment of cholesterol, SM and PS as compared to the lipid composition of basololateral membranes. Therefore, apical microvilli were confirmed to be the precursors of MVs in Saos-2 cell plasma membrane. In addition, we proposed that actin depolymerization and thus actin network retraction lead to the mechanism of MV release from microvilli and cofilin 1, an actin severing protein, could be involved in this process.

Secondly, a proteomic analysis was performed on both MVs and microvilli. Their proteomes were compared and interpreted to identify an *in vivo* mechanism of MV biogenesis. We identified new proteins that could be implicated in mineralization: ectonucleoside triphosphate diphosphohydrolase 3 and inorganic pyrophosphatase 1 affecting P_i and PP_i concentrations; SLC24A3 and voltage-dependent Ca^{2+} channel regulating Ca^{2+} transport; sorcin, another Ca^{2+}-binding protein; SLC4A7, a bicarbonate transporter regulating intravesicular pH. The comparison of the MV proteome with that of microvilli showed 85 % of homology. Proteins associated with mineralization were identified in microvilli as well as microvillar markers were identified in MVs. The common presence of raft markers indicated that MVs are released from apical microvillar lipid rafts. ER markers, vesicular trafficking and cargo proteins shed light on the original pathway of MV formation. Finally, we proposed that actin microfilament retraction responsible for MV release is due to the concomitant action of cofilin 1, gelsolin and contractile myosin.

3. Concludings remarks

Pathological calcification is a process that has similarities with bone formation. Therefore, it is tempting to propose that formation of MVs under physiological conditions may follow the same mechanisms that trigger the vesicular release from microvillar regions of other cells under pathological conditions leading to ectopic mineralization. Key proteins involved in the biogenesis and release of MVs could be another therapeutic targets. However, several key molecules have still to be identified and their role to be elucidated.

REFERENCES

[1] Heinegard D, Oldberg A. Structure and biology of cartilage and bone matrix noncollagenous macromolecules. FASEB J 1989;3:2042-51.

[2] Buckwalter JA, Cooper RR. Bone structure and function. Instr Course Lect 1987;36:27-28.

[3] Marks SC, Popoff SN. Bone cell biology: the regulation of development, structure and function in the skeleton. Am J Anat 1988;183:1-44.

[4] Binette F, McQuaid DP, Haudenschild DR, Yaeger PC, McPherson JM, Tubo R. Expression of a stable articular cartilage phenotype without evidence of hypertrophy by adult human articular chondrocytes in vitro. J Orthop Res 1998;16:207-16.

[5] Paulsen F, Tillmann B. Composition of the extracellular matrix in human cricoarytenoid joint articular cartilage. Arch Histol Cytol 1999;62:149-63.

[6] Reginato AM, Shapiro IM, Lash JW, Jimenez SA. Type X collagen alterations in rachitic chick epiphyseal growth cartilage. J Biol Chem 1988;263:9938-45.

[7] Hatori M, Klatte KJ, Teixeira CC, Shapiro IM. End labeling studies of fragmented DNA in the avian growth plate: evidence of apoptosis in terminally differentiated chondrocytes. J Bone Miner Res 1995;10:1960-8.

[8] Kirsch T, Nah HD, Shapiro IM, Pacifici M. Regulated production of mineralization-competent matrix vesicles in hypertrophic chondrocytes. J Cell Biol 1997;137:1149-60.

[9] Anderson HC. Molecular biology of matrix vesicles. Clin Orthop Relat Res 1995;266-80.

[10] Anderson HC. Matrix vesicles and calcification. Curr Rheumatol Rep 2003;5:222-6.

[11] Anderson HC, Garimella R, Tague SE. The role of matrix vesicles in growth plate development and biomineralization. Front Biosci 2005;10:822-37.

[12] Thouverey C, Bleicher F, Bandorowicz-Pikula J. Extracellular ATP and its effects on physiological and pathological mineralization. Curr Opin Orthop 2007;18:460-6.

[13] Balcerzak M, Hamade E, Zhang L, Pikula S, Azzar G, Radisson J, Bandorowicz-Pikula J, Buchet R. The roles of annexins and alkaline phosphatase in mineralization process. Acta Biochim Pol 2003;50:1019-38.

[14] Glimcher MJ. Mechanism of calcification: role of collagen fibrils and collagen-phosphoprotein complexes in vitro and in vivo. Anat Rec 1989;224:139-53.

[15] Anderson HC, Cecil R, Sajdera SW. Calcification of rachitic rat cartilage in vitro by extracellular matrix vesicles. Am J Pathol 1975;79:237-54.

[16] Boskey AL. Biomineralization: conflicts, challenges, and opportunities. J Cell Biochem Suppl 1998;30-31:83-91.

[17] Anderson HC. Electron microscopic studies of induced cartilage development and calcification. J Cell Biol 1967;35:81-101.

[18] Bonucci E. Fine structure of early cartilage calcification. J Ultrastruct Res 1967;20:33-50.

[19] Anderson HC, Reynolds JJ. Pyrophosphate stimulation of calcium uptake into cultured embryonic bones. Fine structure of matrix vesicles and their role in calcification. Dev Biol 1973;34:211-27.

[20] Ali SY. Analysis of matrix vesicles and their role in the calcification of epiphyseal cartilage. Fed Proc 1976;35:135-42.

[21] Kirsch T, Ishikawa Y, Mwale F, Wuthier RE. Roles of the nucleational core complex and collagens (types II and X) in calcification of growth plate cartilage matrix vesicles. J Biol Chem 1994;269:20103-9.

[22] Kirsch T, Harisson G, Golub EE, Nah HD. The roles of annexins and types II and X collagen in matrix vesicle-mediated mineralization of growth plate cartilage. J Biol Chem 2000;275:35577-83.

[23] Wu LN, Guo Y, Genge BR, Ishikawa Y, Wuthier RE. Transport of inorganic phosphate in primary cultures of chondrocytes isolated from the tibial growth plate of normal adolescent chickens. J Cell Biochem 2002;86:475-89.

[24] Wu LN, Sauer GR, Genge BR, Valhmu WB, Wuthier RE. Effects of analogues of inorganic phosphate and sodium ion on mineralization of matrix vesicles isolated from growth plate cartilage of normal rapidly growing chickens. J Inorg Biochem 2003;94:221-35.

[25] Montessuit C, Caverzasio J, Bonjour JP. Characterization of a Pi transport system in cartilage matrix vesicles. Potential role in the calcification process. J Biol Chem 1991;266:17791-7.

[26] Montessuit C, Bonjour JP, Caverzasio J. Expression and regulation of Na-dependent P(i) transport in matrix vesicles produced by osteoblast-like cells. J Bone Miner Res 1995;10:625-31.

[27] Guicheux J, Palmer G, Shukunami C, Hiraki Y, Bonjour JP, Caverzasio J. A novel in vitro culture system for analysis of functional role of phosphate transport in endochondral ossification. Bone 2000;27:69-74.

[28] Rabinovitch AL, Anderson HC. Biogenesis of matrix vesicles in cartilage growth plates. Fed Proc 1976;35:112-6.

[29] Wuthier RE, Majeska RJ, Collins GM. Biosynthesis of matrix vesicles in epiphyseal cartilage. I. In vivo incorporation of 32P orthophosphate into phospholipids of chondrocyte, membrane, and matrix vesicle fractions. Calcif Tissue Res 1977;23:135-9.

[30] Kardos TB, Hubbard MJ. Are matrix vesicles apoptotic bodies? Prog Clin Biol Res 1982;101:45-60.

[31] Kirsch T, Wang W, Pfander D. Functional differencies between growth plate apoptotic bodies and matrix vesicles. J Bone Miner Res 2003;18:1872-81.

[32] Kirsch T. Physiological and pathological mineralization: a complex multifactorial process. Curr Opin Orthop 2007;18:434-43.

[33] Akisaka T, Shigenaga Y. Ultrastructure of growing epiphyseal cartilage processed by rapid freezing and freeze-substitution. J Electron Microsc 1983;32:305-20.

[34] Akisaka T, Kawaguchi H, Subita GP, Shigenaga Y, Gay CV. Ultrastructure of matrix vesicles in chick growth plate as revealed by quick freezing and freeze substitution. Calcif Tissue Int 1988;42:383-93.

[35] Cecil RN, Anderson HC. Freeze-fracture studies of matrix vesicle calcification in epiphyseal growth plate. Metab Bone Dis 1978;1:89-97.

[36] Morris DC, Masuhara K, Takaoka K, Ono K, Anderson HC. Immunolocalization of alkaline phosphatase in osteoblasts and matrix vesicles of human fetal bone. Bone Miner 1992;19:287-98.

[37] Hale JE, Chin JE, Ishikawa Y, Paradiso PR, Wuthier RE. Correlation between distribution of cytoskeletal proteins and release of alkaline phosphatase-rich vesicles by epiphyseal chondrocytes in primary culture. Cell Motil 1983;3:501-12.

[38] Hale JE, Wuthier RE. The mechanism of matrix vesicle formation. Studies on the composition of chondrocyte microvilli and on the effects of microfilament-perturbing agents on cellular vesiculation. J Biol Chem 1987;262:1916-25.

[39] Wuthier RE. Lipid composition of isolated epiphyseal cartilage cells, membranes and matrix vesicles. Biochim Biophys Acta 1975;409:128-43.

[40] Glaser JH, Conrad HE. Formation of matrix vesicles by cultured chick embryo chondrocytes. J Biol Chem 1981;256:12607-11.

[41] Wuthier RE. Effect of phospholipids on the transformation of amorphous calcium phosphate to hydroxapatite in vitro. Calcif Tissue Res 1975;19:197-210.

[42] Balcerzak M, Malinowska A, Thouverey C, Sekrecka A, Dadlez M, Buchet R, Pikula S. Proteome analysis of matrix vesicles isolated from femurs of chicken embryo. Proteomics 2008;8:192-205.

[43] Xiao Z, Camalier CE, Nagashima K, Chan KC, Lucas DA, de la Cruz MJ, Gignac M, Lockett S, Issaq HJ, Veenstra TD, Conrads TP, Beck GR Jr. Analysis of the extracellular matrix vesicle proteome in mineralizing osteoblasts. J Cell Physiol 2007;210:325-35.

[44] Stewart AJ, Roberts SJ, Seawright E, Davey MG, Fleming RH, Farquharson C. The presence of PHOSPHO1 in matrix vesicles and its developmental expression prior to skeletal mineralization. Bone 2006;39:1000-7.

[45] Einhorn TA, Gordon SL, Siegel SA, Hummel CF, Avitable MJ, Carty RP. Matrix vesicle enzymes in human osteoarthritis. J Orthop Res. 1985;3:160-9.

[46] Hsu HHT, Anderson HC. Evidence of the presence of a specific ATPase responsible for ATP-initiated calcification by matrix vesicles isolated from cartilage and bone. J Biol Chem 1996;271:26383-88.

[47] Anderson HC, Sipe JB, Hessle L, Dhanyamraju R, Atti E, Camacho NP, Millán JL. Impaired calcification around matrix vesicles of growth plate and bone in alkaline phosphatase-deficient mice. Am J Pathol 2004;164:841-7.

[48] Register TC, McLean FM, Low MG, Wuthier RE. Roles of alkaline phosphatase and labile internal mineral in matrix vesicle-mediated calcification. J Biol Chem 1986;261:9354-60.

[49] Johnson K, Moffa A, Chen Y, Pritzker K, Goding J, Terkeltaub R. Matrix vesicle plasma cell membrane glycoprotein-1 regulates mineralization by murine osteoblastic MC3T3 cells. J Bone Miner Res 1999;14:883-92.

[50] Register TC, Wuthier RE. Effect of pyrophosphate and two diphosphonates on 45Ca and $32P_i$ uptake and mineralization by matrix vesicle-enriched fractions and by hydroxyapatite. Bone 1985;6:307-12.

[51] Johnson KA, Hessle L, Vaingankar S, Wennberg C, Mauro S, Narisawa S, Goding JW, Sano K, Millan JL, Terkeltaub R. Osteoblast tissue-nonspecific alkaline phosphatase antagonizes and regulates PC-1. Am J Physiol Regul Integr Comp Physiol 2000;279:R1365-77.

[52] Anderson HC, Harmey D, Camacho NP, Garimella R, Sipe JB, Tague S, Bi X, Johnson K, Terkeltaub R, Millán JL.. Sustained osteomalacia of long bones despite major improvement in other hypophosphatasia-related mineral deficits in tissue nonspecific alkaline phosphatase/nucleotide pyrophosphatase phosphodiesterase 1 double-deficient mice. Am J Pathol 2005;166:1711-20.

[53] Hessle L, Johnson KA, Anderson HC, Narisawa S, Sali A, Goding JW, Terkeltaub R, Millan JL. Tissue-nonspecific alkaline phosphatase and plasma cell membrane glycoprotein-1 are central antagonistic regulators of bone mineralization. Proc Natl Acad Sci USA 2002;99:9445-9.

[54] Golub EE, Boesze-Battaglia K. The role of alkaline phosphatase in mineralization Curr Opin Orthop 2007;18:444-8.

[55] Seaton BA, Dedman JR. Annexins. Biometals 1998;11:399-404.

[56] Majeska RJ, Holwerda DL, Wuthier RE. Localization of phosphatidylserine in isolated chick epiphyseal cartilage matrix vesicles with trinitrobenzenesulfonate. Calcif Tissue Int 1979;27:41-6.

[57] Wu LN, Yoshimori T, Genge BR, Sauer GR, Kirsch T, Ishikawa Y, Wuthier RE. Characterization of the nucleational core complex responsible for mineral induction by growth plate cartilage matrix vesicles. J Biol Chem 1993;268:25084-94.

[58] Genge BR, Wu LN, Wuthier RE. In vitro modeling of matrix vesicle nucleation: synergistic stimulation of mineral formation by annexin A5 and phosphatidylserine. J Biol Chem 2007;282:26035-45.

[59] Genge BR, Wu LN, Wuthier RE. Analysis and molecular modeling of the formation, structure, and activity of the phosphatidylserine-calcium-phosphate complex associated with biomineralization. J Biol Chem 2008;283:3827-38.

[60] Wu LN, Sauer GR, Genge BR, Wuthier RE. Induction of mineral deposition by primary cultures of chicken growth plate chondrocytes in ascorbate-containing media. Evidence of an association between matrix vesicles and collagen. J Biol Chem 1989;264:21346-55.

[61] Kirsch T, Wuthier RE. Stimulation of calcification of growth plate cartilage matrix vesicles by binding to type II and X collagens. J Biol Chem 1994;269:11462-9.

[62] Takagi M, Sasaki T, Kagami A, Komiyama K. Ultrastructural demonstration of increased sulfated proteoglycans and calcium associated with chondrocyte cytoplasmic processes and matrix vesicles in rat growth plate cartilage. J Histochem Cytochem 1989;37:1025-33.

[63] Wu LN, Genge BR, Wuthier RE. Association between proteoglycans and matrix vesicles in the extracellular matrix of growth plate cartilage. J Biol Chem 1991;266:1187-94.

[64] D'Angelo M, Billings PC, Pacifici M, Leboy PS, Kirsch T. Authentic matrix vesicles contain active metalloproteases (MMP). a role for matrix vesicle-associated MMP-13 in activation of transforming growth factor-beta. J Biol Chem 2001;276:11347-53.

[65] Dean DD, Schwartz Z, Muniz OE, Gomez R, Swain LD, Howell DS, Boyan BD. Matrix vesicles are enriched in metalloproteinases that degrade proteoglycans. Calcif Tissue Int 1992;50:342-9.

[66] Dean DD, Schwartz Z, Bonewald L, Muniz OE, Morales S, Gomez R, Brooks BP, Qiao M, Howell DS, Boyan BD. Matrix vesicles produced by osteoblast-like cells in culture become significantly enriched in proteoglycan-degrading metalloproteinases after addition of beta-glycerophosphate and ascorbic acid. Calcif Tissue Int 1994;54:399-408.

[67] Fedde KN. Human osteosarcoma cells spontaneously release matrix-vesicle-like structures with the capacity to mineralize. Bone Miner 1992;17:145-51.

[68] Muhlrad A, Bab I, Deutsch D, Sela J. Occurrence of actin-like protein in extracellular matrix vesicles. Calcif Tissue Int 1982;34:376-81.

[69] Muhlrad A, Setton A, Sela J, Bab I, Deutsch D. Biochemical characterization of matrix vesicles from bone and cartilage. Metab Bone Dis 1984;5:93-9.

[70] Wu LN, Genge BR, Kang MW, Arsenault AL, Wuthier RE. Changes in phospholipid extractability and composition accompany mineralization of chicken growth plate cartilage matrix vesicles. J Biol Chem 2002;277:5126-33.

[71] Balcerzak M, Pikula S, Buchet R. Phosphorylation-dependent phospholipase D activity of matrix vesicles. FEBS Lett 2006;580:5676-80.

[72] Hosokawa R, Uchida Y, fujiwara S, Noguchi T. Lactate dehydrogenase isoenzymes are present in matrix vesicles. J Biol Chem 1988;263:10045-7.

[73] Stechschulte DJ Jr, Morris DC, Silverton SF, Anderson HC, Väänänen HK. Presence and specific concentration of carbonic anhydrase II in matrix vesicles. Bone Miner 1992;17:187-91.

[74] Hoebertz A, Arnett TR, Burnstock G. Regulation of bone resorption and formation by purines and pyrimidines. Trends Pharmacol Sci 2003;24:290-7.

[75] Garimella R, Bi X, Anderson HC, Camacho NP. Nature of phosphate substrate as a major determinant of mineral type formed in matrix vesicle-mediated in vitro mineralization: an FTIR imaging study. Bone 2006;38:811-7.

[76] Bowler WB, Tattersall JA, Hussein R, Dixon CJ, Cobbold PH, Gallagher JA. Real time measurement of ATP release from human osteoblasts. J Bone Miner Res 1998;13:524.

[77] Buckley KA, Golding SL, Rice JM, Dillon JP, Gallagher JA. Release and interconversion of P2 receptor agonists by human osteoblast-like cells. FASEB J 2003;17:1401-10.

[78] Romanello M, Pani B, Bicego M, D'Andrea P. Mechanically induced ATP release from human osteoblastic cells. Biochem Biophys Res Commun 2001;289:1275-81.

[79] Romanello M, Codognotto A, Bicego M, Pines A, Tell G, D'Andrea P. Autocrine/paracrine stimulation of purinergic receptors in osteoblasts: contribution of vesicular ATP release. Biochem Biophys Res Commun 2005;331:1429-38.

[80] Hatori, M., Teixeira, C. C., Debolt, K., Pacifici, M., Shapiro, I. M. Adenine nucleotide metabolism by chondrocytes in vitro: role of ATP in chondrocyte maturation and matrix mineralization. J Cell Physiol 1995;165:468-74.

[81] Graff, R., Lazarowski, E. R., Banes, A. J., Lee, G. M. ATP release by mechanically loaded chondrons in pellet culture. Arthitis & Rheum 2000;43:1571-9.

[82] Graff RD, Picher M, Lee GM. Extracellular nucleotides, cartilage stress, and calcium crystal formation. Curr Opin Rheumatol 2003;15:315-20.

[83] Harada S, Rodan GA. Control of osteoblast function and regulation of bone mass. Nature 2003;423:349-55.

[84] Orriss IR, Knight GE, Ranasinghe S, Burnstock G, Arnett TR. Osteoblast responses to nucleotides increase during differentiation. Bone 2006;39:300-9.

[85] Burnstock G. Purinergic signaling – an overview. Novartis Found Symp 2006;276:26-48.

[86] Khakh BS, North RA. P2X receptors as cell-surface ATP sensors in health and disease. Nature 2006;442:527-32.

[87] Katz S, Boland R, Santillan G. Modulation of ERK 1/2 and p38 MAPK signaling pathways by ATP in osteoblasts: involvement of mechanical stress-activated calcium influx, PKC and Src activation. Int J Biochem Cell Biol 2006;38:2082-91.

[88] Hiken JF, Steinberg TH. ATP downregulates P2X7 and inhibits osteoclast formation in RAW cells. Am J Physiol Cell Physiol 2004;287:C403-C412.

[89] Korcok J, Raimundo LN, Du X, Sims SM, Dixon SJ. P2Y6 nucleotide receptors activate NF-kB and increase survival of osteoclasts. J Biol Chem 2005;280:16909-15.

[90] Bonewald LF. Mechanosensation and transduction in osteocytes. Bonekey Osteovision 2006;3:7-15.

[91] Panupinthu N, Zhao L, Possmayer F, Ke HZ, Sims SM, Dixon SJ. P2X7 nucleotide receptors mediate blebbing in osteoblasts through a pathway involving lysophosphatidic acid. J Biol Chem 2007;282:3403-12.

[92] Roy AA, Nunn C, Ming H, Zou MX, Penninger J, Kirshenbaum LA, Dixon SJ, Chidiac P. Up-regulation of endogenous RGS2 mediates cross-desensitization between Gs and Gq signaling in osteoblasts. J Biol Chem 2006;281:32684-93.

[93] Samways DS, Egan TM. Acidic amino acids impart enhanced Ca(2+) permeability and flux in two members of the ATP-gated P2X receptor family. J Gen Physiol 2007;129:245-56.

[94] Coppi E, Pugliese AM, Urbani S, Melani A, Cerbai E, Mazzanti B, Bosi A, Saccardi R, Pedata F. ATP modulates cell proliferation and elicits two different electrophysiological responses in human mesenchymal stem cells. Stem Cells 2007;25:1840-9.

[95] Plotkin LI, Manolagas SC, Bellido T. Dissociation of the pro-apoptotic effects of bisphosphonates on osteoclasts from their antiapoptotic effects on osteoblasts/osteocytes with novel analogs. Bone 2006;39:443-52.

[96] Yoon MJ, Lee HJ, Lee YS, Kim JH, Park JK, Chang WK, Shin HC, Kim DK. Extracellular ATP is involved in the induction of apoptosis in murine hematopoietic cells. Biol Pharm Bull 2007;30:671-6.

[97] Riddle RC, Taylor AF, Rogers JR, Donahue HJ. ATP release mediates fluid flow-induced proliferation of human bone marrow stromal cells. J Bone Miner Res 2007;22:589-600.

[98] Rossi L, Manfredi R, Bertolini F, Ferrari D, Fogli M, Zini R, Salati S, Salvestrini V, Gulinelli S, Adinolfi E, Ferrari S, Di Virgilio F, Baccarani M, Lemoli RM. The extracellular nucleotide UTP is a potent inducer of hematopoietic stem cell migration. Blood 2007;109:533-42.

[99] Henriksen Z, Hiken JF, Steiberg TH, Jorgensen NR. The predominant mechanism of intercellular calcium wave propagation changes during long-term culture of human osteoblast-like cells. Cell Calcium 2006;39:435-44.

[100] Evans BAJ, Elford C, Pexa A, Francis K, Hughes AC, Deussen A, Ham J. Human osteoblast precursors produce extracellular adenosine, which modulates their secretion of IL-6 and osteoprotegerin. J Bone Miner Res 2006;21:228-36.

[101] Miyazaki T, Tanaka S, Sanjay A, Baron R. The role of c-Src kinase in the regulation of osteoclast function. Mod Rheumatol 2006; 16:68–74.

[102] Morimoto R, Uehara S, Yatsushiro S, Juge N, Hua Z, Senoh S, Echigo N, Hayashi M, Mizoguchi T, Ninomiya T, Udagawa N, Omote H, Yamamoto A, Edwards RH, Moriyama Y. Secretion of L-glutamate from osteoclasts through transcytosis. EMBO J 2006;25:4175-86.

[103] Yao G, Feng H, Cai Y, Qi W, Kong K. Characterization of vacuolar-ATPase and selective inhibition of vacuolar-H+-ATPase in osteoclasts. Biochem Biophys Res Commun 2007;357:821-7.

[104] Dalgarno D, Stehle T, Narula S, Schelling P, van Schravendijk MR, Adams S, Andrade L, Keats J, Ram M, Jin L, Grossman T, MacNeil I, Metcalf C 3rd, Shakespeare W, Wang Y, Keenan T, Sundaramoorthi R, Bohacek R, Weigele M, Sawyer T. Structural basis of Src tyrosine kinase inhibition with a new class of potent and selective trisubstituted purine-based compounds. Chem Biol Drug Des 2006;67:46-57.

[105] Fitzgerald JB, Jin M, Dean D, Wood DJ, Zheng MH, Grodzinsky AJ. Mechanical compression of cartilage explants induces multiple time-dependent gene expression patterns and involves intracellular calcium and cyclic AMP. J Biol Chem 2004;279:19502-11.

[106] Kono T, Nishikori T, Kataoka H, Uchio Y, Ochi M, Enomoto K. Spontaneous oscillation and mechanically induced calcium waves in chondrocytes. Cell Biochem Funct 2006;24:103-11.

[107] Millward-Sadler SJ, Wright MO, Flatman PW, Salter DM. ATP in the mechanotransduction pathway of normal human chondrocytes. Biorheology 2004;41:567-75.

[108] Milner PI, Fairfax TPA, Browning JA, Wilkins RJ, Gibson JS. The effect of O2 tension on pH homeostasis in equine articular chondrocytes. Arthritis Rheum 2006;54:3523-32.

[109] Mouw JK, Imler SM, Levenston ME. Ion-channel regulation of chondrocyte matrix synthesis in 3D culture under static and dynamic compression. Biomech Model Mechanobiol 2007;6:33-41.

[110] Mobasheri A, Genta TC, Nash AI, Womack MD, Moskaluk CA, Barrett-Jolley R. Evidence for functional ATP-sensitive (K(ATP)) potassium channels in human and equine articular chondrocytes. Osteoarthritis Cartilage 2007;15:1-8.

[111] Zhang L, Balcerzak M, Radisson J, Thouverey C, Pikula S, Azzar G, Buchet R. Phosphodiesterase activity of alkaline phosphatase in ATP-initiated Ca2+ and phosphate deposition in isolated chicken matrix vesicles. J Biol Chem 2005;280:37289-96.

[112] Balcerzak M, Radisson J, Azzar G, Farlay D, Boivin G, Pikula S, Buchet R. A comparative analysis of strategies for isolation of matrix vesicles. Anal Biochem 2007;361:176-82.

[113] Bathori G, Csordas G, Garcia-Perez C, Davies E, Hajnóczky G. Ca2+-dependent control of the permeability properties of the mitochondrial outer membrane and voltage-dependent anion-selective channel (VDAC). J Biol Chem 2006;281:17347-58.

[114] Shoshan-Barmatz V, Israelson A, Brdiczka D, Sheu SS. The voltage-dependent anion channel (VDAC): function in intracellular signaling, cell life and cell death. Curr Pharm Des 2006;12:2249-70.

[115] Schwartz Z, Sylvia VL, Larsson D, Nemere I, Casasola D, Dean DD, Boyan BD. 1a,25(OH)2D3 regulates chondrocyte matrix vesicle protein kinase C (PKC) directly via G-protein-dependent mechanisms and indirectly via incorporation of PKC during matrix vesicle biogenesis. J Biol Chem 2002;277:11828-37.

[116] Kirsch T. Determinants of pathological mineralization. Curr Opin Rheumatol 2006;18:174-80.

[117] Sweet MB, Thonar EJ, Immelman AR, Solomon L. Biochemical changes in progressive osteoarthrosis. Ann Rheum Dis 1977;36:387-98.

[118] Kirsch T, Swoboda B, Nah HD. Activation of annexin II and V expression, terminal differentiation, mineralization and apoptosis in human osteoarthritic cartilage. Osteoarthritis and Cartilage 2000;8:294-302.

[119] Nanba Y, Nishida K, Yoshikawa T, Sato T, Inoue H, Kuboki Y. Expression of osteonectin in articular cartilage of osteoarthritic knees. Acta Med Okayama 1997;51:239

[120] Nakase T, Miyaji T, Tomita T, Kaneko M, Kuriyama K, Myoui A, Sugamoto K, Ochi T, Yoshikawa H. Localization of bone morphogenetic protein-2 in human osteoarthritic cartilage and osteophyte. Osteoarthritis and Cartilage 2003;11:278-84.

[121] Wang X, Manner PA, Horner A, Shum L, Tuan RS, Nuckolls GH. Regulation of MMP-13 expression by RUNX2 and FGF2 in osteoarthritic cartilage. Osteoarthritis and Cartilage 2004;12:963-73.

[122] Pritzker KP. Crystal-associated arthropathies: what's new in old joints. J Am Geriatr Soc 1980;28:439-45.

[123] Ali SY. Apatite-type crystal deposition in arthritic cartilage. Scan Electron Microsc 1985;4:1555-66.

[124] Anderson HC. Mechanisms of pathologic calcification. Rheum Dis Clin North Am 1988;14:303-19.

[125] Derfus BA, Kurtin SM, Camacho NP, Kurup I, Ryan LM. Comparison of matrix vesicles derived from normal and osteoarthritic human articular cartilage. Connect Tissue Res 1996;35:337-42.

[126] Derfus B, Kranendonk S, Camacho N, Mandel N, Kushnaryov V, Lynch K, Ryan L. Human osteoarthritic cartilage matrix vesicles generate both calcium pyrophosphate dihydrate and apatite in vitro. Calcif Tissue Int 1998;63:258-62.

[127] Cheung HS, Kurup IV, Sallis JD, Ryan LM. Inhibition of calcium pyrophosphate dihydrate crystal formation in articular cartilage vesicles and cartilage by phosphocitrate. J Biol Chem 1996;271:28082-5.

[128] Derfus BA, Camacho NP, Olmez U, Kushnaryov VM, Westfall PR, Ryan LM, Rosenthal AK. Transforming growth factor beta-1 stimulates articular chondrocyte elaboration of matrix vesicles capable of greater calcium pyrophosphate precipitation. Osteoarthritis and Cartilage 2001;9:189-94.

[129] Serra R, Johnson M, Filvaroff EH, et al. Expression of a truncated, kinase-defective TGF(type II receptor in mouse skeletal tissue promotes terminal chondrocyte differentiation and osteoarthritis. J Cell Biol 1997;139:541-52.

[130] Cecil DL, Rose DM, Terkeltaub R, Liu-Bryan R. Role of interleukin-8 in PiT-1 expression and CXCR1-mediated inorganic phosphate uptake in chondrocytes. Arthritis Rheum 2005;52:144-54.

[131] Mitchell PG, Struve JA, McCarthy GM, Cheung HS. Basic calcium phosphate crystals stimulate cell proliferation and collagenase message accumulation in cultured adult articular chondrocytes. Arthritis Rheum 1992;35:343-50.

[132] Ea HK, Monceau V, Camors E, Cohen-Solal M, Charlemagne D, Lioté F. Annexin V overexpression increased joint chondrocyte apoptosis induced by basic calcium phosphate crystals. Ann Rheum Dis. 2008.

[133] Walhmu WB, Wu LN, Wuthier RE. Effects of Ca/P_i ratio, Ca^{2+} x P_i ion product, and pH of incubation fluid on accumulation of $45Ca^{2+}$ by matrix vesicles in vitro. Bone Miner 1990;8:195-209.

[134] Boskey AL, Boyan BD, Schwartz Z. Matrix vesicles promote mineralization in a gelatin gel. Calcif Tissue Int 1997;60:309-15.

[135] Anderson HC. The role of matrix vesicles in physiological and pathological calcification. Curr Opin Orthop 2007;18:428-33.

[136] Gohr C. In vitro models of calcium crystal formation. Curr Opin Rheumatol 2004;16:263-7.

SUPPLEMENTAL MATERIAL

SUPPLEMENTAL TABLE 1: Proteomic analysis of matrix vesicles and Saos-2 cell microvilli.

GI number	Protein name	MW	CRMVs	Microvilli	TM/PTM
gi|21361181	Na^+/K^+ ATPase alpha 1	112896	990.0 (31)	1577.0 (38)	10 TM
gi|62089374	Integrin alpha V	116038	390.0 (14)	522.0 (13)	1 TM
gi|19743813	Integrin beta 1	91620	489.0 (21)	629.0 (18)	1 TM
gi|4504747	Integrin alpha 3	118755	462.0 (12)	243.0 (9)	1 TM
gi|4507657	Tripeptidyl peptidase II	138449	751.0 (18)	561.0 (7)	
gi|55959864	Nicastrin	78411	84.0 (3)	208.0 (2)	1 TM
gi|4758012	Clathrin heavy chain 1	191614	1224.0 (33)	1746.0 (47)	
gi|6731237	Myoferlin	234708	339.0 (9)	738.0 (17)	1 TM
gi|126376	Lysosome-associated membrane glycoprotein 1	44882	88.0 (3)	259.0 (5)	1 TM
gi|56237029	Integrin alpha 5	114536	147.0 (4)	261.0 (4)	1 TM
gi|4507877	Vinculin	123799	509.0 (11)	792.0 (12)	
gi|6006515	Spliceosome associated protein 130	135577	317.0 (5)	193.0 (4)	
gi|12667788	Myosin heavy polypeptide 9 non-muscle	226532	2775.0 (46)	2730.0 (51)	
gi|61742777	Leucyl cystinyl aminopeptidase	117349	305.0 (6)	535.0 (9)	1 TM
gi|13606056	DNA dependent protein kinase catalytic subunit	469088	308.0 (6)	468.0 (8)	
gi|229532	Ubiquitin	8500	93.0 (2)	128.0 (3)	
gi|62088088	Transferrin receptor	84901	308.0 (14)	463.0 (13)	1 TM; Palmitoylation
gi|13936336	DNA-dependent protein kinase	469088	346.0 (5)		
gi|116256327	Membrane metallo-endopeptidase	85514	363.0 (12)	694.0 (12)	1 TM
gi|19913410	Major vault protein	99327	1296.0 (27)	57.0 (1)	
gi|23510338	Ubiquitin-activating enzyme E1	117849	511.0 (12)	877.0 (15)	
gi|6005942	Valosin-containing protein	89322	296.0 (7)	517.0 (10)	
gi|4501891	Actinin alpha 1	103057	387.0 (11)	1111.0 (13)	
gi|306891	Heat shock 90 kDa protein 1 beta	83264	437.0 (12)	1111.0 (23)	
gi|116734717	Tissue non-specific alkaline phosphatase	57305	2723.0 (48)	2858.0 (67)	GPI
gi|48145665	U5-116 kDa protein	109460	161.0 (2)	319.0 (4)	
gi|20127446	Integrin beta 5	88054	239.0 (7)	265.0 (5)	1 TM
gi|12025678	Actinin alpha 4	104854	401.0 (9)	877.0 (12)	
gi|4505257	Moesin	67820	297.0 (12)	498.0 (7)	
gi|12652633	Solute carrier family 1 member 5	56598	304.0 (10)	544.0 (10)	9 TM
gi|29789006	Kindlin 2	77860	97.0 (2)	62.0 (1)	
gi|62088530	Protein kinase C alpha	76764	111.0 (4)	312.0 (6)	
gi|5031631	Scavenger receptor class B member 2	54290	110.0 (4)	268.0 (5)	1 TM
gi|16507237	Heat shock 70 kDa protein 5	72333	245.0 (4)	751.0 (14)	
gi|61744475	Solute carrier family 3 member 2	71123	522.0 (14)	739.0 (16)	1 TM
gi|21314632	Solute carrier family 1 member 4	55723	98.0 (2)	229.0 (6)	9 TM
gi|40254816	Heat shock 90 kDa protein 1 alpha 2	98113	122.0 (1)	223.0 (1)	
gi|119631391	Integrin alpha 4	114899	354.0 (7)	533.0 (6)	1 TM
gi|187387	Myristoylated alanine-rich C kinase substrate	31545	372.0 (8)	452.0 (5)	Myristoylation
gi|4557425	Ectonucleoside triphosphate diphosphohydrolase 3	59133	75.0 (1)	61.0 (2)	1 TM
gi|14286326	Phosphofructokinase, liver type	90203	81.0 (1)	63.0 (1)	
gi|37267	Transketolase	67877	233.0 (4)	299.0 (7)	
gi|71773329	Annexin A6	75873	873.0 (27)	1064.0 (22)	
gi|46812315	Macroglobulin alpha 2	163292	79.0 (2)		
gi|10863945	ATP-dependent DNA helicase II, 80 kDa subunit	82704	434.0 (15)	144.0 (5)	
gi|5729877	Heat shock 70 kDa protein 8	70898	907.0 (16)	932.0 (13)	
gi|24307939	Chaperonin containing TCP1 subunit 5 (epsilon)	59671	226.0 (6)	212.0 (5)	
gi|35505	Pyruvate kinase 3	58062	454.0 (11)	589.0 (14)	
gi|36796	T-complex polypeptide 1	60343	443.0 (13)	522.0 (6)	
gi|14124984	Chaperonin containing TCP1 subunit 3 (gamma)	60534	282.0 (8)	696.0 (15)	
gi|4505897	Plastin 1	70352	107.0 (1)	88.0 (1)	
gi|41152506	Prostaglandin F2 receptor negative regulator	98556	261.0 (7)	124.0 (3)	1 TM
gi|4503841	ATP-dependent DNA helicase II, 70 kDa subunit	69843	858.0 (19)	487.0 (7)	
gi|4557251	ADAM metallopeptidase domain 10	84142	84.0 (2)	90.0 (2)	1 TM

gi|18201905	Glucose phosphate isomerase	63147	362.0 (6)	354.0 (7)	
gi|12653493	Brain abundant membrane attached signal protein 1	22693	303.0 (10)	247.0 (6)	Myristoylation
gi|7768938	Phenylalanyl tRNA synthetase	66115	117.0 (1)	78.0 (2)	
gi|4502673	CD47 antigen	35214	64.0 (1)	62.0 (1)	5 TM
gi|55584155	Annexin A7	52739	249.0 (8)	379.0 (13)	
gi|55665593	Eukaryotic translation elongation factor 1 alpha-like 3	50141	318.0 (10)	235.0 (8)	
gi|14389309	Tubulin alpha 6	49895	437.0 (9)	724.0 (12)	
gi|303618	Phospholipase C alpha	57065	152.0 (6)	513.0 (7)	
gi|4503529	Eukaryotic translation initiation factor 4A	46154	256.0 (5)	315.0 (5)	
gi|57209813	Tubulin beta	49907	820.0 (25)	861.0 (22)	
gi|40068518	Phosphogluconate dehydrogenase	53140	174.0 (6)	495.0 (9)	
gi|4501885	Actin beta	41737	765.0 (16)	1067.0 (23)	
gi|119620146	Chaperonin containing TCP1 subunit 7 (eta)	59366	237.0 (7)	350.0 (6)	
gi|3122595	Probable DEAD (Asp-Glu-Ala-Asp) box protein 17	80457	79.0 (1)	57.0 (1)	
gi|4502679	CD63 antigen	25637	83.0 (2)	89.0 (2)	4 TM
gi|16579885	Ribosomal protein L4	47697	211.0 (7)	243.0 (6)	
gi|24431933	Reticulon 4	108450	135.0 (4)	284.0 (6)	2 TM
gi|4503571	Enolase 1	47169	720.0 (21)	1102.0 (24)	
gi|5031573	Actin-related protein 3	47371	190.0 (6)	301.0 (4)	
gi|4502277	Na^+/K^+ ATPase beta 1 subunit	35061	177.0 (2)	196.0 (3)	1 TM
gi|5453603	Chaperonin containing TCP1 subunit 2	57488	444.0 (13)	429.0 (9)	
gi|1703322	Annexin A11	54390	105.0 (1)	466.0 (9)	
gi|4506649	Ribosomal protein L3	46109	606.0 (7)	402.0 (9)	
gi|4503481	Eukaryotic translation elongation factor 1 gamma	50119	146.0 (3)	284.0 (5)	
gi|56410847	GDP dissociation inhibitor 2	50663	101.0 (3)		
gi|19913428	Vacuolar H^+ ATPase subunit B	56501	138.0 (2)	61.0 (1)	
gi|20146101	Basigin	42200	136.0 (7)	263.0 (6)	1 TM
gi|5453599	F-actin capping protein alpha-2 subunit	32949	109.0 (3)	89.0 (1)	
gi|4502101	Annexin A1	38714	593.0 (15)	1390.0 (23)	
gi|4506617	Ribosomal protein L17	21397	212.0 (4)	270.0 (4)	
gi|16753227	Ribosomal protein L6	32728	456.0 (10)	121.0 (4)	
gi|33386564	MHC class I antigen B	40460	129.0 (2)	221.0 (3)	1 TM
gi|15718687	Ribosomal protein S3	26688	725.0 (15)	287.0 (9)	
gi|5803023	Lectin mannose-binding 2	40229	95.0 (4)		1 TM
gi|4504041	Guanine nucleotide binding protein G (i) alpha 2 subunit	40451	381.0 (8)	751.0 (16)	
gi|18645167	Annexin A2	40411	753.0 (18)	803.0 (20)	
gi|5174539	Cytosolic malate dehydrogenase	36426	158.0 (5)	447.0 (7)	
gi|14591909	Ribosomal protein L5	34363	564.0 (12)	109.0 (2)	
gi|4557032	Lactate dehydrogenase B	36638	327.0 (9)	232.0 (5)	
gi|5031857	Lactate dehydrogenase A	36689	232.0 (4)		
gi|19923362	Thy-1 cell surface antigen	17935	119.0 (1)	85.0 (2)	GPI
gi|5453597	F-actin capping protein alpha-1 subunit	32923	148.0 (4)	235.0 (5)	
gi|62088624	Band 4.1-like protein 2	112588	286.0 (10)	300.0 (5)	
gi|24981008	Solute carrier family 7 member 5	55010	200.0 (2)	111.0 (1)	11 TM
gi|230867	D-glyceraldehyde-3-phosphate dehydrogenase chain R	36024	133.0 (1)	178.0 (3)	
gi|306785	Guanine nucleotide binding protein beta 1 subunit	37377	159.0 (2)	449.0 (8)	
gi|15082586	Ribosomal protein L8	28025	124.0 (4)	97.0 (3)	
gi|4506723	Ribosomal protein S3a	29945	446.0 (10)	158.0 (3)	
gi|5174447	Guanine nucleotide binding protein beta 2 like 1	35077	477.0 (14)	277.0 (5)	
gi|356168	Histone H1b	21865	164.0 (5)	78.0 (3)	
gi|1703319	Annexin A4	36085	417.0 (11)	612.0 (13)	
gi|809185	Annexin A5	35937	710.0 (16)	2148.0 (26)	
gi|337514	Ribosomal protein S6	28681	736.0 (4)	218.0 (3)	
gi|62896539	Chaperonin containing TCP1 subunit 8 (theta)	59620	412.0 (8)	469.0 (12)	
gi|67464424	14-3-3 protein epsilon	29174	108.0 (5)	169.0 (2)	
gi|121490543	Chaperonin containing TCP1 subunit 6A	58024	169.0 (3)	244.0 (4)	
gi|119607218	Syntenin 1	32444	524.0 (9)	68.0 (1)	
gi|4506725	Ribosomal protein S4 X-linked	29598	487.0 (12)	286.0 (6)	

gi|15431295	Ribosomal protein L13	24261	274.0 (5)	75.0 (1)	
gi|4506743	Ribosomal protein S8	24205	186.0 (6)	372.0 (5)	
gi|15431301	Ribosomal protein L7	29226	204.0 (4)	135.0 (2)	
gi|4506609	Ribosomal protein L19	23466	140.0 (2)	142.0 (1)	
gi|88496	Proteasome alpha chain	?	65.0 (1)	60.0 (1)	
gi|22538467	Proteasome subunit beta type 4	29204	354.0 (6)	246.0 (5)	
gi|4885377	Histone H1d	21365	116.0 (2)		
gi|4507953	14-3-3 protein zeta	27745	319.0 (5)	582.0 (7)	
gi|4506183	Proteasome subunit alpha type 3	28433	143.0 (3)		
gi|34234	Laminin receptor 1	32854	1151.0 (11)	559.0 (9)	
gi|15055539	Ribosomal protein S2	31324	389.0 (13)	219.0 (5)	
gi|7513316	Ribosomal protein L14	23432	141.0 (3)	85.0 (1)	
gi|38455427	Chaperonin containing TCP1 subunit 4 (delta)	57924	212.0 (5)	415.0 (11)	
gi|56204043	Proteasome subunit alpha type 7	27887	197.0 (2)		
gi|14141193	Ribosomal protein S9	22591	239.0 (6)	145.0 (4)	
gi|550021	Ribosomal protein S5	22876	1610.0 (7)	445.0 (6)	
gi|4507207	Sorcin	21676	197.0 (4)	167.0 (4)	
gi|5031599	Actin related protein 2/3 complex subunit 2	34333	69.0 (1)	70.0 (1)	
gi|558528	Proteasome subunit beta type 6	25358	219.0 (3)	84.0 (2)	
gi|11415026	Ribosomal protein L18a	20762	322.0 (4)	182.0 (2)	
gi|4506607	Ribosomal protein L18	21634	324.0 (6)	228.0 (3)	
gi|15431303	Ribosomal protein L9	21863	454.0 (8)	133.0 (2)	
gi|34147513	RAB7	23490	301.0 (8)	491.0 (9)	Prenylation
gi|4505591	Peroxiredoxin 1	22110	151.0 (5)	120.0 (4)	
gi|4507357	Transgelin 2	22391	67.0 (2)	324.0 (5)	
gi|1172607	Proteasome subunit beta type 5	28480	304.0 (8)	337.0 (7)	
gi|6912634	Ribosomal protein L13a	23577	133.0 (2)	71.0 (1)	
gi|123296530	Proteosome subunit beta type 9	23264	105.0 (2)	211.0 (3)	
gi|5803149	Cop-coated vesicle membrane protein p24	22761	96.0 (1)	271.0 (5)	1 TM
gi|5174431	Ribosomal protein L10	24577	572.0 (6)	226.0 (6)	
gi|55669683	Eukaryotic translation initiation factor 3 subunit k	25060	70.0 (1)	111.0 (1)	
gi|4502693	CD9 antigen	25416	87.0 (1)		4 TM
gi|4758970	Proteasome subunit beta type 8	30354	69.0 (1)	78.0 (1)	
gi|22538465	Proteasome subunit beta type 3	22949	298.0 (7)	343.0 (5)	
gi|619788	Ribosomal protein L21	18565	130.0 (2)	96.0 (1)	
gi|7661678	RAP1B	20825	97.0 (1)	682.0 (7)	Prenylation
gi|10835165	CD59 antigen	14177	187.0 (3)	358.0 (3)	GPI
gi|88193084	Ras-related protein	23480	141.0 (3)	276.0 (5)	Prenylation
gi|4506597	Ribosomal protein L12	17819	473.0 (7)	262.0 (4)	
gi|55665353	Ribosomal protein L11	20252	238.0 (5)	122.0 (1)	
gi|292435	Ribosomal protein L26	17258	162.0 (4)	128.0 (3)	
gi|4502201	ADP-ribosylation factor 1	20697	197.0 (4)	294.0 (5)	Myristoylation
gi|4506681	Ribosomal protein S11	18431	347.0 (5)	205.0 (5)	
gi|4502205	ADP-ribosylation factor 4	20511	99.0 (1)	116.0 (3)	
gi|4506701	Ribosomal protein S23	15808	232.0 (3)	63.0 (1)	
gi|4505893	Proteolipid protein 2	16691	116.0 (2)	78.0 (2)	4 TM
gi|98986464	Transmembrane trafficking protein	24976	154.0 (3)	198.0 (3)	1 TM
gi|118090	Peptidylprolyl isomerase B	23742	112.0 (2)	236.0 (4)	
gi|57997105	Hypothetical protein	20294	139.0 (2)	409.0 (6)	?
gi|17105394	Ribosomal protein L23a	17695	92.0 (1)	98.0 (2)	
gi|478813	Non-histone chromosomal protein HMG-1	9539	103.0 (2)		
gi|2914478	Small guanine nucleotide binding protein rac1	23467	74.0 (1)	91.0 (1)	
gi|5453740	Myosin regulatory light chain MRCL3	19794	346.0 (7)	338.0 (6)	
gi|15451856	Caveolin 1	20472	91.0 (2)		1 TM; Palmitoylation
gi|119964726	Insulin growth factor 2 receptor	274275	1364.0 (25)	917.0 (18)	1 TM
gi|67476453	Fatty acid synthase	273426	495.0 (17)	1051.0 (29)	
gi|119604095	Filamin C gamma	291021	599.0 (9)	1537.0 (27)	
gi|1708865	Low density lipoprotein receptor-related protein 1	504605	439.0 (10)	956.0 (14)	1 TM

gi|119602166	Dynein cytoplasmic heavy chain 1	532406	250.0 (6)	2091.0 (35)	
gi|3694920	ADP-ribosyltransferase like 1	192594	275.0 (4)		
gi|53791221	Filamin A	280017	1172.0 (21)	1933.0 (38)	
gi|14286105	Plasma membrane Ca^{2+} ATPase type 4	133930	366.0 (9)	302.0 (9)	8 TM
gi|1228049	Glutamine dependent carbamoyl phosphate synthase	242983	64.0 (1)	246.0 (7)	
gi|16753233	Talin 1	269667	406.0 (11)	1301.0 (23)	
gi|119620171	Dysferlin	237294	814.0 (14)	1075.0 (18)	1 TM
gi|31657142	Integrin alpha 1	130847	401.0 (9)	446.0 (10)	1 TM
gi|473583	DNA topoisomerase I	90725	240.0 (12)		
gi|110624774	Mannose receptor, C type 2	166674	145.0 (2)	676.0 (15)	1 TM
gi|55665772	Solute carrier family 44 member 1	73302	78.0 (3)	67.0 (2)	9 TM
gi|4557803	Niemann Pick C1 protein	142148	81.0 (1)	242.0 (4)	12 TM
gi|5031931	Nascent polypeptide-associated complex alpha subunit	23384	178.0 (4)	219.0 (4)	
gi|134142345	ATP binding cassette subfamily C member 1	171591	119.0 (1)	482.0 (9)	5 TM
gi|134288865	Solute carrier family 4 member 7	136044	140.0 (3)	177.0 (3)	11 TM
gi|51315727	Histone H4	11367	430.0 (10)	140.0 (5)	
gi|4504255	Histone H2A z	13553	85.0 (3)		
gi|4506633	Ribosomal protein L31	14632	147.0 (2)		
gi|31542331	Cysteine-rich angiogenic inducer 61	42026	103.0 (2)		
gi|4506679	Ribosomal protein S10	18898	170.0 (1)	65.0 (1)	
gi|4506625	Ribosomal protein L27a	16561	122.0 (2)	68.0 (1)	
gi|4506699	Ribosomal protein S21	9111	146.0 (2)	54.0 (1)	
gi|28195394	Histone H2A	13995	1203.0 (14)	84.0 (1)	
gi|4506613	Ribosomal protein L22	14787	573.0 (5)	205.0 (1)	
gi|4506667	Ribosomal protein P0	34273	1154.0 (12)	309.0 (8)	
gi|4506715	Ribosomal protein S28	7841	226.0 (3)		
gi|31979	Histone H2B2	13906	1175.0 (6)	153.0 (3)	
gi|4506605	Ribosomal protein L23	14865	315.0 (3)	107.0 (1)	
gi|4506685	Ribosomal protein S13	17222	211.0 (3)		
gi|4506671	Ribosomal phosphoprotein P2	11665	1212.0 (8)	328.0 (4)	
gi|55956788	Nucleolin	76614	194.0 (2)	451.0 (9)	
gi|4506631	Ribosomal protein L30	12784	222.0 (4)	143.0 (3)	
gi|2697005	Proliferation-associated protein 2G4	43787	66.0 (2)	106.0 (2)	
gi|4506703	Ribosomal protein S24	15069	257.0 (3)	83.0 (1)	
gi|4506635	Ribosomal protein L32	15860	194.0 (3)	66.0 (1)	
gi|14277700	Ribosomal protein S12	14515	513.0 (4)	105.0 (1)	
gi|17986258	Myosin light chain 6	17557	193.0 (6)	139.0 (2)	
gi|4506741	Ribosomal protein S7	22127	95.0 (2)		
gi|53692187	Actin-related protein 2	45376	104.0 (1)	228.0 (4)	
gi|17932940	Ribosomal protein L15	24146	212.0 (1)	92.0 (1)	
gi|4506693	Ribosomal protein S17	15550	733.0 (5)	259.0 (4)	
gi|457262	Major histocompatibility complex, class II, Y box binding protein	35924	139.0 (1)	201.0 (2)	
gi|4506669	Ribosomal protein P1	11514	993.0 (8)	433.0 (2)	
gi|4506695	Ribosomal protein S19	16060	247.0 (3)	76.0 (1)	
gi|119623780	MHC class I antigen C	40648	420.0 (2)	182.0 (1)	1 TM
gi|4506643	Ribosomal protein L37a	10275	156.0 (1)	57.0 (1)	
gi|5032051	Ribosomal protein S14	16273	301.0 (6)	230.0 (3)	
gi|5031635	Cofilin 1	18502	289.0 (3)	354.0 (5)	
gi|4503053	Hyaluronan and proteoglycan link protein 1	40165	484.0 (9)	129.0 (1)	
gi|4757944	CD81 antigen	25809	171.0 (3)	195.0 (3)	4 TM
gi|4502899	Clathrin light polypeptide A	27077	86.0 (1)	75.0 (1)	
gi|386772	Histone H3	15388	433.0 (7)		
gi|115527968	CADM1 protein	48509	125.0 (1)	342.0 (2)	
gi|13491174	MARCKS-like protein	19529	162.0 (6)	163.0 (3)	
gi|38014007	DIP2B protein	171491	76.0 (2)	63.0 (1)	
gi|119582923	Transmembrane protein 2	154373	122.0 (4)		1 TM
gi|141797011	IQ motif containing GTPase activating protein 1	189251	278.0 (8)	841.0 (13)	
gi|119629737	Solute carrier family 19 member 1	64868	75.0 (1)	73.0 (1)	12 TM

gi|61743954	AHNAK nucleoprotein	629099	67.0 (1)	1586.0 (33)	
gi|4507047	Solute carrier family 7 member 1	67638	141.0 (3)	184.0 (3)	14 TM
gi|119582796	Solute carrier family 12 member 2	131447	126.0 (3)	155.0 (3)	12 TM
gi|4505807	Phosphatidylinositol 4 kinase type 3 alpha	100000	55.0 (1)	54.0 (1)	
gi|95113664	Leucine rich repeat containing 1	59242	102.0 (2)	61.0 (1)	
gi|74754588	Transmembrane protein 119	29119	139.0 (4)	95.0 (1)	1 TM
gi|62089338	Tetraspanin 6	27563	77.0 (1)	85.0 (1)	4 TM
gi|16418453	Pannexin 3	44683	98.0 (3)	113.0 (2)	4 TM
gi|1174915	Utrophin	394465	58.0 (1)	1060.0 (17)	
gi|10835049	Ras homolog gene family member A	21768	84.0 (2)	459.0 (8)	
gi|1705852	Voltage-dependent calcium channel, alpha 2/delta subunit 1	123183	188.0 (5)	227.0 (5)	
gi|3850044	Tubulin specific chaperone D	132600	62.0 (1)	78.0 (1)	
gi|148536855	Coatomer protein complex, subunit alpha	139324	99.0 (2)	151.0 (3)	
gi|757924	Epidermal growth factor receptor	134277	116.0 (1)	198.0 (4)	1 TM
gi|44889481	Myosin IB	124950	207.0 (5)	609.0 (9)	
gi|24307969	Cytoplasmic FMR1 interacting protein 1	145182	145.0 (4)	185.0 (2)	
gi|21237748	CD151 antigen	28295	65.0 (1)	56.0 (1)	4 TM
gi|249616	Insulin-like growth factor I receptor	154793	174.0 (3)	169.0 (2)	1 TM
gi|4506303	Protein tyrosine phosphatase, receptor type, alpha	90719	109.0 (2)		1 TM
gi|1373019	Cysteine-rich fibroblast growth factor receptor	91867	76.0 (1)	321.0 (4)	1 TM
gi|34782987	TBP-Interacting protein	136375	213.0 (6)	121.0 (4)	
gi|114319027	Immunoglobulin J chain	18099	76.0 (1)		
gi|42556032	Prominin 1	97202	162.0 (4)		4 TM
gi|13375569	Hp95	96023	432.0 (9)	536.0 (6)	
gi|119568427	Ectonucleotide pyrophosphatase/phosphodiesterase 1	99930	74.0 (1)	384.0 (5)	1 TM
gi|384062	Solute carrier family 24 member 3	71992	85.0 (1)		
gi|5031633	FERM, RhoGEF, and pleckstrin domain protein 1	122139	115.0 (2)		
gi|119593392	Glycogen debranching enzyme	174763	67.0 (1)	145.0 (2)	
gi|58331222	ATPase class VI type 11C	129560	108.0 (2)	260.0 (4)	7 TM
gi|119593571	Protein kinase C like 2	112034	133.0 (2)		
gi|16757970	Niban protein	79855	98.0 (3)	184.0 (2)	
gi|238236	Polymeric immunoglobulin receptor	83283	120.0 (1)		1 TM
gi|119588731	Transmembrane protein 16E	107187	193.0 (4)	180.0 (3)	8 TM
gi|4506773	S100 calcium-binding protein A9	13242	65.0 (1)		
gi|33598948	Phospholipase C gamma 1	148532	106.0 (1)		
gi|7657683	Solute carrier family 7 member 11	55423	104.0 (1)	69.0 (1)	12 TM
gi|19882251	Cystatin SN	16388	145.0 (2)		
gi|4504529	Histatin 1	6963	108.0 (1)		
gi|21361602	Solute carrier family 38 member 2	56026	198.0 (3)	77.0 (1)	9 TM
gi|2226273	Trans-golgi network glycoprotein 46	45879	71.0 (2)	68.0 (1)	1 TM
gi|19913416	Adaptor-related protein complex 2 alpha 1 subunit	107546	175.0 (5)	141.0 (3)	
gi|158937236	Aminopeptidase puromycin sensitive	98503	207.0 (4)	331.0 (4)	
gi|30583505	Catenin delta 1	108170	104.0 (2)	197.0 (5)	
gi|19744759	Rho guanine nucleotide exchange factor 2	111471	250.0 (5)	63.0 (1)	
gi|62088652	Synapse associated protein 97	103321	143.0 (4)	283.0 (4)	
gi|13699868	Methylenetetrahydrofolate dehydrogenase 1	101531	331.0 (8)	407.0 (5)	
gi|9716092	Sortilin	92067	124.0 (3)	179.0 (2)	1 TM
gi|119631361	NCK-associated protein 1	43000	129.0 (3)		1 TM
gi|603074	ATP citrate lyase	120839	259.0 (5)	254.0 (4)	
gi|3560557	Cellular apoptosis susceptibility protein	110416	150.0 (3)	159.0 (2)	
gi|4885505	N-acetylated alpha-linked acidic dipeptidase 2	83591	256.0 (4)	125.0 (2)	1 TM
gi|55770844	Catenin alpha 1	100071	432.0 (10)	584.0 (9)	
gi|119594339	Damage-specific DNA binding protein 1, 127 kDa	126968	74.0 (1)	86.0 (1)	
gi|4503131	Catenin beta 1	85496	126.0 (5)	306.0 (6)	
gi|5453998	Importin 7	119516	60.0 (1)	203.0 (2)	
gi|51100974	Myosin ID	116202	73.0 (1)		
gi|38014621	Autophagy related 9 homolog A	94447	61.0 (2)	58.0 (1)	5 TM
gi|799177	EBNA2 coactivator p100	101997	204.0 (4)	424.0 (6)	

gi|33873479	USO1 protein	62000	96.0 (2)		
gi|387019	Phosphoribosylglycinamide formyltransferase	107767	163.0 (2)		
gi|38327039	Heat shock 70 kDa protein 4	94331	336.0 (8)	512.0 (8)	
gi|42544159	Heat shock 105 kDa protein	96865	202.0 (4)	287.0 (5)	
gi|4758648	Kinesin family member 5B	109685	111.0 (2)	421.0 (5)	
gi|45751608	Myosin IC	121681	172.0 (4)	281.0 (4)	
gi|7705369	Coatomer protein complex subunit beta	107142	63.0 (1)	141.0 (3)	
gi|94721259	Solute carrier family 26 member 6	80910	141.0 (2)		12 TM
gi|4503483	Eukaryotic translation elongation factor 2	95338	201.0 (4)	222.0 (3)	
gi|1015321	Alanyl-tRNA synthetase	106810	94.0 (2)	239.0 (3)	
gi|119600540	Adaptor-related protein complex 2 beta 1 subunit	105691	102.0 (3)	246.0 (5)	
gi|6912530	Transmembrane 4 superfamily member 15	33165	102.0 (2)	147.0 (2)	4 TM
gi|4033763	Importin beta 3	125545	208.0 (4)	625.0 (9)	
gi|4507943	Exportin 1	123386	169.0 (3)	225.0 (3)	
gi|2873377	Exportin t	109964	61.0 (1)	66.0 (1)	
gi|116242779	Solute carrier family 12 member 7	119106	68.0 (1)	248.0 (5)	11 TM
gi|14250440	EphA2 protein	108266	166.0 (1)	168.0 (3)	1 TM
gi|55666319	Calcium/calmodulin-dependent serine protein kinase	104480	145.0 (2)		
gi|5880490	Lectomedin 1 alpha	157177	91.0 (1)	331.0 (4)	7 TM
gi|4758032	Coatomer protein complex subunit beta 2	102487	55.0 (1)	183.0 (6)	
gi|38511752	CD276 antigen	57235	76.0 (1)	61.0 (1)	1 TM
gi|493066	Glycyl-tRNA synthetase	84648	85.0 (2)	59.0 (1)	
gi|119631610	Dynein cytoplasmic 1 intermediate polypeptide 2	71456	69.0 (1)	75.0 (1)	
gi|134244281	Melanoma-associated antigen p97	80214	402.0 (7)	611.0 (7)	
gi|119600034	ATPase, H+ transporting, lysosomal alpha polypeptide, 70 KD	68304	77.0 (1)	371.0 (7)	
gi|13514809	DEAD (Asp-Glu-Ala-Asp) box polypeptide 3 Y-linked	73153	107.0 (2)	99.0 (1)	
gi|89954531	Sphingomyelin phosphodiesterase 3	71081	172.0 (5)	325.0 (5)	2 TM
gi|4506467	Radixin	68564	168.0 (2)	208.0 (2)	
gi|38202255	Threonyl-tRNA synthetase	83435	200.0 (5)	190.0 (3)	
gi|149363636	Plexin B2	53975	63.0 (1)	286.0 (5)	
gi|119612222	Polyadenylate binding protein 1	70671	64.0 (1)	214.0 (5)	
gi|119585402	Acylpeptide hydrolase	81224	65.0 (1)	72.0 (1)	
gi|94681046	Cyclin M4	86607	77.0 (1)	86.0 (1)	4 TM
gi|5107666	Importin beta 1	97170	138.0 (2)	151.0 (5)	
gi|984145	Lanosterol synthase	83309	73.0 (1)	213.0 (3)	
gi|32425737	Niban-like protein	84138	112.0 (3)	167.0 (3)	
gi|5123454	Heat shock 70 kDa protein 1A	70038	386.0 (6)	527.0 (8)	
gi|119620257	Glutamine-fructose-6-phosphate transaminase 1	76747	257.0 (4)	454.0 (5)	
gi|180117	CD36 antigen	53053	109.0 (1)	109.0 (1)	Palmitoylation
gi|3170407	Glycogen phosphorylase	97092	140.0 (2)	189.0 (3)	
gi|2039383	ADAM 17	93021	99.0 (1)		1 TM
gi|90265805	Phospholipase C delta 1	85665	103.0 (1)		
gi|7656959	Calpain 7	92652	56.0 (1)		
gi|56204623	Phosphoglycerate dehydrogenase	56650	209.0 (5)	244.0 (3)	
gi|20127454	Bifunctional purine biosynthesis protein PURH	64616	487.0 (9)	370.0 (6)	
gi|31542868	Glycogen synthase 1	83785	103.0 (2)	84.0 (1)	
gi|24431958	Solute carrier family 16 member 7	52200	65.0 (1)	75.0 (1)	12 TM
gi|4503939	Guanine nucleotide binding protein 1	67902	96.0 (2)		Prenylation
gi|16933537	Glomulin	68208	145.0 (2)	87.0 (1)	
gi|4507297	Syntaxin binding protein 1	68736	258.0 (3)	215.0 (3)	
gi|4506675	Ribophorin I	68569	88.0 (2)	174.0 (3)	1 TM
gi|11066968	EH domain-containing protein 3	60887	269.0 (7)	148.0 (2)	
gi|119616317	Chondroitin sulfate proteoglycan 2	372819	62.0 (2)		
gi|7549809	Plastin 3	70811	275.0 (10)	520.0 (9)	
gi|30240932	EH-domain containing 1	60627	217.0 (3)	74.0 (1)	
gi|189428	Phosphatase 2A regulatory subunit A	65308	127.0 (4)	172.0 (2)	
gi|4503015	Copine III	60130	124.0 (2)	223.0 (3)	
gi|28592	Albumin	69366	98.0 (2)	72.0 (1)	

gi|27881593	Syntaxin binding protein 3	67764	84.0 (1)	146.0 (2)	
gi|4505815	Phosphatidylinositol-4-phosphate 5-kinase type 1 alpha	62633	79.0 (1)		
gi|4503377	Dihydropyrimidinase-like 2	62293	156.0 (3)	350.0 (4)	
gi|1050527	Seryl-tRNA synthetase	58282	136.0 (1)		
gi|7656991	Coronin 1C	53249	96.0 (2)	150.0 (2)	
gi|13276615	Membrane protein, palmitoylated 2	61585	75.0 (1)	84.0 (1)	Palmitoylation
gi|460789	Transformation upregulated nuclear protein	51028	62.0 (1)	79.0 (3)	
gi|62897087	WD repeat-containing protein 1	66193	77.0 (1)	240.0 (7)	
gi|73909112	Stress induced phosphoprotein 1	62639	199.0 (1)	292.0 (3)	
gi|4757810	ATP synthase, H+ transporting, mitochondrial F1 complex, alpha	59750	115.0 (4)	625.0 (8)	
gi|449441	UDP-glucose pyrophosphorylase	56940	80.0 (2)	273.0 (4)	
gi|4758958	cAMP-dependent protein kinase, regulatory subunit alpha 2	45518	115.0 (3)	279.0 (5)	
gi|4929561	RuvB-like 2 protein	51156	110.0 (3)	86.0 (1)	
gi|182871	Glucose-6-phosphate dehydrogenase	88892	167.0 (3)		
gi|41281489	Putative MAPK activating protein PM28	39928	69.0 (1)	88.0 (2)	
gi|62089044	Replication factor A protein 1	68138	93.0 (4)		
gi|149589008	Peptidase D	54383	62.0 (1)	121.0 (2)	
gi|1581615	Oligosaccharyltransferase	50702	63.0 (1)	188.0 (2)	1 TM
gi|4759112	Solute carrier family 16 member 3	49469	62.0 (1)	122.0 (2)	12 TM
gi|19224660	Protein kinase C and casein kinase substrate in neurons 3	48487	63.0 (1)	83.0 (1)	
gi|4335941	Leucine aminopeptidase	56166	143.0 (3)	215.0 (3)	
gi|4507145	Sorting nexin 4	51909	61.0 (1)		
gi|119591141	Aspartyl aminopeptidase	52428	116.0 (2)		
gi|62896685	RuvB-like 1 protein	50228	134.0 (2)	400.0 (5)	
gi|4557317	Annexin A11	54390	358.0 (9)	466.0 (9)	
gi|32189394	ATP synthase, H^+ transporting, mitochondrial F1 complex, beta	56560	117.0 (2)	781.0 (9)	
gi|18379349	Vesicle amine transport protein 1	41920	440.0 (6)	314.0 (6)	
gi|10720285	Sorting nexin 6	47804	76.0 (1)	72.0 (1)	
gi|19923193	Heat shock 70 kDa protein binding protein	41332	106.0 (1)	205.0 (2)	
gi|4506439	Retinoblastoma binding protein 7	47820	98.0 (1)		
gi|62896713	Eukaryotic translation initiation factor 2 subunit 3	51109	74.0 (1)	85.0 (1)	
gi|435487	Aldehyde dehydrogenase 9	56292	64.0 (1)	71.0 (1)	
gi|9622850	Vacuolar sorting protein 35	91707	71.0 (1)	233.0 (3)	
gi|1710248	Protein disulfide isomerase A5	59594	91.0 (1)	458.0 (5)	
gi|4502281	Na^+/K^+ -ATPase beta 3 subunit	31512	113.0 (5)	327.0 (6)	1 TM
gi|20070158	Serine/threonine kinase 24	49308	106.0 (1)	88.0 (1)	
gi|119615779	Solute carrier family 7 member 5	55010	65.0 (1)	58.0 (1)	11 TM
gi|8922699	Glutamate carboxypeptidase-like protein 1	52779	59.0 (1)	63.0 (1)	
gi|4504169	Glutathione synthetase	52385	90.0 (1)	113.0 (2)	
gi|8439415	Tryptophanyl-tRNA synthetase	53165	119.0 (2)	65.0 (1)	
gi|4758756	Nucleosome assembly protein 1-like 1	45374	80.0 (1)	102.0 (2)	Farnesylation
gi|31127085	Ephrin receptor B4	108270	58.0 (1)	75.0 (1)	1 TM
gi|16445029	Immunoglobulin superfamily, member 8	65034	141.0 (1)	227.0 (2)	1 TM
gi|4505061	Cation-dependent mannose-6-phosphate receptor	30993	268.0 (3)	284.0 (3)	1 TM
gi|5453539	Phosphorybosylaminoimidazole carboxylase	47958	299.0 (7)	477.0 (6)	
gi|5453854	Poly(rC) binding protein 1	37526	104.0 (2)	64.0 (1)	
gi|12005493	NPD011	24353	150.0 (2)	112.0 (1)	
gi|5174557	Milk fat globule-EGF factor 8 protein	43123	197.0 (6)	63.0 (2)	
gi|21410823	Integrin binding protein DEL1	53765	214.0 (5)	93.0 (4)	
gi|24307907	Plasminogen activator inhibitor type 1 member 2	44002	99.0 (2)		
gi|10863955	Phosphoserine aminotransferase	35188	175.0 (3)	172.0 (2)	
gi|21361547	Ribonuclease/angiogenin inhibitor	49973	203.0 (3)	118.0 (1)	
gi|3641398	Isocitrate dehydrogenase 1	46659	93.0 (2)	367.0 (5)	
gi|9836652	Adipocyte plasma membrane-associated protein	46480	147.0 (2)	244.0 (3)	1 TM
gi|9951915	S-adenosylhomocysteine hydrolase	47716	71.0 (2)	271.0 (5)	
gi|24111250	Guanine nucleotide binding protein, alpha 13	44049	269.0 (5)	218.0 (8)	Palmitoylation
gi|1906670	Acyl-CoA thioester hydrolase	41150	69.0 (2)	91.0 (1)	
gi|94538362	Flotillin 2	47064	55.0 (1)	222.0 (5)	

gi|33415057	Transformation-related protein 14	42819	106.0 (2)	210.0 (3)	
gi|157502193	Proteasome 26S non-ATPase subunit 13	42945	101.0 (1)	152.0 (2)	
gi|119590191	ADP ribosyl transferase	113135	130.0 (4)		
gi|58761502	GTP-binding protein PTD004	44743	108.0 (2)		
gi|5031699	Flotillin 1	47355	85.0 (1)	516.0 (7)	
gi|13160478	Inositol polyphosphate-5-phosphatase A	47819	114.0 (2)	151.0 (2)	
gi|47938093	Protein tyrosine kinase 7	118391	204.0 (3)	293.0 (5)	1 TM
gi|4758158	Septin 2	41487	146.0 (3)	261.0 (4)	
gi|231382	MHC class I antigen B*13	40474	276.0 (5)	262.0 (3)	1 TM
gi|180570	Creatine kinase brain type	42644	296.0 (5)	302.0 (5)	
gi|4519417	Serine/threonine kinase receptor associated protein	38438	72.0 (1)	62.0 (1)	
gi|4504813	CD82 antigen	29625	90.0 (1)		4 TM
gi|4505763	Phosphoglycerate kinase 1	44615	568.0 (6)	653.0 (9)	
gi|21396504	Ephrin receptor B2	110030	161.0 (2)	209.0 (2)	1 TM
gi|55960300	Gelsolin	85697	103.0 (1)	96.0 (1)	Myristoylation
gi|6912420	Heparan sulfate 2-O-sulfotransferase 1	41881	61.0 (1)	61.0 (1)	
gi|52487191	Thioredoxin domain containing 4	46971	77.0 (1)	136.0 (2)	
gi|20986531	Mitogen-activated protein kinase 1	41390	88.0 (1)		
gi|46249758	Villin 2 (Ezrin)	69413	163.0 (2)	156.0 (2)	
gi|180687	2',3'-cyclic-nucleotide 3'-phosphodiesterase	47578	80.0 (1)	74.0 (2)	
gi|119624661	Solute carrier family 29 member 1	50219	70.0 (2)	59.0 (1)	11 TM
gi|115583685	Solute carrier family 16 member 1	53944	62.0 (1)	62.0 (2)	11 TM
gi|312137	Fructose-bisphosphate aldolase	39456	127.0 (1)	217.0 (3)	
gi|31645	Glyceraldehyde-3-phosphate dehydrogenase	36054	510.0 (9)	803.0 (15)	
gi|28614	Aldolase A	39420	121.0 (4)	593.0 (7)	
gi|1633574	MHC class I antigen A2	40841	231.0 (6)	352.0 (6)	1 TM
gi|20149560	Syntaxin 4A	34180	100.0 (3)		1 TM
gi|6912328	Dimethylarginine dimethylaminohydrolase 1	31122	211.0 (5)	189.0 (2)	
gi|3929617	SNAP alpha	33233	159.0 (5)	113.0 (3)	
gi|4506005	Protein phosphatase 1 catalytic subunit beta	37187	126.0 (4)		
gi|4506061	AMP-activated protein kinase, noncatalytic gamma-1 subunit	37579	106.0 (1)	62.0 (1)	
gi|4885381	Histone 1, H1b	22580	130.0 (4)	124.0 (2)	
gi|4504753	Integrin alpha 7	124287	76.0 (1)		1 TM
gi|6912594	Phosphatidylinositol transfer protein, beta	31540	147.0 (4)		
gi|4505641	Proliferating cell nuclear antigen	28769	162.0 (3)		
gi|13375926	Vacuolar protein sorting 37B	31307	194.0 (4)		
gi|4758256	Eukaryotic translation initiation factor 2, subunit alpha	36112	166.0 (3)	55.0 (1)	
gi|38522	Eukaryotic translation elongation factor 1, delta	71408	84.0 (1)	70.0 (1)	
gi|8393516	NAD(P)H steroid dehydrogenase like protein	41900	74.0 (1)		1 TM
gi|19913432	ATPase, H+ transporting, lysosomal, V0 subunit D	40329	188.0 (3)	216.0 (3)	
gi|28827795	Chromatin modifying protein 4B	24950	89.0 (1)	84.0 (1)	
gi|10863877	Phospholipid scramblase 1	35049	160.0 (2)	169.0 (3)	1 TM
gi|11056044	Inorganic pyrophosphatase 1	32660	150.0 (4)	84.0 (1)	
gi|4506017	Protein phosphatase 2A, catalytic subunit	35594	100.0 (2)	121.0 (2)	
gi|4502599	Carbonyl reductase 1	30375	133.0 (3)	77.0 (1)	
gi|14714483	OTU domain containing ubiquitin aldehyde binding 1	31284	94.0 (1)		
gi|133252	Heterogeneous nuclear ribonucleoprotein A1	38747	104.0 (1)	88.0 (1)	
gi|150439236	Deoxyribonuclease I-like 1	33893	103.0 (1)		1 TM
gi|15788437	Cyclin-box carrying protein	39337	74.0 (1)		
gi|181184	Stomatin	31731	292.0 (7)	505.0 (8)	Palmitoylation
gi|2343185	Tubulin folding cofactor B	27325	70.0 (1)	88.0 (1)	
gi|4826659	F-actin capping protein beta subunit	30629	214.0 (5)	102.0 (1)	
gi|387033	Purine nucleoside phosphorylase	32148	64.0 (1)	65.0 (1)	
gi|42734438	Family with sequence similarity 49, member B	36748	412.0 (7)	81.0 (1)	
gi|4885079	Mitochondrial ATP synthase, gamma subunit 1	32996	78.0 (1)	86.0 (1)	
gi|14251209	Chloride intracellular channel 1	26923	166.0 (3)	114.0 (1)	
gi|4506179	Proteasome subunit alpha type 1	29556	67.0 (2)	126.0 (2)	
gi|119574954	Voltage-dependent anion channel 2	38093	60.0 (1)	114.0 (3)	

gi|15930199	Glucosamine-6-phosphate deaminase 2	31085	192.0 (3)	78.0 (1)	
gi|30410792	Proteasome activator complex subunit 2	27402	104.0 (1)	95.0 (1)	
gi|7705855	Hydroxysteroid (17-beta) dehydrogenase 12	34324	89.0 (1)	64.0 (1)	3 TM
gi|158259997	Family with sequence similarity 125, member A	28783	128.0 (1)		
gi|119609801	Ubiquitin-conjugating enzyme E2O	141383	99.0 (1)		
gi|4503143	Cathepsin D preproprotein	44552	140.0 (2)	359.0 (8)	
gi|13477169	Vitronectin	54305	86.0 (1)		
gi|116063554	Phosphodeoxyriboaldolase	35231	284.0 (4)		
gi|4506129	Phosphoribosyl pyrophosphate synthetase 2	34769	114.0 (1)		
gi|4758874	Transmembrane 9 superfamily member 2	75775	71.0 (1)		9 TM
gi|7656922	Chromatin modifying protein 2A	25104	115.0 (1)		
gi|4506203	Proteasome subunit beta type 7	29965	139.0 (3)	124.0 (2)	
gi|25188179	Voltage-dependent anion channel 3	30659	85.0 (2)	294.0 (5)	
gi|847724	Methylthioadenosine phosphorylase	31236	110.0 (2)	150.0 (2)	
gi|7524354	Dimethylarginine dimethylaminohydrolase 2	29644	244.0 (4)	497.0 (5)	
gi|4505773	Prohibitin	29804	64.0 (1)	158.0 (2)	
gi|1374813	SNAP-23	23354	55.0 (1)	118.0 (1)	Palmitoylation
gi|7661922	RAB21	24348	165.0 (3)	297.0 (3)	
gi|34485714	RAB23	26659	156.0 (3)	312.0 (4)	
gi|41393545	RAB5C	23482	338.0 (6)	494.0 (6)	
gi|178790	Apolipoprotein B100	515529	80.0 (1)		Palmitoylation
gi|19923989	Collagen triple helix repeat-containing 1	26224	135.0 (2)		
gi|36038	Rho GDP dissociation inhibitor alpha	23207	125.0 (3)	297.0 (5)	
gi|4507951	14-3-3 Eta	28219	277.0 (3)	220.0 (2)	
gi|4504483	Hypoxanthine phosphoribosyltransferase 1	24579	62.0 (1)	163.0 (2)	
gi|7656952	Calcyclin binding protein	26210	77.0 (2)		
gi|5729941	Tetraspanin 9	26779	119.0 (2)	77.0 (1)	4 TM
gi|296736	Proteosome subunit alpha type 6	27399	204.0 (3)	299.0 (3)	
gi|23397554	Leucine rich repeat containing 57	26740	127.0 (2)	245.0 (3)	
gi|4758638	Peroxiredoxin 6 (Lysosomal phospholipase A2)	25035	305.0 (5)	283.0 (3)	
gi|5453990	Proteasome activator subunit 1	28602	118.0 (2)	257.0 (3)	
gi|30425420	PHOSPHO1	29713	80.0 (1)	138.0 (2)	
gi|54696300	Proteosome subunit alpha type 5	26579	83.0 (2)	62.0 (1)	
gi|4885371	H1 histone family, member 0	20863	116.0 (3)	74.0 (1)	
gi|23065552	Glutathione S-transferase M3	26560	199.0 (3)	254.0 (3)	
gi|23491735	Ribosomal protein L10a	24831	135.0 (3)	74.0 (1)	
gi|73536235	RAB14	23897	168.0 (3)	220.0 (4)	
gi|4502013	Adenylate kinase 2	26478	93.0 (1)	164.0 (3)	
gi|16877641	Proline-rich coiled-coil 1	46701	68.0 (1)	90.0 (1)	
gi|4506405	Ras related protein RAL B	23408	95.0 (1)	144.0 (2)	
gi|4506185	Proteasome subunit alpha type 4	29484	310.0 (3)	195.0 (5)	
gi|20147713	Ras related protein RAL A	23567	97.0 (1)	251.0 (3)	
gi|82407948	14-3-3 gamma	28303	222.0 (2)	369.0 (3)	
gi|5052202	Chloride intracellular channel 4	28772	141.0 (2)		
gi|4505753	Phosphoglycerate mutase 1	28804	99.0 (2)	425.0 (6)	
gi|119598698	Clathrin adaptor complex AP2, MU subunit	49389	100.0 (2)		
gi|726098	Glutathione S-transferase 3	23356	494.0 (5)	265.0 (3)	
gi|14589951	RNA polymerase II polypeptide E	24611	105.0 (1)	111.0 (1)	
gi|21361091	Ubiquitin carboxyl-terminal esterase L1	24824	65.0 (1)	170.0 (3)	
gi|4757834	BCL2-associated athanogene 2	23772	146.0 (3)	118.0 (2)	
gi|4506181	Proteasome subunit alpha type 2	25899	230.0 (3)	265.0 (3)	
gi|7705885	Vacuolar protein sorting 28	26462	319.0 (6)		
gi|8922491	Transmembrane protein 33	27951	98.0 (1)	98.0 (1)	3 TM
gi|19923231	RAB6A	23593	72.0 (1)	333.0 (7)	Prenylation
gi|4502011	Adenylate kinase 1	21635	105.0 (2)	132.0 (2)	
gi|33695095	RAB10	22469	246.0 (4)	329.0 (4)	
gi|5020074	Glyoxalase I	20778	91.0 (2)	145.0 (3)	
gi|31543380	DJ-1 protein	19891	162.0 (5)	201.0 (4)	Sumoylation

gi|6005731	Calcium binding protein P22	22456	103.0 (2)	352.0 (4)	Myristoylation
gi|8218049	Histidine triad nucleotide binding protein 3	20375	128.0 (2)		
gi|62897873	Lin-7 homolog C	21834	118.0 (2)	193.0 (3)	
gi|39725636	Transmembrane emp24 protein transport domain containing 9	27277	73.0 (1)	242.0 (3)	1 TM
gi|5803135	RAB35	23025	137.0 (2)	298.0 (4)	
gi|12585534	Transmembrane emp24 domain-containing protein 5	26017	74.0 (1)	67.0 (1)	1 TM
gi|156071462	Solute carrier family 25 member 6	32926	58.0 (1)	290.0 (5)	2 TM
gi|4885417	Huntingtin interacting protein 2	22407	97.0 (1)	170.0 (2)	
gi|4506365	RAB2A	23545	125.0 (1)	278.0 (3)	
gi|4502419	Biliverdin reductase B	22119	108.0 (1)	125.0 (1)	
gi|4506363	RAB13	22774	238.0 (6)	406.0 (6)	Prenylation
gi|4092054	RAN	24423	70.0 (1)	85.0 (1)	
gi|7706563	RAB8B	23584	197.0 (3)	178.0 (3)	
gi|4506193	Proteasome subunit beta type 1	26489	214.0 (4)	163.0 (4)	
gi|21361884	RAB2B	24214	95.0 (2)	176.0 (2)	
gi|913159	Raf kinase inhibitor protein	21057	60.0 (1)	324.0 (4)	
gi|125987848	VHL-binding protein 1	22626	100.0 (1)	66.0 (1)	
gi|4506195	Proteasome subunit beta type 2	22836	110.0 (1)	160.0 (2)	
gi|4506413	RAP1A	20987	103.0 (2)	522.0 (8)	
gi|4758988	RAB1A	22678	443.0 (7)	483.0 (10)	Prenylation
gi|13569962	RAB1B	22171	350.0 (3)	519.0 (5)	
gi|2978560	Neuropilin 1	103085	122.0 (1)	100.0 (1)	1 TM
gi|3002951	Breakpoint cluster region protein 1	15522	146.0 (3)		
gi|49168476	RAB11B	24574	87.0 (2)	155.0 (3)	
gi|54696598	ADP-ribosylation factor 6	20082	84.0 (2)	132.0 (2)	
gi|29436553	Syndecan 2	22160	88.0 (1)		
gi|4503249	DEK oncogene	42674	93.0 (2)		
gi|4826962	RAC3	21379	139.0 (3)	332.0 (6)	
gi|4506691	Ribosomal protein S16	16445	65.0 (1)		
gi|55669748	Golgi-Associated protein 1	17218	105.0 (1)	167.0 (2)	
gi|1942977	Macrophage migration inhibitory factor	12476	73.0 (1)		
gi|4506661	Ribosomal protein L7a	29996	192.0 (3)	312.0 (5)	
gi|4826898	Profilin 1	15054	251.0 (3)	287.0 (3)	
gi|208115	H-Ras	21298	103.0 (2)	216.0 (3)	Palmit; Farn; Pren
gi|4506623	Ribosomal protein L27	15798	103.0 (2)		
gi|4505751	Profilin 2	15046	72.0 (1)	74.0 (1)	
gi|4757952	CDC 42	21259	80.0 (1)	433.0 (5)	
gi|1237406	Superoxide dismutase 1	15936	55.0 (1)	67.0 (1)	
gi|4432748	Ribosomal protein S27	9461	85.0 (1)	58.0 (1)	
gi|400059	Interferon-induced transmembrane protein 2	14546	106.0 (1)	112.0 (2)	2 TM
gi|15530277	Ferritin, light polypeptide	20020	92.0 (1)	269.0 (3)	
gi|19557691	Surfeit 4	30394	71.0 (1)	109.0 (1)	5 TM
gi|4505183	CD99 antigen	18848	76.0 (1)	67.0 (1)	1 TM
gi|296452	Ribosomal protein S26	13015	88.0 (1)	95.0 (1)	
gi|1772345	Ras-related GTP-binding protein	20497	95.0 (1)		
gi|10863927	Peptidylprolyl isomerase A	18012	179.0 (2)	120.0 (2)	
gi|825635	Calmodulin 1	16838	62.0 (1)	258.0 (5)	
gi|14165469	Ribosomal protein S15a	14839	103.0 (1)	165.0 (1)	
gi|4507669	Tumor protein, translationally controlled 1	19595	61.0 (1)	186.0 (2)	
gi|5174764	Metallothionein 2A	6042	64.0 (1)		
gi|307348	Prothymosin alpha	12203	140.0 (1)	229.0 (1)	
gi|124219	Eukaryotic translation initiation factor 4B	69151	127.0 (2)	112.0 (2)	
gi|4759140	Solute carrier family 9 member 3 regulatory factor 1	38868	59.0 (1)	80.0 (1)	
gi|10716563	Calnexin	67568	150.0 (1)	311.0 (8)	1 TM
gi|20664042	Calcyclin	10180	61.0 (1)		
gi|8922720	Transmembrane protein 30A	40684	52.0 (1)		2 TM
gi|4507793	Ubiquitin-conjugating enzyme E2N	17138	78.0 (1)	95.0 (2)	
gi|60416394	XRP2 protein	39642	84.0 (1)	66.0 (2)	Myristoyl; Palmitoyl

LIST OF PUBLICATIONS

Experimental papers:

-Zhang L., Balcerzak M., Radisson J., **Thouverey C.**, Pikuła S., Azzar G., Buchet R. (2005). Phosphodiesterase activity of alkaline phosphatase in ATP-initiated Ca2+ and phosphate deposition in isolated chicken matrix vesicles. *J Biol Chem;* 280:37289-96.

-Gorecka K.M., **Thouverey C.**, Buchet R., Pikuła S. (2007). Potential role of AnnAt1 from *Arabidopsis thaliana* in pH-mediated cellular response to environmental stimuli. *Plant Cell Physiol*; 48:792-803.

-Balcerzak M., Malinowska A., **Thouverey C.**, Sekrecka A., Dadłez M., Buchet R., Pikuła S. (2007). Proteome analysis of matrix vesicles isolated from femurs of chicken embryo. *Proteomics*; 8:192-205.

-**Thouverey C.**, Bechkoff G., Pikuła S., Buchet R. (2008). Inorganic pyrophosphate as a regulator of hydroxyapatite or calcium pyrophosphate dihydrate mineral deposition by matrix vesicles. *Osteoarthritis and Cartilage;* accepted (#OAC4312R1). *

-**Thouverey C.**, Strzelecka-Kiliszek A., Balcerzak M., Buchet R., Pikuła S. (2008). Matrix vesicles originate from apical membrane microvilli of mineralizing osteoblast-like Saos-2 cells. Manuscript submitted to *J Cell Biochem;* under revision (JCB-08-0177). *

-**Thouverey C.**, Malinowska A., Balcerzak M., Strzelecka-Kiliszek A., Buchet R., Pikuła S. (2008). Proteomic Characterization of the Origin and Biogenesis of Calcifying Matrix Vesicles from Osteoblast-like Saos-2 cells. Manuscript under preparation. *

Reviews:

-Sekrecka A., Balcerzak M., **Thouverey C.**, Buchet R., Pikuła S. (2007). Annexins in mineralization. *Postepy Biochem*; 53:159-63.

-**Thouverey C.**, Bleicher F., Bandorowicz-Pikuła J. (2007). Extracellular ATP and its effects on physiological and pathological mineralization. *Curr Opin Orthop*; 18:460-6. *

* Publications reported in the PhD thesis.

LIST OF PRESENTATIONS

Oral presentation

-**Thouverey C.** (2007). Origin of matrix vesicles in mineralization competent osteoblast-like Saos-2 cells. Seminar of Department of Biochemistry, Nencki Institute of Experimental Biology, October 8, Warsaw, Poland.

Poster presentations

-Gorecka K.M., **Thouverey C.**, Buchet R., Pikuła S. (2007). Annexin AnnAt1 from *A. thaliana* as an intracellular pH sensor in stress response in plants. 6th Parnas Conference, May 31, Krakow, Poland. *Acta Biochim Pol*; 54, supplement 2:15.

-**Thouverey C.**, Balcerzak M., Strzelecka-Kiliszek A., Pikuła S., Buchet R. (2008). Origin of matrix vesicles in mineralization competent osteoblast-like saos-2 cells. IBMS Davos Workshops: Bone Biology & Therapeutics, March 10, Davos, Switzerland. *Bone;* 42, supplement 1:S31-S32.

-**Thouverey C.**, Balcerzak M., Strzelecka-Kiliszek A., Malinowska A., Buchet R., Pikuła S. (2008). Apical microvilli of osteoblast-like Saos-2 cells as precursors of calcifying matrix vesicles: A comparative proteomic study. Abstracts of the 35th European Symposium on Calcified Tissues, May 27, Barcelona, Spain. *Calcif Tissue Int;* 82, supplement 2:S120.

Origin, characterization and roles of matrix vesicles in physiological and pathological mineralization

Matrix vesicles (MVs) are involved in the initiation of mineralization in tissues undergoing physiological and pathological calcification. Pyrophosphate (PP_i) has a dual effect on mineralization: a source of phosphate (P_i) to sustain hydroxyapatite (HA) formation and an inhibitor of HA growth. We found that formation of HA was optimal when the P_i/PP_i molar ratio was above 140, while calcium pyrophosphate dihydrate, identified in osteoarthritis was exclusively produced by MVs when the ratio was below 6. Proteomic analysis and lipid compositions on both MVs and microvilli from osteoblast-like Saos-2 cells, revealed that MVs have an endoplasmic reticular origin and characteristic lipids and proteins as in lipid rafts. Finally, we demonstrated that MV release from microvilli is caused by the concomitant actions of actin-depolymerizing and contractile motor proteins. Proteins involved in MV biogenesis could be new therapeutic targets to prevent pathological calcification.

Keywords: Biogenesis, bone, cartilage, chondrocytes, matrix vesicles, microvilli, mineralization, osteoarthritis, osteoblasts, pyrophosphate.

Pęcherzyki macierzy pozakomórkowej (MV) uczestniczą we wczesnych etapach mineralizacji tkanek, zarówno w normie, jak i w patologii. Nieorganiczny pirofosforan (PP_i) odgrywa podwójną rolę w tym procesie: jest źródłem nieorganicznego fosforanu (P_i), związku niezbędnego w produkcji hydroksyapatytu (HA), i jest jednocześnie inhibitorem tworzenia kryształów HA. W niniejszej pracy pokazano, że powstawanie HA w wyizolowanych z tkanki pęcherzykach MV zachodzi z optymalną szybkością w warunkach, kiedy stosunek molowy P_i/PP_i przekracza 140, podczas gdy pirofosforan wapnia·$2H_2O$, zidentyfikowany w przypadkach osteoartretyzmu (artrozy), tworzy się w kiedy stosunek P_i/PP_i jest niższy niż 6. Proteomiczna i lipidomiczna analiza składu chemicznego pęcherzyków MV i frakcji mikrokosmków wyizolowanych z hodowli osteoblastów linii Saos-2 wskazuje na pochodzenie tych struktur z siateczki śródplazmatycznej, a ich skład białkowy i lipidowy przypomina frakcję mikrodomen błony plazmatycznej, tzw. tratw (ang. *rafts*). W niniejszej pracy zaprezentowano także dane świadczące, że pączkowanie pęcherzyków MV od błony plazmatycznej (rejon mikrokosmków) zachodzi przy współudziale białek uczestniczących w depolimeryzacji F-aktyny i białek motorycznych. Białka biorące udział w procesie powstawania pęcherzyków MV mogą stanowić dogodne cele przyszłej interwencji farmakologicznej, zapobiegającej rozwojowi stanów chorobowych związanych z nieprawidłowym przebiegiem mineralizacji.

Słowa kluczowe: Biogeneza, kość, chrząstka, chondrocyty, pęcherzyki macierzy pozakomórkowej, mikrokosmki, mineralizacja, artroza, osteoblasty, nieorganiczny pirofosforan.

Université Claude Bernard Lyon 1
UFR Chimie – Biochimie
UMR CNRS UCBL 5246 – ICBMS
Bâtiment Chevreul
43 Boulevard du 11 Novembre 1918
69622 Villeurbanne Cedex

Nencki Institute of Experimental Biology
Polish Academy of Sciences
Department of Biochemistry
Laboratory of Biochemistry of Lipids
3 Pasteur Street
02-093 Warsaw, Poland

Origin, characterization and roles of matrix vesicles in physiological and pathological mineralization

Matrix vesicles (MVs) are involved in the initiation of mineralization in tissues undergoing physiological and pathological calcification. Pyrophosphate (PP_i) has a dual effect on mineralization: a source of phosphate (P_i) to sustain hydroxyapatite (HA) formation and an inhibitor of HA growth. We found that formation of HA was optimal when the P_i/PP_i molar ratio was above 140, while calcium pyrophosphate dihydrate, identified in osteoarthritis was exclusively produced by MVs when the ratio was below 6. Proteomic analysis and lipid compositions on both MVs and microvilli from osteoblast-like Saos-2 cells, revealed that MVs have an endoplasmic reticular origin and characteristic lipids and proteins as in lipid rafts. Finally, we demonstrated that MV release from microvilli is caused by the concomitant actions of actin-depolymerizing and contractile motor proteins. Proteins involved in MV biogenesis could be new therapeutic targets to prevent pathological calcification.

Keywords: Biogenesis, bone, cartilage, chondrocytes, matrix vesicles, microvilli, mineralization, osteoarthritis, osteoblasts, pyrophosphate.

Les vésicules matricielles (VM) sont impliquées dans l'initiation des minéralisations physiologique ou pathologique. Le pyrophosphate (PP_i) est une source de phosphate (P_i) pour maintenir la formation d'hydroxyapatite (HA) mais aussi un inhibiteur de la croissance de ces minéraux. Nous avons montré que la formation d'HA était optimale lorsque le rapport molaire P_i/PP_i était supérieur à 140, tandis que du calcium pyrophosphate dihydraté, marqueur de l'arthrose, était exclusivement formé lorsque ce rapport était inférieur à 6. Des analyses protéomiques et en compositions lipidiques sur les VM et les microvillosités des cellules Saos-2 ont révélé que les VM étaient formées dans le réticulum endoplasmique et qu'elles possèdent des lipides et protéines caractéristiques de radeaux lipidiques. Finalement, nous avons montré que les VM sont libérées à partir des microvillosités grâce aux actions coordonnées de protéines dépolymérisant l'actine et de protéines contractiles. Les protéines impliquées dans la biogenèse des VM peuvent être des nouvelles cibles thérapeutiques pour prévenir des calcifications pathologiques.

Mots-clés: Biogénèse, cartilage, chondrocytes, microvillosités, minéralisation, os, ostéoarthrose, ostéoblastes, pyrophosphate, vésicules matricielles.

Université Claude Bernard Lyon 1
UFR Chimie – Biochimie
UMR CNRS UCBL 5246 – ICBMS
Bâtiment Chevreul
43 Boulevard du 11 Novembre 1918
69622 Villeurbanne Cedex

Nencki Institute of Experimental Biology
Polish Academy of Sciences
Department of Biochemistry
Laboratory of Biochemistry of Lipids
3 Pasteur Street
02-093 Warsaw, Poland